UiT The Arctic University of Norway

Faculty of Science and Technology
Department of Physics and Technology

Wind energy and economic assessment of a wind farm at Senja

A techno-economic analysis

Ola Wang Ørjavik

EOM-3901 Master's thesis in Energy, Climate and Environment
June 2022

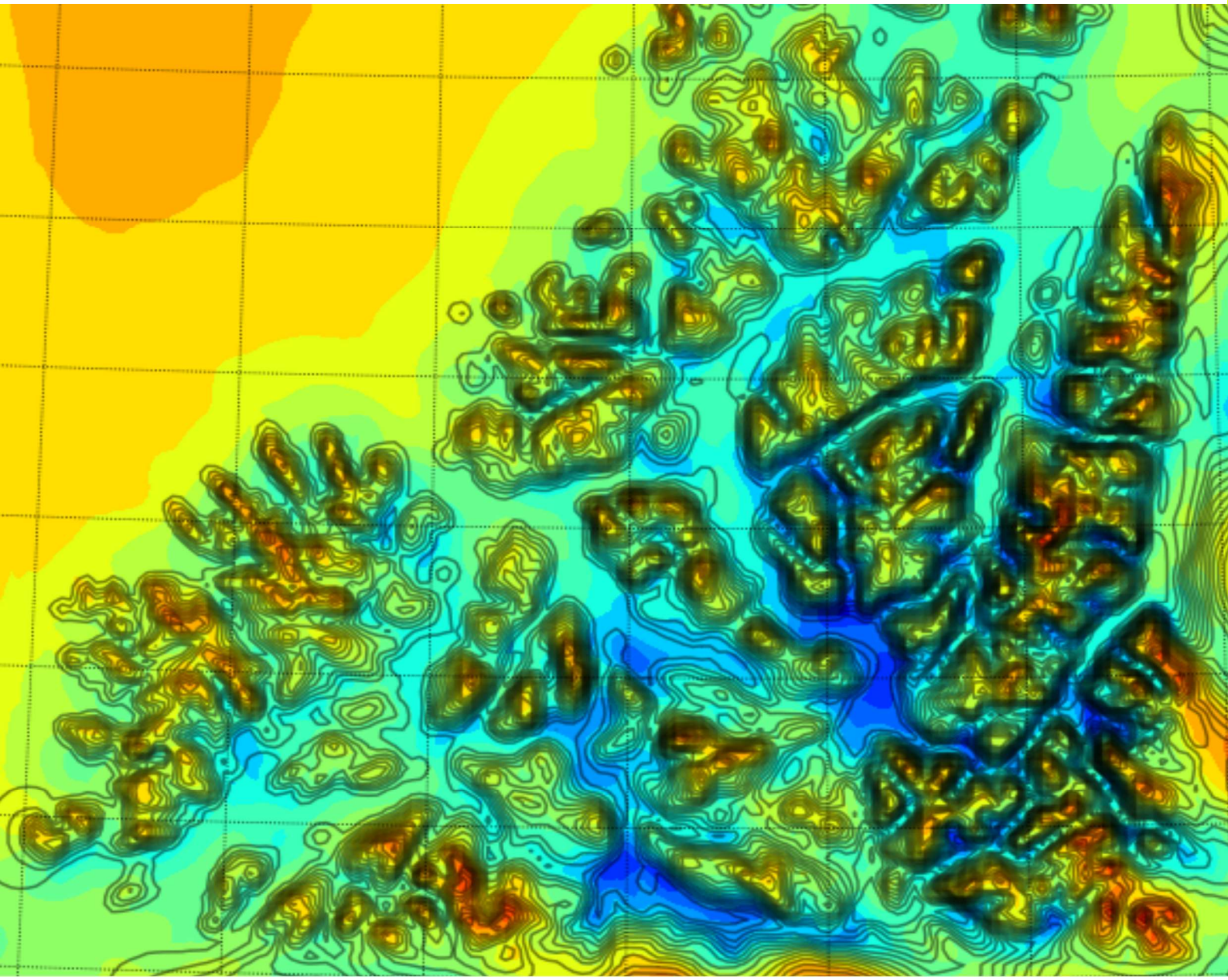

Abstract

In order to deliver on the emission cuts in the Paris Agreement, additional renewable energy production is required to cover the rising energy demand. This thesis assesses the wind resources, energy production potential and the economic sustainability of a new potential wind farm, located at Senja island in northern Norway.

The aim of this thesis is to decide if a new wind farm at Senja is an economic sustainable investment, based on the Levelized Cost of Electricity (LCOE) and the Net Present Value (NPV). The wind resources and the potential energy production was mapped by using a Numerical Weather Prediction (NWP) model, called Weather Research and Forecasting (WRF) model. The area of interest was chosen due to the current and future growth in energy demand at Senja. Troms Kraft has estimated that the energy consumption will increase by six times in 2030 from today's levels. Development of a new local renewable energy plant would cover parts of this upcoming demand and increase the energy self-sufficiency at Senja.

This thesis has shown that the wind farm at Senja is an economic sustainable investment, with energy production from 2030. The LCOE of the wind farm and the NPV was estimated to 39.65 øre/kWh and 55.42MNOK, respectively. This result was based on a yearly average energy production of 288.53GWh during an average weather year. This resulted in a capacity factor of 39.10%, which was higher than all the other wind farms in the vicinity of new wind farm. In the sensitivity analysis, the LCOE of the wind farm showed high sensitivity to variation in yearly energy production and initial Capital Expenditure (CAPEX).

Acknowledgements

First of all, I want to thank my supervisor Professor Yngve Birkelund for great guidance and discussions throughout this master thesis. Yngve has contributed with valuable expertise and experience regarding the WRF-simulations. I would also thank Ronald Hardersen for sharing his knowledge and experience about projecting a wind power plant and putting me in touch with people working in the industry.

In addition, I would thank Ivar Bredesen at OsloMet, for contributing with valuable feedback and guidance regarding the economic assessment. I would thank Tom Erik Olsen at Ishavskraft, for contributing with the latest electricity price predictions for NO4. Finally, I would thank Espen Erdal at Magnora for additional feedback on the economic assessment and good discussions about the wind energy industry.

These five years at UiT had never been the same without my classmates. I will always be grateful for the friendships and memories we have together. Thank you all!

Last but not least, I would thank my family for always supporting me and believing in me. You have made it possible for me to achieve my goals, I will always be grateful.

Ola Wang Ørjavik

Contents

Abbreviations

CAPM: Capital Asset Pricing Model

CAPEX: Capital expenditure, initial costs of an investment

DO1: Outermost domain in the WRF simulation, 25km resolution

DO2: Intermediate domain in the WRF simulation, 5km resolution

DO3: Innermost domain in the WRF simulation, 1km resolution

ECMWF: European Center for Medium-range Weather Forecasts

ERA-Interim: Global atmospheric reanalysis data from ECMWF

GWh: Giga Watt hour

IRR: Internal Rate of Return

kWh: Kilo Watt Hour

LCOE: Levelized Cost of Electricity

NCL: National Center for Atmospheric Research command language

OPEX: Operating expenses

MASL: Meter above sea level

NPV: Net Present Value

NWP: Numerical Weather Prediction model

PPA: Power Purchase Agreement

RIX: Measurement of the steepness of the terrain

TWh: Terra Watt hour

WRF: Weather Research and Forecasting model

WPS: WRF pre-processing system

1 Introduction

1.1 Background

Through the Paris Agreement, Norway has stated a goal of cutting between 50-55% of their national greenhouse gas emissions by 2030, compared to 1990 levels [1]. To achieve this goal, an energy transition from fossil fuel to renewable energy is required among several segments of the society. This will increase the demand of renewable energy substantially and will require growth in new renewable energy capacity.

As of 2022, Norway has a positive energy balance of 15-20TWh during an average weather year [4][27]. Towards 2030, the energy demand in Norway will increase more than the additional supply. This will decrease the energy balance towards 5-7TWh, based on estimates from NVE and Statnett [4][28]. There are related uncertainties to these estimates, and in a high demand growth scenario the energy balance in Norway is estimated towards zero in 2030 [28]. To cover the increasing demand, wind energy is estimated to stand for the largest additional supply in Norway from 2020 to 2030, with 10TWh [28].

Decreasing power balance will result in higher prices in Norway [4]. For Norway to remain attractive for new industrial development and take a leading role in the fast-growing renewable technology sector, it is important to maintain the edge with lower electricity prices compared to central Europe. To achieve this, a growth in new renewable energy production is necessary and it is therefore highly relevant to map new possible sites for wind energy production.

Increased industrial activity in the fishing and aquaculture industry in northern Norway leads to an increased need for energy. In addition to traditional aquaculture, new projects in both large-scale sea farming and land-based farming are under development. Production growth entails increased transport volumes, both at sea and along the roads. To meet the political requirements in relation to emission cuts, increased electrification of production, slaughterhouse and transport of the industry will be necessary.

Senja island, located in northern Norway, has experienced strong growth in energy consumption due to growth in the aquaculture sector. In 2030, Troms Kraft has estimated that the energy demand will be six times higher at Senja, compared to 2021(Erling Dalberg, Director of market and technology, Troms Kraft, personal communication, 24.05.06). The current transmission lines are already struggling to handle todays load and are not dimensioned for the upcoming consumption growth. Smart Senja is an initiative lead by Troms kraft, where leading actors in the energy sector and researchers at the University of Tromsø works on solutions related to this issue [9]. To cover the growing energy demand at Senja within the obligations of The Paris Agreement, its relevant to map the potential of new renewable power plants located close to the end user. Establishment of new renewable power generation will also improve the energy self-sufficiency at Senja.

1.2 Former research

Areas well suited for wind energy are often located remote and in areas where observation data from weather masts are limited. In the start phase of a project where several areas are considered, it would be costly to put a weather mast on each location. It is therefore often more convenient to run a Numerical Weather Prediction model (NWP), like the Weather research and Forecasting (WRF) model. This method gives an indication of the available wind resources much faster than a weather mast, and the results can be used to rank the different options for further assessment.

There has been done several earlier studies on how well the WFR model is able to estimate and predict wind speed and wind direction in coastal areas in northern Norway [2][13][3]. In the following article “Evaluation of the Weather Research and Forecasting (WRF) model with respect to wind in complex terrain” [2], on-site measurements at Hekkingen, Andøya and Tromsø was used to evaluate the WRF-model. It was found that the model was able to reproduce the annual wind direction properly for all locations. At Tromsø and Andøya, it was found that the WRF-model tends to overestimate the frequency of wind speeds above 6 m/s. At Hekkingen, the frequency of wind speed above 7m/s and below 2 m/s was underestimated. This highlights the uncertainties related to WRF-simulations in complex terrain. In total, it

was shown that the model performed best at Hekkingen by comparing the Weibull probability density function between model data and measurement data.

In a case study at Havøygavelen wind farm [13], the performance of WRF was evaluated with respect to wind speed and wind direction at hub height of the turbine. The results showed that the model was vulnerable for rapid changes in wind speed but performed better under stabile and moderate wind speeds. In addition, the annual wind resources were underestimated at lower resolutions, but enhanced at finer resolutions. In a study by Bilal, Solbakken and Birkelund [3], it was found that the WRF model tends to underestimate wind speed during high wind speeds, similar as in [13] and at Hekkingen in [2].

1.3 Idea and aim of the thesis

The idea of the thesis came from discussions with Professor Yngve Birkelund and Ronald Hardersen, in relation to Smart Senja and the future energy demand. By developing a wind farm at Senja, parts of the upcoming demand growth can be supplied by local energy production and make Senja more self-sufficient. The area of interest chosen in this thesis was suggested by Ronald Hardersen, due to its interesting topographical location and proximity to the energy consumers. The economic part of the thesis was integrated to investigate the economic sustainability of the wind farm.

The main goal of this thesis is to decide if the new wind farm at Senja is an economic sustainable investment, based on an evaluation of the NPV and the LCOE. This is achieved by mapping wind resources and estimating yearly energy production.

The wind resource assessment and the estimation of yearly energy production are based on a NWP, called WRF. To map the wake loss of the wind farm two simulations have been completed, one clean simulation and one simulation including wind turbines and the respective power curve. The result from the simulation is analyzed to suggest changes on the wind farm design, in order to obtain higher energy production, hence higher profitability. A sensitivity analysis is performed in the economic part to highlight the sensitivity of the LCOE and NPV of the project if main parameters changes.

Structure of the thesis

In addition to the introduction, this thesis consists of 5 chapters; Theory, method, result and discussion, and conclusion. Each chapter focus on the three distinct segments of the wind farm project: wind resource assessment, energy production and economic analysis.

Chapter 2 -Theory: The theoretical section includes necessary information to understand the methodology of the thesis. Background information about wind resource assessment, energy production estimation and economic analysis are presented. The chapter include an energy market outlook summing up the latest analysis.

Be aware that parts of the theory are completely similar/copied from my project paper written autumn 2021.

Chapter 3 – Method: The methodology chapter describe how the wind assessment, wind energy estimation and the economic analysis was performed to achieve the results. It includes information about how to set up and run the WRF.

Be aware that parts of the Method, describing the WRF model, are completely similar/copied from my project paper written autumn 2021.

Chapter 4 – Results and discussion: The result section is divided in three distinct segments. First are the results from the WRF simulation presented, showing the yearly average wind speed for the wind farm. Secondly, is the yearly estimated energy production for the wind farm presented. In the last part, the estimated energy production is used to calculate the NPV and LCOE of the wind farm. A sensitivity analysis is performed to map the sensitivity of the project if main parameters changes.

Uncertainties related to the WRF simulation and how this affect the results are discussed. Based on observations from the results, several suggestions related to optimizing turbine placements and wind farm design is presented.

Chapter 5 – Conclusion: The conclusion summarizes the results and proposes ideas for future studies.

2 Theory

2.1 Atmospheric motions

The magnitude of incoming solar energy varies between low and high latitudes at the earth. This result in differential heating between geographical areas and result in atmospheric motions on a large range of scales. When the ground is heated by the incoming solar irradiation the air parcels will rise upwards, resulting in a low atmospheric pressure at the heated surface. This result in horizontal differences in atmospheric pressure, called the *pressure gradient*. Large pressure differences between areas result in a large *pressure gradient force,* where the magnitude of the force is dependent on the pressure gradient. The force will cause the air to move from a high pressure to a low-pressure area. As the air starts to move it will be deflected by the *Coriolis force,* which appear due to the rotational movement of the earth. The *Coriolis force* will deflect the wind to the right in the northern hemisphere and to the left in the southern hemisphere. The magnitude of the *Coriolis force* varies by latitude and the speed of the moving parcel. Increased wind speed will also increase the *Coriolis force* and therefor will higher wind speed result in greater deflection. The *Coriolis force* has an increasing effect on the air parcel as it moves closer to the poles [14].

In the boundary layer the friction forces must be considered, resulting in ageostrophic winds. The friction force varies dependent on the surface properties and roughness and will slow down the wind. In the atmospheric general circulation, tropospheric jet streams and mesospheric jet streams are prominent features. The tropospheric jet stream has strongest magnitude during winter and blows from the west throughout the year. The mesospheric jet stream has seasonal variations, blowing from west during winter and east during the summer [15].

To describe the atmospheric motions there are three velocity components used, the zonal- (1), the meridional- (2) and the vertical (3) velocity component [15]. The zonal component describes the fluid flow pattern along the latitudinal lines in the west-eastern direction and the meridional component describe the fluid flow along the longitude lines in the north-south direction. The vertical component describes the vertical motion of the atmosphere.

$$u = \frac{dx}{dt} = R_E \, cos(\phi) \frac{d\lambda}{dt} \tag{1}$$

$$v = \frac{dy}{dt} = R_E \frac{d\phi}{dt} \tag{2}$$

$$w = \frac{dz}{dt} \tag{3}$$

Based on the zonal component *u* (1) and the meridional component *v* (2), one can derive an expression for the horizontal velocity (4). Where **i** and **j** are the unit vectors for the zonal and meridional directions. The SI unit for the wind velocity is given in [m/s]. Positive zonal velocities are referred to as *westerly* winds, negative zonal velocities are referred to as *easterly* winds. For the meridional component, positive velocities are referred to as *southerly* winds and negative velocities are referred to as *northerly* winds, this is valid for both the *southern* and *northern* hemisphere [15].

$$\boldsymbol{V} = u\boldsymbol{i} + v\boldsymbol{j} \tag{4}$$

When examine the Earth's atmosphere in a scale larger than 100km, the length scale, zonal- and meridional components, is significantly larger than the vertical depth scale component. This result in a magnitude of (4) which exceed the size of the velocity component (3) by several orders. The term *wind* is therefore used as a synonym for the *horizontal velocity component* (4) when the scale is above 100km.

Equation (5) shows how to calculate the magnitude of the horizontal velocity based on the *u* and *v* -component.

$$V = |\boldsymbol{V}| = sqrt(v^2 + u^2) \tag{5}$$

$$\angle \mathrm{V} = \left(arctan2(u, v) * \left(\frac{45}{\arctan(1)} \right) \right) + 180 \tag{6}$$

Equation (6) shows how to calculate the wind direction based on the *u,* and *v*- component of the wind. The output value is in degrees, where North is defined as 0 degrees and South as 180 degrees.

2.2 Wind phenomena in complex terrain

Mountain waves

Mountain waves are internal gravity waves occurring in the air mass due to vertical displacement. The phenomenon can occur due to orographic lifting when air masses flow over a mountain. There are several conditions that need to be fulfilled before mountain waves can occur. Firstly, the air masses ned to have a high stability, which is characterized by a positive change in vertical potential temperature. Secondly, the wind needs to have a distinct cross barrier air flow over the mountain ridge. The magnitude of the wind speed is also important and impact the magnitude of the wave's propagation and the amplitude of the waves [15].

The waves will propagate with decreasing amplitude due to natural damping. A result of horizontal displacement is that lee waves can form on the lee side of the mountain. The lee wind extends downwards from the mountain top and are trapped between the land surface and the upper level of where the wave is reflected downwards. As a result, lee waves can result in high wind speeds at the lee side of the mountain.

Breaking mountain waves is another phenomenon that occur when the amplitude of the vertical propagation get very large, and the isobars gets a vertically direction. This result in strong vertical mixing and the mountain wave will break. This can result in down slope windstorms on the lee side of the mountain, where the wind speed can reach a magnitude that is 2-3 times larger than on the mountain top [14].

Mountain gap wind winds

Gap winds are a wind phenomenon that occur when winds flow through a natural gap or funnels in the terrain. Fjords and mountain ranges are typically terrain types where this can appear. In front of the gap a local high pressure will be formed, as the wind blows through the narrow gap, the wind will accelerate from the high pressure towards the local low pressure at the exit of the gap. The wind speed will therefore have highest speed at the exit of the gap.

Mountain gap winds are strongest during the winter when cold air is trapped near the ground surface due to a strong temperature inversion. This can occur in fjords and valleys where there

is a sufficient elevation gradient that contribute to trap the cold air at the surface. The temperature above can be several degrees warmer, contributing to strong gap winds [14].

2.3 Numerical Weather Prediction model

An NWP model is a program that solves equations describing the processes in the atmosphere over time. To calculate the movements in the atmosphere, the atmosphere is divided into cubes where each box has a grid point in the centre. The forecasted value from the model is the average value from the box. A model with high resolution would have closer and more grid points to increase the accuracy of the model. Higher resolution also results in more demanding computations and need of more powerful computers [10].

Model resolution has a large impact on the terrain and topography in the model. Mountain tops in the models are often lower than in real life, due to the grid point averaging of the elevation values. Also, valleys will be smoothed out and be less distinct in the model. Topographical features like downslope wind, lee waves and convection will not be fully described [10]. The vertical layers are divided into layers to describe the atmospheric movements. Higher resolution will hence describe the movements more accurate but requires more computational power. To better describe the phenomena that occur under the boundary layer, many models dived this part of the atmosphere in smaller section to get higher resolution where most of the weather phenomena develops. The main constraint for running high resolution NWP models is computational power.

NWP models are an alternative and a supplement to metrological weather stations when it comes to mapping wind energy resources. Even though weather station will return more exact measurements at a specific location, NWP has several benefits. Firstly, many NWP models are freely available and cheaper than placing a weather mast at a fixed location. Secondly the model can give a larger overview of an area and produce data for remote locations where it is hard to place weather masts. NWP will provide vertical data at higher altitudes, providing a more holistic view of the weather situation. Finally, an NWP model can provide data for a hole year in a relatively short time, compared to a weather mast where one year is acquired to get seasonal variations [10].

There are also some uncertainties related to use of NWP. Firstly, the model is defined as an approximation of the real world. This result in simplifications and smoothing of the topography and terrain. Due to limitations in computational power, physicals processes like convection, solar irradiation and turbulence are simplified [10]. There are also several physical process that is not fully understood and can therefore not be represented as a feature in the model. The characteristics of the surface play also an important role in the boundary layer and affect the friction coefficient. Finally, the access to computational power is important to be able to run models with high resolution over large time horizons.

2.4 Fundamentals of wind power

2.4.1 Wind power and energy production

The energy of a moving air parcel can be derived from kinetic energy (7), where *m* is the mass of the air parcel in [kg], and *v* is the horizontal velocity of the parcel in [m/s]. The unit of the kinetic energy is given in [Joules].

$$E_k = \frac{1}{2}mv^2 = \frac{1}{2}(\rho Ax)v^2 \tag{7}$$

From equation (7), ρ is the density of the air in [kg/m³] and *A* is the swept area of the turbine blades in [m²], and *x* is the thickness of the air parcel in meter [m].

The power in the air parcel can be expressed as the derivative of the kinetic energy with respect to time (8). This result in equation (9), which represent the total available power in the air parcel in watt [w].

$$P_w = \frac{dE_k}{dt} = \frac{1}{2}(\rho Ax)v^2\frac{dx}{dt} \tag{8}$$

$$P_w = \frac{1}{2}\rho Av^3 \tag{9}$$

Equation (9) shows that the available power is strongly dependent on the speed of the air parcel due to the cubic relationship. Variations in wind speed will results in large fluctuations in power production. The swept area *A* is defined as the area that the turbine blades cover (10), where *r* is the length of the turbine blade. Increasing the length of the turbine blade will increase the power production.

$$A = \pi r^2 \tag{10}$$

The density of an air parcel is defined by the *ideal gas law* (11). Where p is the pressure, T is the temperature inn Kelvin and R is the ideal gas constant for air [J/kg K]. To consider humidity, the RT term can be replaced with $R_d T_v$, as expressed in equation (12). Here is T_v the virtual temperature, which is defined as the temperature that dry air would have at the same density as moist air at a specific pressure, and R_d is the gas constant of dry air.

$$\rho = \frac{p}{RT} \tag{11}$$

$$\rho = \frac{p}{R_d T_v} \tag{12}$$

From equation (11) and (12) it is visible that the density of an air parcel is proportional with the power output. Increasing pressure and decreasing temperature will result in higher power production. In humid air the water vapor takes up space for nitrogen and oxygen molecules that has a higher molar mass than the water molecule. This makes humid air lighter than dry air. The most ideal conditions for wind power production are therefore cold and dry air, due to higher air density [16].

Air flow towards a wind turbine

When a tube of moving air with pressure p1, speed u1 and diameter d1 moves towards a wind turbine the speed will decrease. When the speed of the wind tube decrease, the diameter will increase to the size of the swept area of the turbine. Some of the kinetic energy will be converted to potential energy and result in increased air pressure right in front of the wind turbine. When the air mass has passed the turbine blades the pressure will fall below atmospheric pressure. Kinetic energy is then converted to potential energy to normalize the pressure and obtain equilibrium. The speed of the air tube will therefore decrease until it has

the same pressure as the surrounding air. When the speed of the tube has reached its minimum, it will start to receive kinetic energy from the surrounding air flow [17].

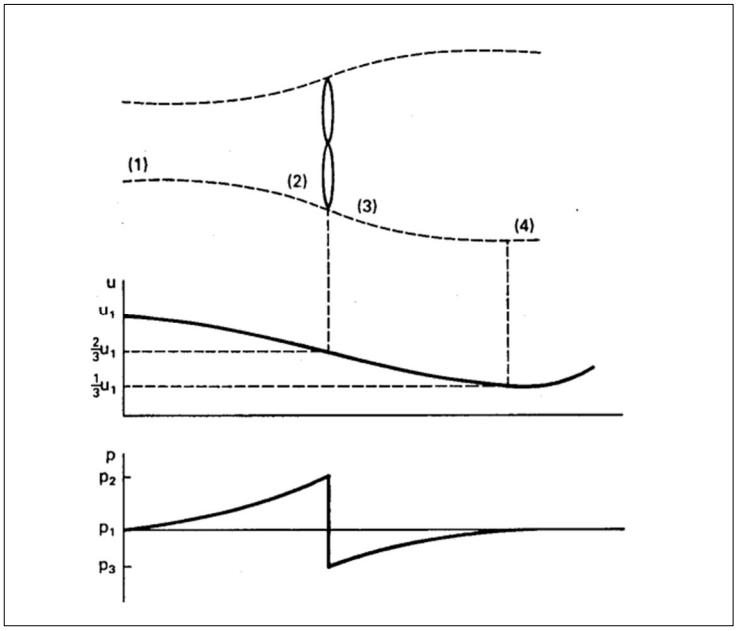

Figure 1: Air flow through an ideal wind turbine [17]

Practical turbines- power output

The maximum theoretical efficiency of a wind turbine is 59%, defined by Betz' limit [18]. This is a theoretical limit including assumptions like, idealized turbine with infinitely many thin turbine blades, no electrical losses, and no turbulence in the air flow [26]. None of these assumptions are valid in real life, which make Betz limit at theoretical limit. The theoretically maximum power possible to extract from wind is defined as (12), where $\frac{16}{27}$ represent Betz' limit.

$$P_{Betz} = \frac{1}{2}\rho A\, v^3(\frac{16}{27}) \tag{12}$$

For a wind turbine the power coefficient is the ratio of produced power from the wind turbine P_0, compared to the available power in the wind P_w.

$$C_p = \frac{P_0}{P_w} \tag{13}$$

The performance coefficient will vary with wind speed and the wind turbine blade parameters. Dependent on turbine size and manufacture, rotational speed, pitch angel and blade parameters will vary and result in various performance coefficients for different wind turbines. Larger and newer turbines can change the pitch angel dependent on the wind speed to maximize the power coefficient and hence the mechanical power output [17].

Figure 2 illustrates the different 'steps' of an electrical wind power system. The available power in the wind (P_w) is the input to the system The mechanical power output from the turbine (P_m), at a given angular velocity (w_m), is dependent on the performance coefficient(C_p). The mechanical power output is then coupled to the transmission, where transmission power output (P_t) is a product of the mechanical power (P_m) and the transmission efficiency (n_m). The power generator output is a product of the transmission output (P_t) and the efficiency of the generator (n_g).

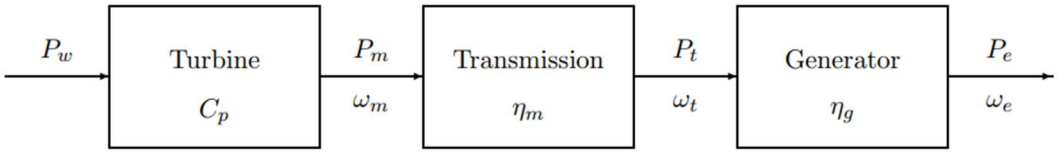

Figure 2: Generation of electricity from a wind turbine [17]

The power output from a wind turbine is expressed in the equation (14). The overall efficiency can be expressed by equation (15)

$$P_e = C_p n_m n_g P_w \tag{14}$$

$$n_0 = C_p n_m n_g \tag{15}$$

Energy output from a turbine is defined as power output multiplied with time (16). The performance of the turbine can be expressed by the capacity factor (17), which is defined as the total energy output from a wind turbine over a defined period, dived by the maximum possible energy output for that period.

$$E_e = P_e * t \tag{16}$$

$$C_f = \frac{E_e}{E_{max}} \tag{17}$$

The capacity factor describes how the turbine perform in relation to its maximum potential. It is the ratio of its actual energy production, with respect to it is maximum energy production potential. Capacity factor varies between renewable energy technologies due to their different dependency on the weather.

2.4.2 Power curve

A power curve describes the electrical power output from a wind turbine at different wind speeds. The power curve is obtained from theoretical derivation based on measurement in stable conditions with minimal turbulence and where the angle of attack of the wind is faced directly on the turbine blades [17]. Vc is the cut in speed, which indicates the wind speed the turbine starts to produce power at. The power production increases until it reaches rated speed, Vr. The power production is constant from rated speed and up to the cut-out speed, Vf. At Vf the rotor is stooped to prevent high mechanical load on the turbine which can cause damages. The power curve is just a theoretical estimation of what the turbine can produce in terms of power, but the actual production will fluctuate based on different weather conditions [17].

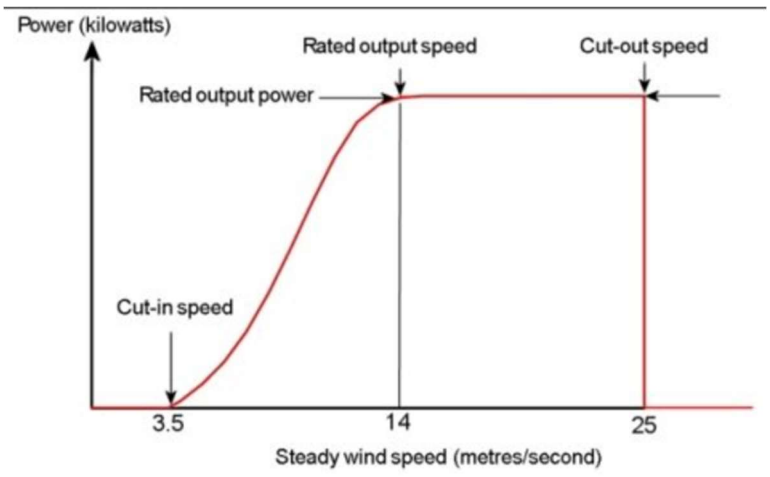

Figure 3: Power curve for a wind turbine [74]

For wind turbines with high installed capacity, the power curve can be optimized to avoid unwanted high mechanical load during high wind speeds. This is done by gradually decrees the power production above a certain wind speed level. This cut off strategy system is referred to as High Wind Ride Trough (HWRT). It is earlier shown that this system increases the energy production from a wind turbine, due to more continuous production [73].

2.5 Factors reducing power production

There are several factors contributing to reduce the theoretical power output from a wind turbine. Some of the most important factors are, wake loss, ice and dirt on turbine blades, mechanical losses due to friction, losses in electrical cabling and transformers, and downtime due to planned maintenance. When estimating energy production, it is important to be aware of these factors and how they affect the total energy production. The net output from a wind turbine is usually estimated to be 10-15% under the theoretical estimated energy production from the power curve [41]. Since the total energy production is an important factor in the economic assessment, it' important to be aware of the magnitude of the loss factors mentioned above.

2.5.1 Wake loss

For a wind power plant consisting of several rows of wind turbines, the wake effect will have an impact on the total energy production [23]. The wind turbines extract energy from the wind, resulting in less energy in the wind leaving behind the turbine. This results in reduced wind speed and turbulent in the downstream wind from a wind turbine [19]. Behind the turbine the wake will begin to spread and gradually return to free stream flow. If turbines are located close to each other, a wake can intersect the swept area of the next turbine. In this case the second turbine is said to lay in the wind shadow of the turbine producing the wake. There are two main effects of a wake: (1) the wind speed is reduced, which result in lower energy production from the wind turbines; (2) increased turbulence in the wind can potentially increase the dynamic mechanical load on the turbines and reduce power output [19]. It is

important to consider these wakes effects when designing a wind farm. Turbine locations should be optimized to reduce the wake affect, in order to maximize power production and lifetime of the turbines.

2.5.2 Icing

When developing a wind farm in northern Norway, icing on the turbine blades is a phenomenon that can occur. During sever icing the wind turbine can in a worst-case scenario stop, resulting in temporary stop in energy production. This leads to economic losses from both increased maintenance and lost revenue. Also, miner icing will affect the power production, even though the turbine does not stop. These phenomena are covered in detail in this study [20]. In addition to loss in energy production, icing on turbines can poeses a risk for people who stay close to a wind turbine.

There are many ways the turbine can stop due to severe icing. Firstly, ice can disrupt the aerodynamics of the blade in such a way that the force of the wind is not able to rotate the blade [20]. Secondly, the load of the ice can cause imbalance on the blade, resulting in vibrations. This can trigger the vibration alarm in the turbine and by that stop the turbine. Finally, the turbine can stop if the rotor torque exceeds a preprogrammed level, which is based on the expected torque at different wind speeds.

It is mentioned in [20] that ice often accumulate easier on thin surfaces than thicker surfaces. From a study at Nygårdsfjellet [20], there was low production loss despite indications of icing. It was suggested that the large and thick turbines blades were less susceptible for ice accumulation than smaller turbines.

Nygårdsfjellet wind farm has experienced icing, which has resulted in complete stop of the turbines. Normally, these stops have only lasted for one or two days [20]. The turbines at Nygårdsfjellet are located at an elevation of approximately 420-460m above sea level. In the same study it was found that the energy loss due to icing at Nygårdsfjellet was lower compared to other wind farms with smaller turbines.

In the following study [22], estimated production loss due to icing was performed on Kvitfjell and Raudfjell wind farm. The simulation was done between 2014-2016 and used WindSim

combined with a Computational fluid dynamic simulation (CFD) model. The results from the simulation showed a production loss due to icing at 9,5% in a worst-case scenario and 4,75% in the most probable scenario. There are uncertainties associated with the estimates due to the model's capability to cover the actual ice conditions and local variation in atmospheric icing within the park [22].

Figure 4 illustrate expected hours of icing at 80m above sea level for the coastal areas of Troms County [67]. This map can be used as a rough estimate to describe the expected icing conditions for an area.

Figure 4: Expected icing at 80m. The map covers the coastal areas of Troms municipal. The map is made by Kjeller Vindteknikk for NVE [67].

2.5.3 Degradation

Energy conversion system like wind turbines operates under non-stationary conditions. The load on the system will over time lead to decreased performance. In a study that analyzed the performance of a Vestas V52 wind turbine, it was found that the turbine performance declined with 5% over a ten-year period [25]. An important observation was that the decline in performance was a nonlinear relationship as the year passed. The gearbox contributed to approximately 30% of the total degradation. After ten years, the gearbox was replaced, resulting in partly recovery of the performance. It was found that the replacement of the gear box had largest improvement on energy output on sites where the wind was above 6 m/s. The result found in this study [25], was consistent with other studies done on the same topic.

In NVE's estimations of future LCOE for onshore wind in Norway [71], a yearly degradation rate of 0,10% have been used. In a discussion with a person with experience from the wind energy industry, a degradation rate of approximately 0.25% was presented as often used. (Espen E., VP Business Development Magnora, personal comment, 27.05.2022).

2.6 The energy market

Nord Pool is the leading energy market in Europa and offers a dynamic marketplace where energy is sold and bought across countries and geographical areas. The market is deregulated, meaning it is a free competition without any involvement of the state. Hence, the energy price is a result of demand and supply and is strongly connected to the weather situation at the given time. The dynamic market allows the energy to flow from areas with positive energy balance, where supply is larger than demand, to areas with negative energy balance, where demand is larger than supply [66]. This flexibility contributes to increase the energy security and the efficiency of the European energy market. The main energy resources come from coal, hydro, thermal, gas, nuclear, wind and solar. As European countries are gradually phasing out coal and fossil fuels in their energy mix, in line with the Paris Agreement, the share of renewable energy like wind and solar are increasing. As a result, the energy production in Europe will be more weather dependent. The importance of a dynamic and floating energy market will therefore increase in the future. In addition, the electricity prices will be more volatile with large daily fluctuations.

2.6.1 Electricity prices

For companies engaged in energy production, the electricity price is an important factor that has large impact one the probability of the business. As mentioned above, it is the relation between supply and demand that it is the fundamental factor affecting the electricity price [66]. In addition, the energy mix and the relative share of the different energy sources covering the demand is important. Figure 5 illustrates how the electricity price is sat in a dynamic market, dependent on energy demand and the different energy sources available in the energy mix. During low demand, wind and hydro power production is enough to cover the demand. These power producers have a low marginal cost, which makes the electricity price low. As the demand increase, nuclear, coal, gas and oil power plants need to supply the market. Since these power plants has a higher marginal cost, the electricity price will increase for the consumers. In general, it is the power plant contributing with the highest marginal cost, who set the electricity price for the whole market.

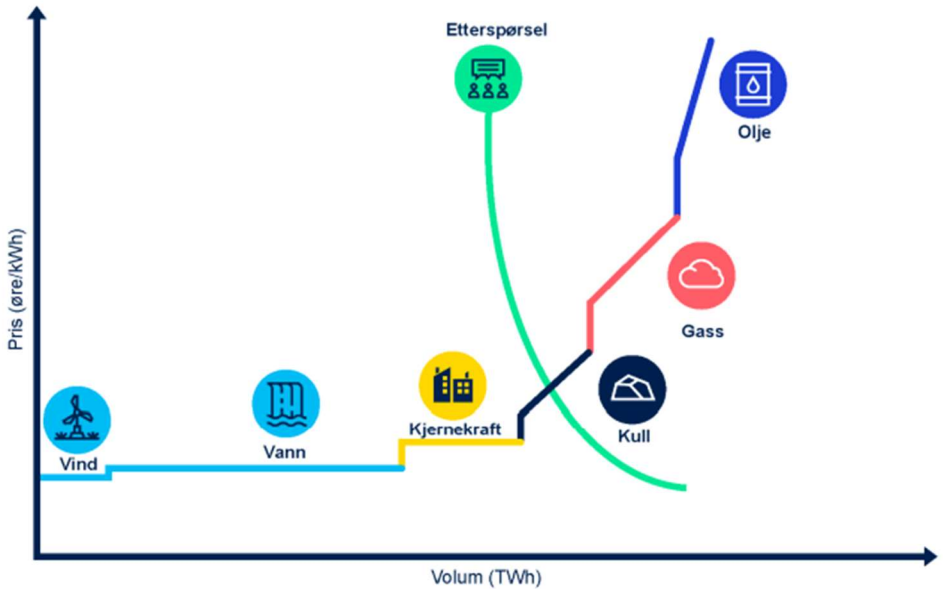

Figure 5: Price setting in a market with perfect competition [68]

2.6.2 Price regions

Figure 6 shows the NordPool price regions in Scandinavia. Norway is divided into five price regions, where NO4 represent northern-Norway. The northern parts of the Nordics stand for 30% of the total energy surplus in the Nordic, but only 15% of the annual consumption. Due to this relationship, the main flow of energy is from the surplus area in the north to the deficit areas in the south [29]. Figure 7 shows the established transmission lines in Scandinavia, due to limitations in the grid, just a portion of the surplus energy in the northern region can flow into the southern regions, resulting in price differences in the Nordic electricity market.

Since the price regions N04 and SE1 is strongly connected, it is relevant to look at the future demand situation for these two regions combined. An overview over the estimated energy demand for these prices regions is presented in section 2.6.3.

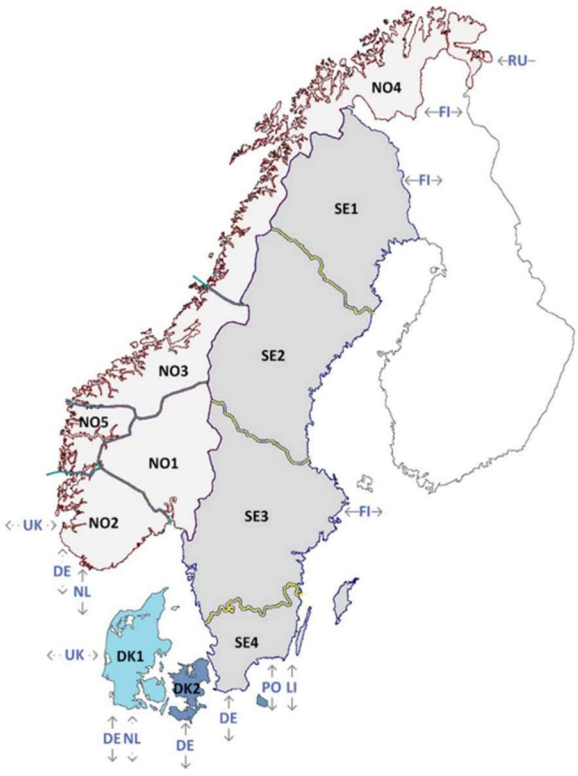

Figure 6: Electricity price regions in Scandinavia [24]

Figure 7: Overview over transmission lines in the Nordic and Baltic countries. The red lines indicate 400 kv, the orange lines 275 kv and the green lines 220 kv transmission lines. The transmission lines have not capacity to transmit all of the surplus energy from the northern regions (NO4 and SE1) and southwards. This result in price differences in the Nordic electricity market [69].

2.6.3 Market outlook

The shift from fossil fuel to more renewable energy will results in changes in the global and Nordic energy market. In this section, market outlook analysis from Statnett and NVE is presented [27] [28][4]. The analysis focus on how the market will develop in Norway and The Nordic region towards 2050, regarding demand, supply, CO2- and electricity prices. The reports were published 2021, before the war in Ukraine. Subsequently, EU has stated a plan to make Europe independent from Russian fossil fuels before 2030, through the REPowerEU incentive [30]. This adds additional factors that affect the energy market in Europe, which is not covered in these reports. A new updated market outlook from Statnett will come during fall 2022. Regardless, the reports describe the fundamental drivers that will affect the energy market in the future.

2.6.4 Situation today

Energy prices in Norway has historically been determined by a combination of the energy balance in the northern parts of Europe and the energy prices Norway's neighboring countries [5]. The last 10 years, Norway, Sweden, Finland, and Denmark have had a positive power balance in total, during normal weather years. This is illustrated in figure 8, which also shows that NO1 is the only region in Norway with negative power balance. Finland and Denmark have a negative power balance during a normal weather year, but the positive power balance in Norway and Sweden compensate for this, resulting in a total positive power balance of 21TWh in the Nordic region [5].

As a result of positive power balance in Norway, the power prices have historically been lower than in Europe. In central-Europe, the energy prices have been more connected to the marginal cost at coal and gas power plants, which again is strongly connected to the prices of coal, gas, and CO2 emissions. After opening two new power cables, North Sea Link to England ,1st October 2021, and Nordlink to Germany, 27th of May 2021, the transport capacity of power out of Norway has increased with 2 8000MW [7][8]. This has led to higher and more volatile electricity prices in the Southern price regions, N01, N02 and N05.

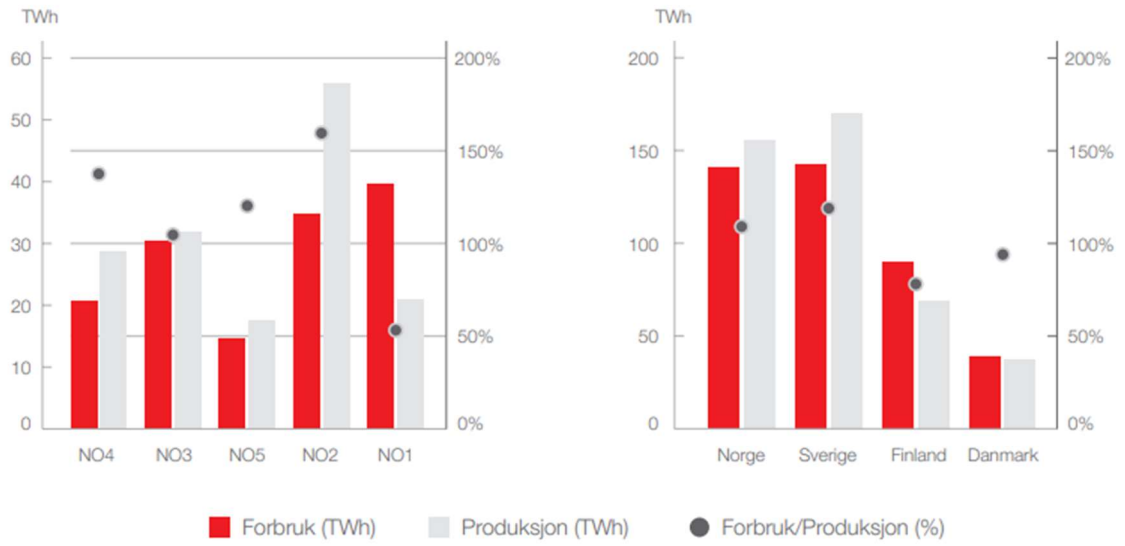

Figure 8: The left figure shows the relation between energy production and consumption for all the price regions in Norway during an average weather year (2021). The dot indicates how large share of the consumption that is covered by production in % (right axis). N01 is the only region in Norway with negative power balance.

The right figure shows the power balance in Norway, Sweden, Finland, and Denmark during an average weather year (2021). Finland and Denmark have a negative power balance, but combined the power balance is positive, with approximately 21TWh [5].

In northern Norway, limitations in the transmission capacity makes the energy region N03 and N04 more isolated from these volatile prices. The last year this has resulted in large national variation in energy prices in Norway, with much lower pieces in northern Norway compared to southern parts of Norway.

From 2023 will the Nordic region establish flow-based market connection [31]. Information about the physical transmission limitations will be considered directly in the calculations of power flow and price. This will optimize the physical transmission capacity and minimize local bottlenecks. As a result, more capacity will be available where the demand is largest. This will contribute to lessen the price differences between North and South [31].

2.6.5 Energy demand in the future

The relationship between demand and supply is the most important factor regarding the formation of the electricity price. In this section the future energy demand situation for Norway, NO4 and SE1 is described based on analyses form Statnett, NVE and Troms Kraft.

In the Nordic region the power production will increase in line with increased consumption towards 2026 [27]. Norway is predicted to have the largest consumption growth among the Nordic countries, with 30TWh in 2030 [27]. This comes from electrification of the petroleum industry, transport sector and new data centres, illustrated in figure 9. As a result, Norway's power surplus is predicted to decrease from today's 15-20TWh (2021) to 3TWh in 2026, in Statnett's analysis. Since the consumption growth is largest in the south, Southern-Norway will have power deficit in 2026 [27][48].

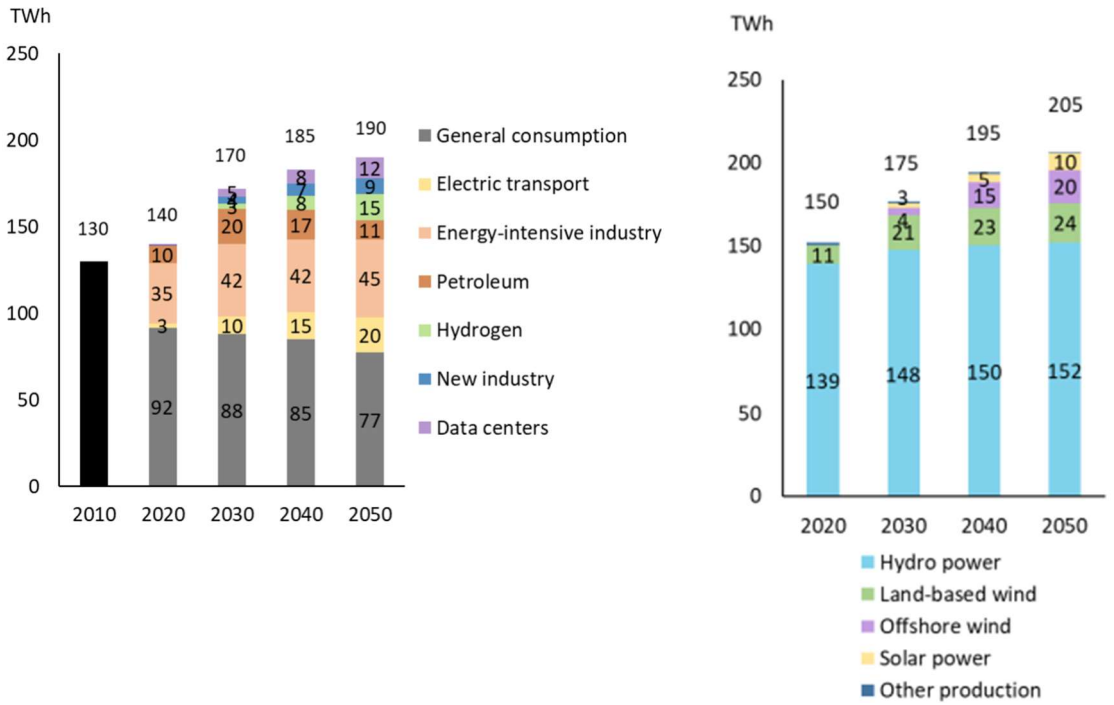

Figure 9: Basis scenario for Norwegian energy consumption to the left and energy production to the right towards 2050. The largest growth is expected to come from energy-intensive industry, data centers, hydrogen, and electric transport. Towards 2030 the largest additional supply is estimated to come from onshore wind, approximately 10TWh. The figure is rounded off to the nearest 5 [27].

Figure 10 shows the energy balance in the Nordic price regions based on the Climate Neutral Nordics Scenario. This scenario assumes that alle the Nordic countries delivers on the goal of decarbonization in 2030-2050 [29]. This implies a large growth in electrification of the industry and the transport sector for all the Nordic countries.

The combined power balance in NO4 and SE1 will develop from a strong energy surplus of 18TWh in 2020, to a deficit of 11TWh in 2040 based on the Climate Neutral Nordics Scenario [29].

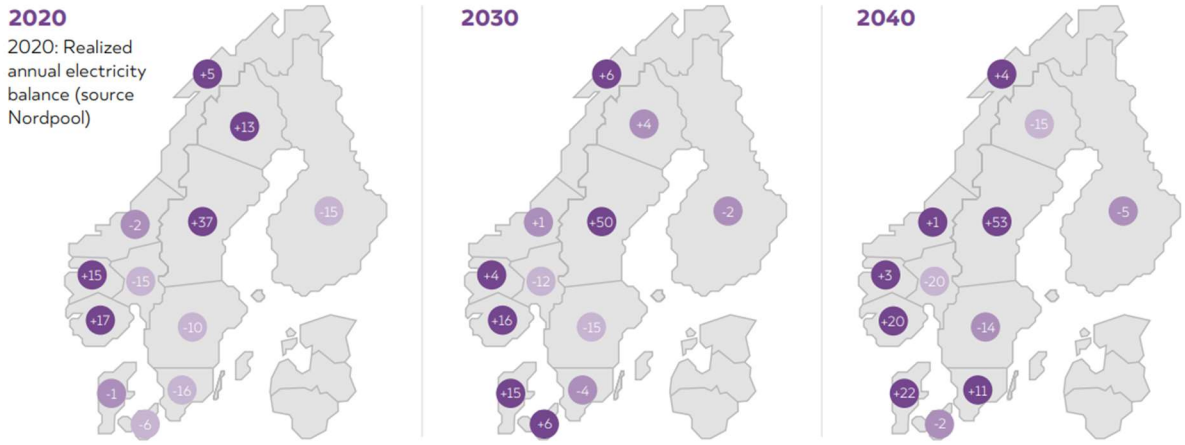

Figure 10: Electricity balance in the Nordic price regions in 2030 and 2040 based on the Climate Neutral Nordics Scenario. This scenario assumes that alle the Nordic countries delivers on the goal of decarbonization in 2030-2050. Values presented in 2020 are confirmed historical values [29].

Energy demand in N04

Towards 2030 it is expected increased focus on electrification of the petroleum industry. Mainly due to great pressure on emission cuts and expected hikes in the CO2 emission tax in Norway. In price region NO4, Melkøya, onshore facilities for gas processing, and Wisting, new oil field in Barentshavet, are suggested to be electrified. Melkøya is the most mature project and is expected to be electrified by 2027, with a yearly energy demand of 2,6 TWh [33]. Wisting is expected to start production in 2028 and from the impact assessment there is an ambition to facilitate electrical power from shore [35]. In the impact assessment it is stated that Wisting will reach maximum energy consumption in 2032, with 0,55TWh. The consumption is predicted to decrease towards 0,45 TWh to end of the production phase. In addition, it is estimated an increased demand of 0,5 TWh from the transport and the general industry in N04 in 2030 [39].

Towards 2040, an additional growth of 10TWh from 2025 levels are expected in NO4, see figure 11. It is predicted an increase of 3TWh due to electrification of the petroleum industry, hydrogen production will stand for 1TWh, Transport sector 1,7TWh and battery production 2 TWh. This will reduce the energy surplus in northern Norway and NO4 and contribute to higher power prices and smaller difference between north and south [33].

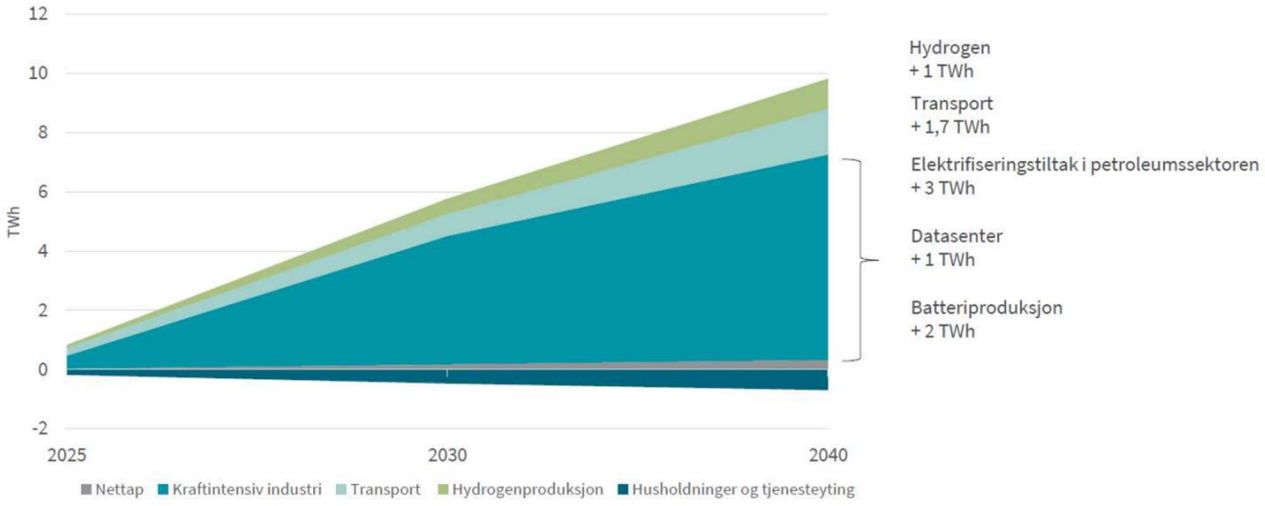

Figure 11: Demand growth towards 2040 in NO4. Most of the demand growth comes from the electrification of Melkøya and Wisting, a total of 3TWh [34].

Senja, located in NO4, is excepting a large growth in energy demand. In 2030 the yearly energy consumption is estimated to be six times higher compared to 2021 (Erling Dalberg, Director of market and technology, Troms Kraft, personal communication, 24.05.06)

This growth will mainly come from consisting and new establishment within the aquaculture industry. In addition, Troms Kraft has stipulated the yearly electricity demand needed, if all fishing vessels above 11m arriving at Tromsø harbour are going to use ammoniac as energy source. This would increase the yearly electricity demand in Tromsø by 6TWh (Erling Dalberg, Director of market and technology, Troms Kraft, personal communication, 24.05.06) and highlight the demand growth that will rise as a part of the green transition.

Demand in SE1

LKAB is Europe's largest iron ore producer, located in Kiruna, northern Sweden. Trough *The Swedish climate policy framework* [36], they are committed to reach net-zero emissions by 2045. To reach this goal the company need to electrify large amount of energy intense processes related to the mining activity. The company has announced an estimated yearly electricity demand of 55TWh from 2045 [37][38]. From a presentation held by Troms Kraft 24.05.2022, it was predicted an energy demand from LKAB at 20 TWh in 2030, 50 TWh in 2040 and 70 TWh in 2050 (Erling Dalberg, Director of market and technology, Troms Kraft, personal communication, 24.05.06)

In NVE's long term analysis they estimate a power surplus in Sweden of 23TWh in 2040, but the analysis only includes a small part of the increased power demand from LKAB [4]. NVE estimates that a total electrification of the Swedish iron ore and cement industry will contribute to a larger rise in the energy demand, hence reducing the power surplus. If the power balance moves towards zero in Sweden in 2040, NVE estimates that it will isolated increase the power prices with 3-5 øre/KWh in Norway [4].

2.6.6 CO2 prices

Towards 2030 the EU has sat a goal of reducing the net emissions of C02 by 55%, compared to 1990 levels [32]. This is a sub-goal towards reaching net zero in 2050. As a result, the C02 price forecast has been raised considerably in the newest market outlook from Statnett [28]. In this analysis, the CO2 prices is predicted to be between 70-80€/t in a basis scenario, and within a range of 50-100 €/ in 2030. An updated market analysis from Statnett will come during the fall in 2022. This analysis will include the latest changes in the European energy market, and the effects regarding Europe's goal of be independent from Russian oil, gas and coal.

The CO2 prices has more than doubled the last year, from 30 €/t in May 2021 to over 80 €/t in May 2022 [27]. The increased prices are a combination of tightening in EU's emission targets and increased demand after CO2 quats, in relation to more power production from coal power plant and very high gas prices in 2021 and 2022 [27]. The price trajectory, shown in figure 12, is expected to increase in line with the emission cuts towards 2030 and 2050, and tight emission budgets. Higher CO2 prices will result in higher marginal cost for fossil power plants, hence higher power prices in Europe and Norway. As wind and solar takes a large share of the total energy mix, the effect from CO2 prices on the power price will decrease. Statnett's analysis [27] except lower correlation between CO2 prices and power prices in 2030 than today. Power prices in northern Norway is less effect by the C02 prices, due to the limitations in grid capacity discussed earlier.

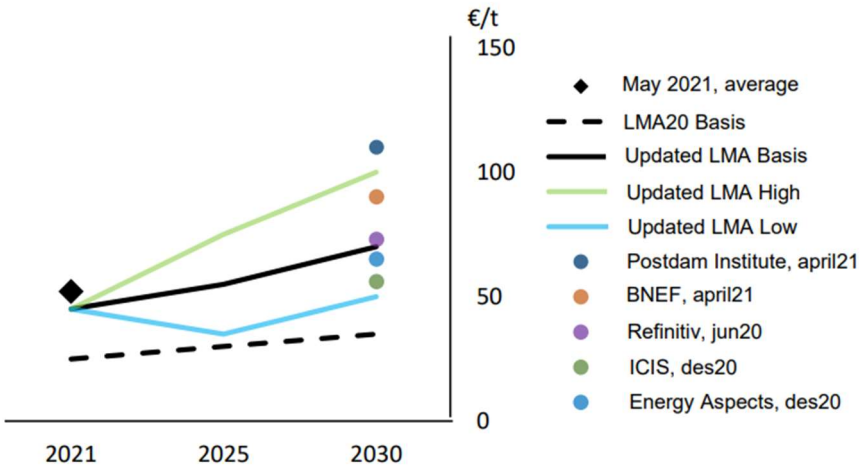

Figure 12: Predicted CO2 prices in Statnett's short-term analysis towards 2030 [27].

2.6.7 Future electricity prices

In Norway, the power prices are predicted to stabilize towards 2026 at a lower level compered to today's historical high level, but they will be above the 10-year average. The large price differences between the North and South in Norway will decline, but still be distinct. In addition, daily and weekly prices will be more volatile in the whole Nordic region.

As a power producer in NO4 it is highly relevant to have knowledge about the predicted power prices for the region, and which drivers that will affect the power prices both in the short and long term. The power prices are predicted to stabilize in southern and northern-Norway towards 2026, at respectively 55 €/MWh and 25 €/MWh [27]. Both coal and gas prices are expected to decline from today's historical high levels, but there is large uncertainty regarding the price trajectories because of REPowerEU. Increased CO2 prices will contribute to increase the marginal cost for fossil fuel power plant, which will support higher power prices.

The large difference in power prices between south and north are caused by several factors. Firstly, large power surplus in northern Sweden due to devolvement of new wind power capacity and limitations on the transmission capacity southwards. To increase the power transmission between north and south, Statnett and Svenska Kraftnat (SvK) has planned several expansions of the transmission capacity. This will expand the capacity north-south with 50-60% [31], but these plans will first show visible effect in 2030. It is associated large uncertainty to the timeline of the expansion of the transmission capacity, which again result in uncertainties in the power prices trajectories. Increased daily volatility will be the new "normal", mainly due to out phasing of coal and nuclear in the energy-mix, which makes the margin between consumption and available production small during hours with low power production from renewable energy plants.

Increased energy efficiency towards 2040 will contribute to decrease the energy consumption within heating and lighting. NVE estimates that this effect will dampen the average Norwegian electricity price with 4-5 øre/kWh in 2040 [4]. The effect is strongest in areas with dens population and tight power balance; hence the effect is largest in southern Norway.

Short term price outlook

Figure 13 shows one basis and one high scenario for the power prices in NO4 towards 2032, based on data from Ishavskraft [6]. The scenario with higher prices considers a stronger growth in energy demand. After almost similar prices in 2023, the price trajectories splits and there is a distinct price difference between the two scenarios towards 2032. How the difference price trajectories affect the profitability of the wind farm will be analysed through a sensitivity analysis in the result section.

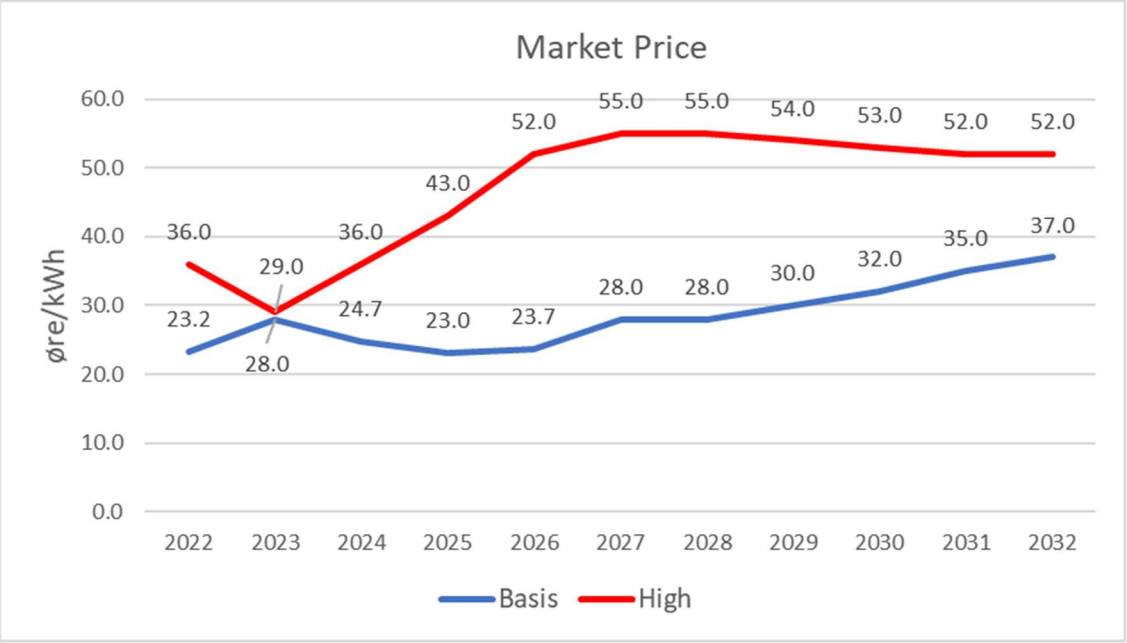

Figure 13: Short term power price estimates for NO4, with data are from Ishavskraft [6]. The high scenario reflects a situation with stronger growth in power demand than in the basis scenario.

Long term price outlook

Figure 14 shows three different price scenarios in NO4 towards 2040. The prices are based on a long-term market analysis from NVE [4]. The high and low-price trajectory are based on scenarios with high and low CO2 and fossil fuel prices. The deviation between the high and low scenario is largest in 2030, with a difference of 23 øre/kWh.

Figure 14: Power price estimates from NVE's long term market analysis towards 2040 for NO4 [4]. The prices are based on the average of 30 weather scenarios. Low and high price trajectory refers to low and high prices for CO2 and fossil fuel prices.

2.7 Economic aspects of wind power

This section describes the economic aspects of a wind power project. Firstly, the cost structure of a wind energy project is explained. Secondly, WACC is defined how it impact a economical part of a project. Finally, two economic evaluation methods used to determine the economic sustainability of a renewable energy project is presented. The first method is LCOE, which represent the cost of producing 1kWh. Comparing the LCOE for a power plant with the expected future electricity prices will show if the project is financially sustainable. Secondly, Net Present Value (NPV) is the current value of all future cash flow that the projects will generate, where a discount rate is applied to calculate the present value of the cash flow. The NPV shows the absolute return of the investment.

2.7.1 Cost structure

The project costs for a wind energy plant can be divided into four distinct segments, investment costs, operational costs, maintenance costs and financial costs [41]. The majority of the total cost's outflows during the initial phase of a wind energy project, making it capital intensive investment.

Investment costs

The investment cost is often referred to as the "initial costs" or Capital Expenditure (CAPEX) and reflect all costs that occur at the beginning of the project. This includes the cost of purchase and installation of all necessary equipment. For a wind farm the largest cost is related to the purchasing of the wind turbines. In addition, acquisition of licenses, wind resources assessment, site preparation and external grid connection are included. The most important factor affecting the probability of a wind power plant are the available wind resources [41]. This points out the importance of a good wind resource assessment and micrositing for optimal turbine placement.

Operational costs

Operational costs are costs related the daily operation of the wind farm after the farm is sat into production. This includes the cost of operating personnel, technical management, insurance, tax payments, land lease and grid rent.

Maintenance costs

This segment includes all costs that are related to ensure operational availability. This can be achieved through frequent maintenance and replacement of lamps, air filters or oil shifts. Larger and infrequent maintenance related to shift of larger components of the turbine is also a part of this cost segment. The maintenance costs will vary dependent on the total mechanical load that the turbine is exposed to. This will vary between wind farms and within the different turbines of a wind farm.

Financial costs

Financial costs are related to all financial expenditures from financing transactions during the lifetime of the project. The most important one is interest payments to lenders. In addition, costs related to financial guarantees, construction consortium and capital acquisition are typical costs under this segment [41].

Renewable energy project has relatively high capital expenses up-front but has in general lower operating cost than fossil fuel energy plants. One of the main reasons is that there is no fuel cost, like gas, coal, or oil. This is illustrated in figure 15, where a general renewable energy project is compered to gas power plant. The cost of the renewable energy plant is taken almost entirely up-front, whereas the cost related to the gas plant is more evenly distributed across the lifetime of the plant.

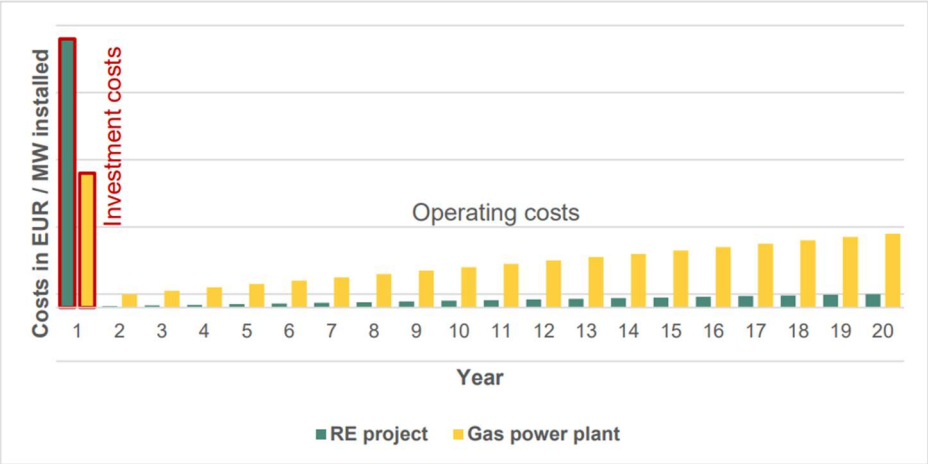

Figure 15: Operating cost and investment cost of a renewable energy project (RE project) and a gas power plant [41].

2.7.2 Weighted average cost of capital

WACC describe the cost of capital and is one of the most important financial variables for renewable energy infrastructure [49]. There is mainly two ways to raise capital for developing projects, either by borrowing cash (debt) or using equity from the company. When aggregating the relative weights of debt and equity one obtains the WACC. The WACC indicates the required rate of return which the project/company need to deliver to provide capital from bondholders and shareholders. High WACC indicates that the company need to pay a higher price for the financing, which indicates higher volatility and risk. By increasing the debt-to-equity-ratio, the overall WACC will decrease, since the cost of debt is typically lower than the cost of equity [52]. There are several variables affecting the WACC, especially interest rates and risks. Risk categories like; political, economic, regulatory, social and policy are the most common. Higher WACC will be required by investors if the investment includes high risk [49].

Equation (18) is show how to calculate the WACC, where; r_{WACC}=Weighted Average Cost of Capital, W_D=Capital structure, r_E= Cost of Equity, r_D=Cost of Debt before tax and t=taxes. The weighted cost of the funding sources is calculated in equation, by dividing the equity on the total (19).

$$r_{WACC} = (1 - W_D)r_E + W_D r_D(1 - t) \quad (18)$$

$$W_D = \frac{Equity}{Eqiuty+Debt} \tag{19}$$

The cost of debt is reflected in the interest rate that the company must pay to the lenders. The corporate tax is the percentage of the profit which the company must pay to the state, 22% in Norway. The cost of equity reflects the minimum required rate of return that the market demands from their investments. Higher risk implies higher rate of return. A common way of calculating the cost of equity is by the Capital Asset Pricing Model (CAPM).

Average WACC for onshore wind in EU

Figure 16 illustrate the reported WACC values for onshore wind farms in EU for 2019 [49]. Central-European countries like Germany, France and Denmark had the lowest reported WACC, with a range between 1.3%-4.3%.

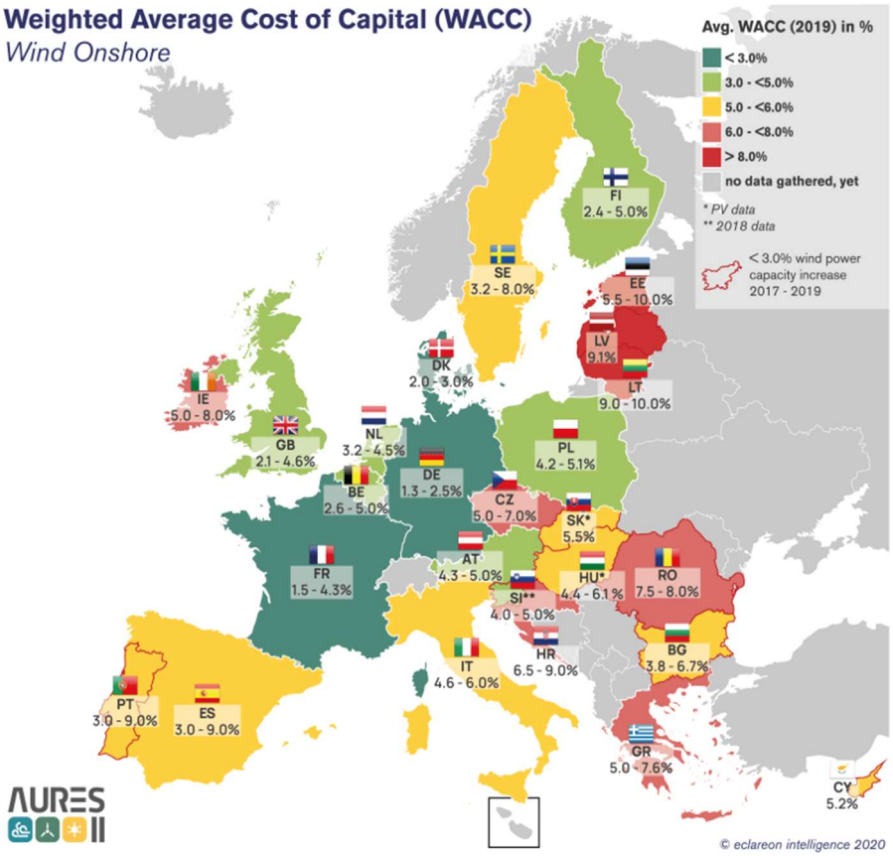

Figure 16: Reported average WACC for onshore wind in EU for 2019 [49].

In 2019, the 10-year government bond yield, often referred to as the risk-free rent, traded well below 0% during large parts of the year for these countries. As a result, investors required a lower rate of return, and hence the WACC for projects was low. As of May 2022, the 10-y government bonds are increasing, and the values in figure 16 is not representative for today's situation. However, it illustrates the difference in WACC between different countries, and how investors rate the risk related to onshore wind projects in different regions.

In Sweden, the maximum reported WACC was on 8% in 2019. This was way above neighbor countries like Denmark and Finland. Large amount of the wind energy farms in Sweden are in the northern parts of the country. As in Norway, the transmission lines are not dimensioned to export all the surplus energy out from the northern region which result in lower electricity prices. Another reason for the high WACC pointed out in [49], was that developers in Sweden explained that projects financed by green certificates where riskier and hence with a higher WACC, than if the project was secured with a long-term Power Purchas Agreement (PPA) [49]. The green certificate prices are low and volatile and hence not enough to compensate for the also low market price [49]. This increases the policy and price uncertainty for long term projects, and hence resulting in a higher WACC.

However, the WACC values presented in figure 15 are from 2019 and cannot be seen as representative today, because the WACC depends on cost of equity and cost of debt that changes along with the global economy. In addition, the 10-year Government bond yields were at historical low levels in 2019, resulting in a very low risk-free rent.

In the following article [53] there was found that Levelized cost of electricity (LCOE) for wind power plants are more sensitive for an increase in WACC than in coal and gas power plants. A low WACC is therefore very important for wind power plants to be competitive among fossil fuel power plants.

2.7.3 Deprecation

All cost related to the wind turbines are depreciated with 20% yearly, according to balance group d. Cost related to electrical transmission is depreciated yearly with 5%, according to balance group e [64].

2.7.4 Capital Asset Pricing Model

The Capital Asset Pricing Model is a widely used method in the financial market to estimate the cost of equity [51]. It describes the relationship between the expected rate of return from the asset and the systematic risk. The systematic risk is a term used to describe the universal risk related to the whole market, thus it is not possible to avoid. To calculate the CAPM one need the rate of return (r_m) of the general market, the risk-free rent (r_f), and the beta coefficient (β_i), see equation (20).

$$r_E = r_f + \beta_i * (r_m - r_f) \tag{20}$$

The risk-free rent, r_f, is the rate of return one can expect from a riskless investment. U.S government bonds with a duration of 10-years is often used as the risk-free rate, because it sated as the best proxy for a riskless investment [51]. Market risk premium is the additional return an investor requires on top of the risk-free rent in order to make an investment. The risk premium is dependent on the total risk of the investment, higher risk results in higher risk premium. The return of the MSCI World Index is often referred to as the general market return, r_m, since it reflects the performance of large and mid-cap equities across 23 devolved markets [51]. The beta coefficient reflects the risk associated with an investment compared to the volatility of the general market. A beta value above one indicate that a stock has higher volatility than the general market, hence higher risk. The most widely applied way of estimating CAPM beta for a stock is by statistical regression [50].

2.7.5 Levelized Cost of Electricity

Levelized cost of electricity is a common way of presenting the cost of producing energy. This model considers the interest rate on the capital that was required to build the plant, total years of energy production, maintenance, and operational costs [42]. For wind power plants there is no fuel cost, which is one of the advantages for wind and solar power plants. But on the other side, the availability of the energy varies seasonally and with the weather. Equation (21) shows how to calculate the LCOE. The upper term calculates the NPV of total costs over the lifetime of the power plant, the denominator term calculates the total energy produced over the lifetime [42].

$$LCOE = \frac{\sum_{t=}^{T} \frac{(I_t + M_t)}{(1+r)^t}}{\sum_{t=0}^{T} \frac{E_t}{(1+r)^t}} \quad (21)$$

Where, I=initial cost of investment, M=maintenance and operations expenditures, E= total energy production during lifetime of the plant, r=discount rate (WACC), t=lifetime of the plant.

NVE has estimated the general cost of electricity (LCOE) for onshore wind power to 29,94 øre/kWh for 2021 [71]. This is based on the parameters given in table 1. In line with technology improvements NVE has estimated that the LCOE for on shore wind power can decrease to 22,15 øre/kWh in 2030 [71].

Table 1: Estimated LCOE in 2021 and 2030 by NVE. The table shows the distinct factors used to calculate the LCOE. For the estimates in 2030 it is used a technology improvement factor based on NVE's assumption on the development of the technology [71].

	LCOE (øre/kWh) 2021	LCOE (øre/kWh) 2030	Size (MW)	Investment costs (kr/kW)	(Rated power hours/ year)	Lifetime (year)	Operation and Maintainance cost (øre/kWh)	Degradiation rate (øre/kWh)
Onshore wind power	29.94	22.15	47 400	10 071	4 008	25	10	10 %

2.7.6 Net Present Value

Net Present Value is an economic evaluation method widely used to determine the absolute return of an investment. The method calculates the present value of the total cash flow generated through the lifetime of the project, see equation (22). This is done by calculating the yearly cash flow and apply a discount rate, in this case the WACC [41].

$$NPV = \sum_{t=0}^{T} \frac{CF}{(1+r)^t} \tag{22}$$

T=project lifetime, CF=cash flow, r= discount rate (WACC), t=number of periods

An investment decision can be done based on the results from the NPV analysis. If the NPV is above zero, it means that the project will generate a return which fulfill the requirements from lend holders and equity investors. If an investor can choose between two projects, the project with the highest NPV should be chosen. A project with negative NPV will return in net loss for the investors.

The method has some disadvantages that may affect the evaluation of the project. In the discount rate, WACC, the cost of capital remains the same trough the lifetime of the project. Through a 30-year period the cost of capital will varies dependent on the global economy and financial markets [41].

Internal rate of return

In addition to the NPV one can use the Internal Rate of Return (IRR) to find which discount rate that will give a NPV of zero. If the IRR is equal or higher than the discount rate, (the discount rate is represented by *r* in equation 23), the project will have a positive NPV [42]. The IRR can also be used as an indicator when considering several different investment opportunities. Where the project with the highest IRR would be the most profitable, but the risk factor of the investment should also be considered.

$$IRR = r \rightarrow NPV = 0 \tag{23}$$

3 Method

3.1 Site and time

Solberg is located at the south-eastern part of Senja, the second largest island in Norway, see figure 17. The terrain and topography surrounding Solberg is illustrated at different scales in both figure 17 and 18. Solberg was chosen based on its interesting location, with open fjords in the South-West (SW), high mountains in the West, its proximity to established infrastructure and energy end users. The elevation in the area differs between 250 and 400 meter above sea level (masl). In the SW part of Solberg, the elevation is 400masl before the elevation gradually decreases towards the North-West. Steep mountain ridges with a height of almost 1000masl, are located 25km West for Solberg. In the SW, Solbergfjorden and Vågsfjorden form an 70km long open passage towards Harstad. In the East, a large valley formation stretches from Sørreisa up to Øverbygd. The largest cities in northern Norway is added on the map to show the distance between Solberg and the areas with largest population, see figure 17.

The vegetation above 300masl consist mainly of heathland with some sporadic birch trees. Some smaller lakes are also located 300m above sea level in the area of the wind farm. Below 300m the forest get gradually denser. There is one dirt road established in the area, which is marked in figure 18. This road goes all the way up to a radio mast marked by the yellow star in figure 19.

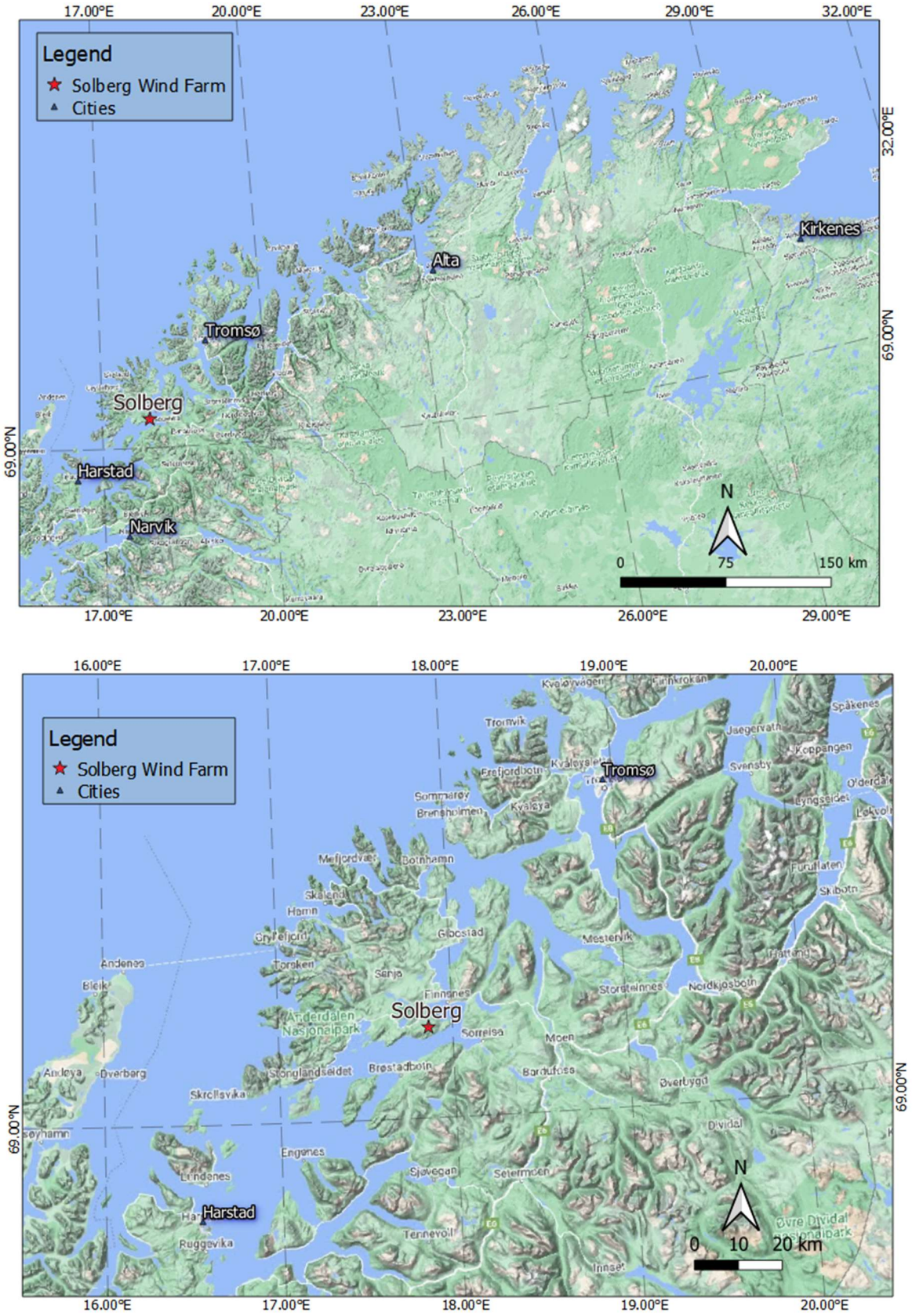

Figure 17: Overview images showing the locations of the wind farm relatively to the largest cities in northern Norway. Solberg is located at the eastern side of the Senja island.

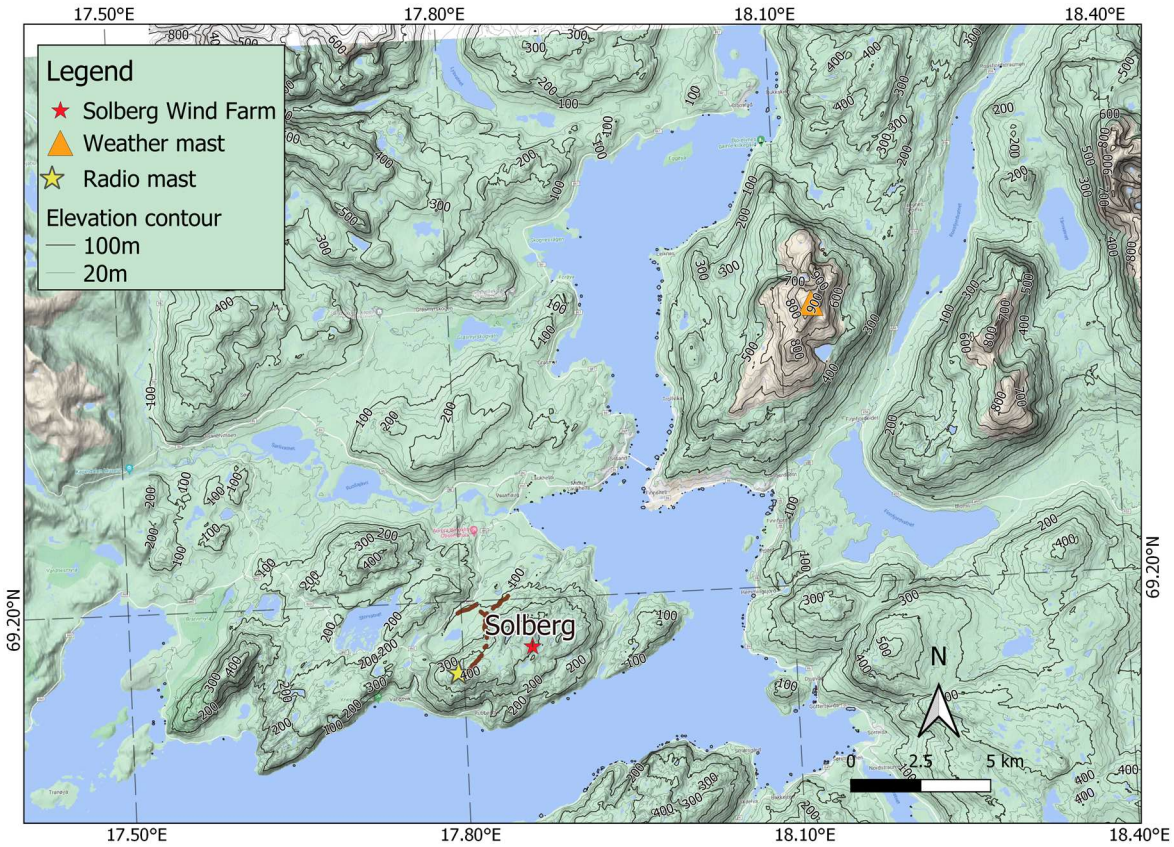

Figure 18: Overview over Solberg. Elevation curves are added to describe the topography.

3.1.1 Terrain complexity

The terrain around Solberg can be described as complex due to high and steep mountains in the vicinity. The terrain complexity is described by a RIX value in the following report by NVE [43], shown in figure 19. The RIX value indicates how large percentage of the surrounding terrain with a radius of 2km that has a terrain slope steeper than 30 degrees. A high RIX value indicate that the area is surrounded by steep terrain, hence a more complex terrain. At Solberg, the SW parts of the farm, including turbine w1, w2, w3 and w4, see figure 20 for turbine placement, lays in an area with RIX values between 10-20%. The remaining turbines are place in an area with RIX values between 5-10%.

Higher terrain complexity and steep terrain can in general cause more turbulence, which is negative for energy production. These phenomena's can be underestimated in the WRF model due to the terrain smoothing as mentioned in section 2.3.

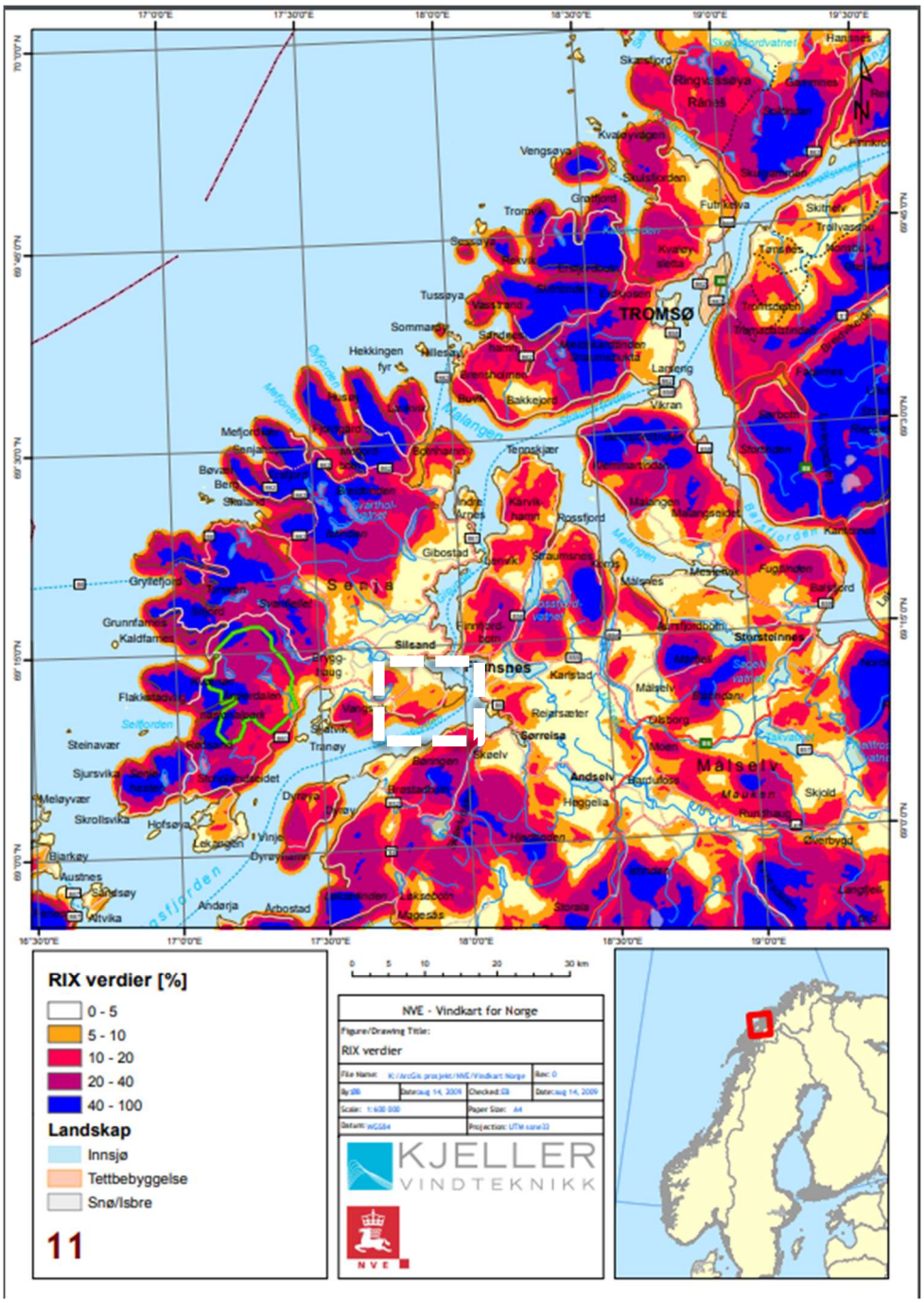

Figure 19: Overview over RIX values at Senja and Solberg. Higher RIX values indicate a more complex terrain [43].

3.1.2 Wind turbine placement

The wind turbines are placed at Solberg with the following criteria: The distance between each turbine in the same row must be at least three times the rotor diameter, and the distance between each row must be at least five times the rotor diameter. The rotor diameter is 162m, resulting in 486m between each turbine and 810m between each row. It is important to comply with these criteria to limit the drag and wake effect in the wind farm. In addition, no turbine can be placed closer than 800m from a house. These criteria are acquired from person with experience from projecting wind power plants. The location of the wind turbines is presented in figure 20.

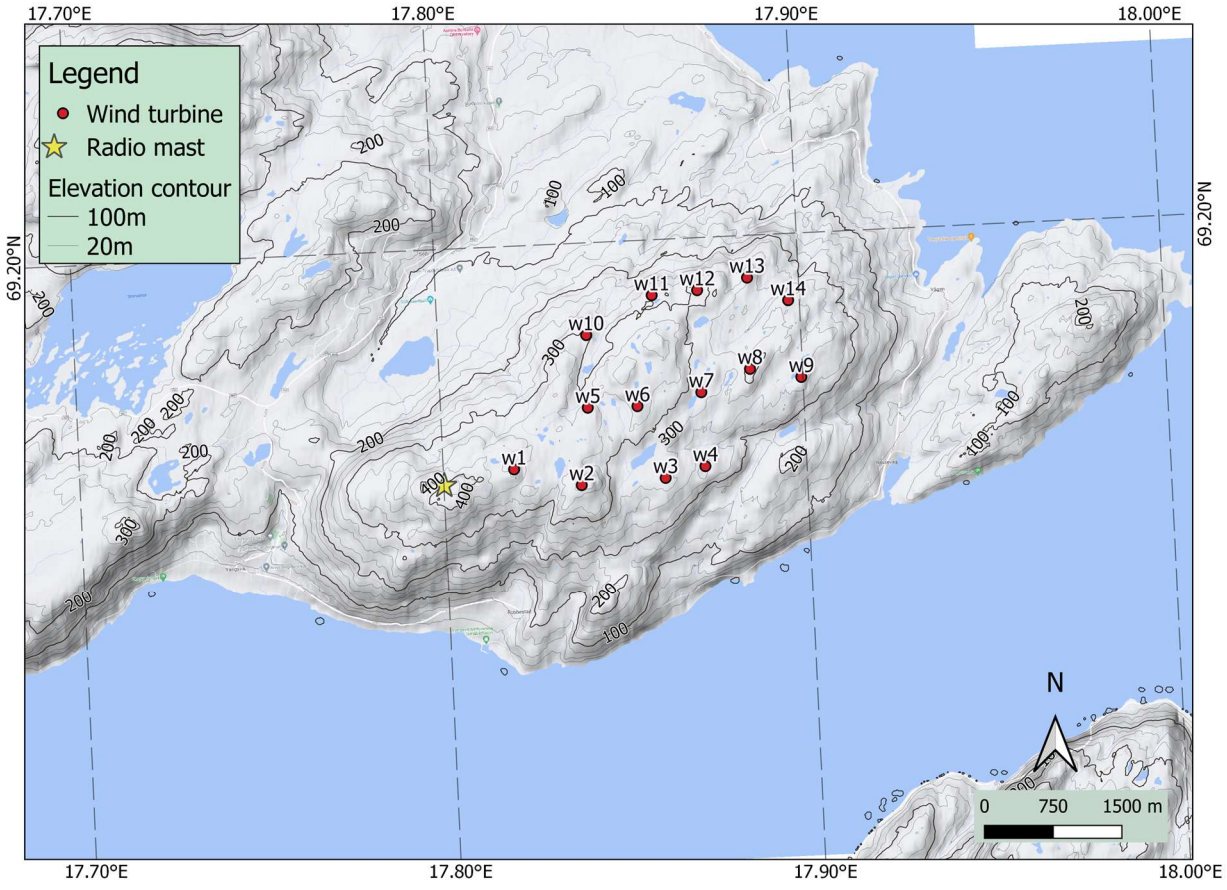

Figure 20: Wind turbine placement at Solberg wind farm. There are 14 turbines with a total installed capacity of 84MW.

3.2 Sources of data

3.2.1 Input weather data

ERA-interim data is a global reanalyzed data set obtained from the European Center for Medium-Range Weather Forecasting (ECMWF), covering the period from 1979 to present time [44]. The reanalyzed data is obtained by assimilating present and historical observation data into a global weather prediction model. The real observation data is mainly obtained from weather stations and measurements from satellites. The data set has a resolution of approximately 80 kilometers horizontally and has 60 vertical levels from the surface and up to 0.1 hPa, which is approximately a resolution of 40km vertically [44]. For this thesis, the ERA-Interim data set from 2016 is used.

3.3 The Weather Research and Forecasting model

In this thesis a Numerical Weather Prediction system (NWP) called: WRF was used to map the wind resources at Solberg. The Advanced Research WRF (ARW) modelling system was applied, which is a state-of-the-art atmospheric simulation model designed for both atmospheric research and mesoscale weather forecasting [10] [11]. The model can be used in a broad filed of applications and is flexible to be used for a large range of different scales. Spatial resolution of the out-put data and a large scale of parameters can be defined by the user. Since the WRF model is open source, it is used by researchers in several Universities, which also contribute with modifications and new schemes. ERA-Interim data is used as input data for the WRF-simulations. Currently, the Mesoscale and Microscale Meteorology Division of NCAR are supporting and maintaining a broad range of the WRF code [45].

Using a WRF model is a convenient method to map the wind resources over an area in the early stage of a survey. The model can return a wide spectre of different variables like, e.g, wind speed and direction at different hights, turbulence, solar irradiation, pressure, precipitation, and temperature. Dependent on the resolution and the available computing power, a one-year simulation can be done in just a few hours. This will give an indication on the wind resources much faster than from a weather mast, which will need one year to gather enough data to map seasonal variations.

The wind resource assessment in this thesis was based on the year 2016. The data from the WRF-simulation returned wind speed and direction data every 10minutes throughout the year. Only hourly data was available from the weather mast during 2016.

In this thesis two high resolution WRF models was simulated. This requires large computational resources, and the simulation was therefore run on FRAM, a national high-performance computing resource run by Sigma2 and available through UiT, The Arctic University of Norway [12]. On FRAM the simulation can be run on several nodes simultaneous, resulting in much faster running time.

WRF - Preprocessing system

The WRF-model need two types of external data sources to run the preprocessing system, static geographical data, and metrological data. As mentioned earlier, ERA-Interim data is used as the metrological input data for the simulation. To run the WRF-Preprocessing System (WPS), specific information about the case must be defined in the *namelist.wps* file. This includes information about time, area of interest, number of domains, spatial resolution, and the projection. The input data, like initial- and boundary conditions is then adapted to the time and area of the simulation specified in the *namelist.wps*.

Figure 21 is a chart flow describing the different steps of the WRF model. After the *namelist.wps* and the external data sources are available, a set of three programs called, geogrid, unigrib and metgird will be completed. These programs will use the information defined in the *namelist.wps* to produce *met* files. The *met* files are the out-put from the WPS and is used as input in the real WRF-simulation.

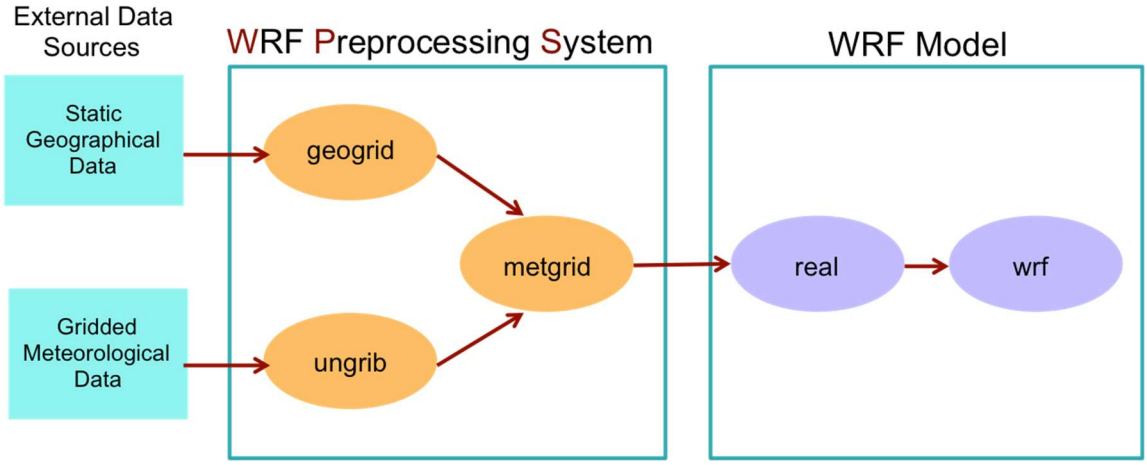

Figure 21: Flow chart of the WRF model. The WPS step need geographical and metrological data as input and return real.exe files as out-put files, which are used as input files in the real WRF-simulation [72].

Geogrid

The coarse domain and nested domains of the model is defined in the "geogrid" section. The number of domains, resolution and parent grid ratio is defined by the user in the *namelist.wps* file. The goal of the section is to interpolate terrestrial data to match the model grid resolution at every grid point. The geogrid program will interpolate terrestrial data like terrain elevation, landuse, soil temperature, monthly vegetation friction, monthly albedo, and slope category and make a static landscape model. These parameters are time-invariant and are downloaded through a Geographical Static Data Downloads page [46]. The default terrestrial fields are often enough to interpolate the categorical fields to the simulation domain. Additional data sets may be interpolated to the simulation domain, this is defined in the GEOGRID.TBL. The landscape does not change often, so the geogrid is usually only run once.

Ungrib

The unigrib program extracts time-varying metrological fields from GRIB-formatted files. Before the GRIB files can be used in the WRF-simulation they are "ungribbed" and rewritten in a simpler format called intermediate format. Variable tables are used to identify the correct field and identify correct levels and variables in the GRIB file. In these simulations, the ERA-interim data set was used as input data for the unigrib program.

Metgrid

The metgrid uses the output data from the geogrid and ungrid programs as input files. The metrological data from the ungrib program is horizontally interpolated onto the static landscape model defined in the geogrib program. The real WRF-simulation will use these interpolated metgrid files as input files. The metgrid program is time-dependent like the ungrib program.

Weather Research and Forecasting model

WRF – namelist

From the *namelist.input* file the WRF program read specified parameters that defines the configuration of the simulation, much like in the WPS namelist. The *namelist.input* have a more complex configuration, where boundary conditions and physical options can be modified based on the desired simulation. Time and dates, nesting domains and domain size need to match the *namelist.wps*. However, there is a flexibility to run simulations for shorter time periods as long it is inside the time-period defined in the WPS. One can also run the simulation for only the outermost domain. If high resolution is not a necessity, this will save a large amount of computing power and time.

Domain and nesting

For the WRF-simulations in this thesis, 3 domains with a parent grid ratio of 1:5 was used. The resolution of the different domains was:

- D01: dx = 25 000m, dy = 25 000m
- D02: dx = 5 000m , dy = 5 000m
- D03: dx = 1 000m , dy = 1 000m

The outermost domain, d01, has resolution of 25km, the second domain, d02, has a resolution of 5km and the innermost domain, d03, has a resolution of 1km. This set up gives both a wide overview of the overall weather situation in d01 and a finer and more detailed overview in the area around the wind farm.

Figure 22 shows the domain configuration, where Solberg is marked by a red dot. This type of configuration is often called *telescoping* domains. In this set up the finer domain will get its initial values and boundary values from the larger domain enclosing the small domain. In general, it is desirable to avoid "cutting" trough lateral boundaries and important topography at the edges of the domain, mainly to improve the performance of the model.

In figure 22 Solberg is located in the lower left corner of the d03. It was prioritized to include the Lyngen Alps in d03, due to its known impact on the local weather system. This is the reason why Solberg is not placed in the centre of d03, but in the lower left corner.

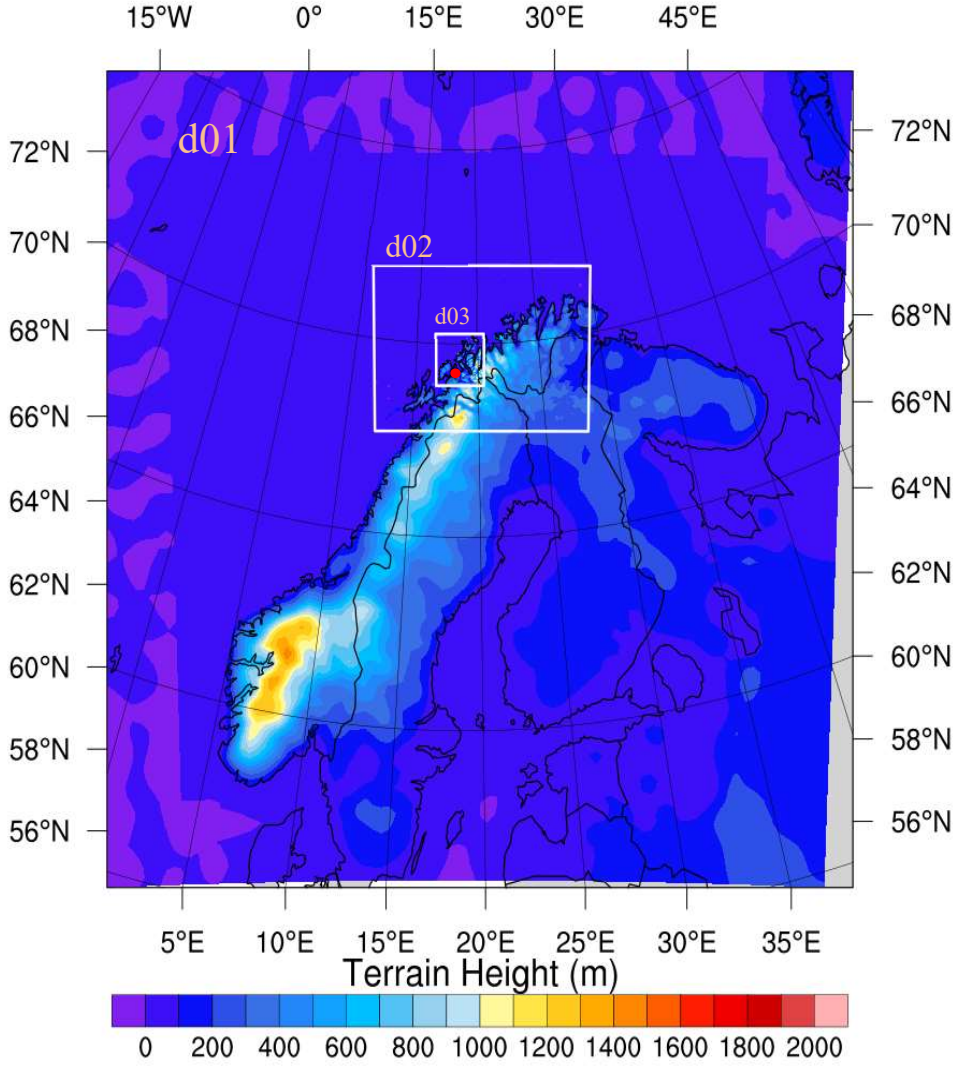

Figure 22: WPS Domain configuration for the WRF-model. Solberg is marked with a red dot.

Model height and terrain smoothing

Figure 23 shows two different plots of the terrain height in the innermost domain of the WRF-model. In the figure to the left all terrain under 25m is colored with blue. In the figure to the right, all areas with green color are land with elevation in the WRF-model. Large parts of Lyngsfjorden at the edge of the image is almost completely green. Meaning that this area has got false elevation in the model. Finer resolution will result in less smoothing but will also increases the need of computing power. Mapping wind resource in areas close to steep mountain ridges is therefore a complex task since the terrain is smoothed and it is hard to recreate "real" wind phenomena.

Another factor of terrain smoothing is that the model elevation at Solberg is lower than in the real terrain. Therefore, the wind turbines placed in the WRF simulation will be placed on a lower elevation.

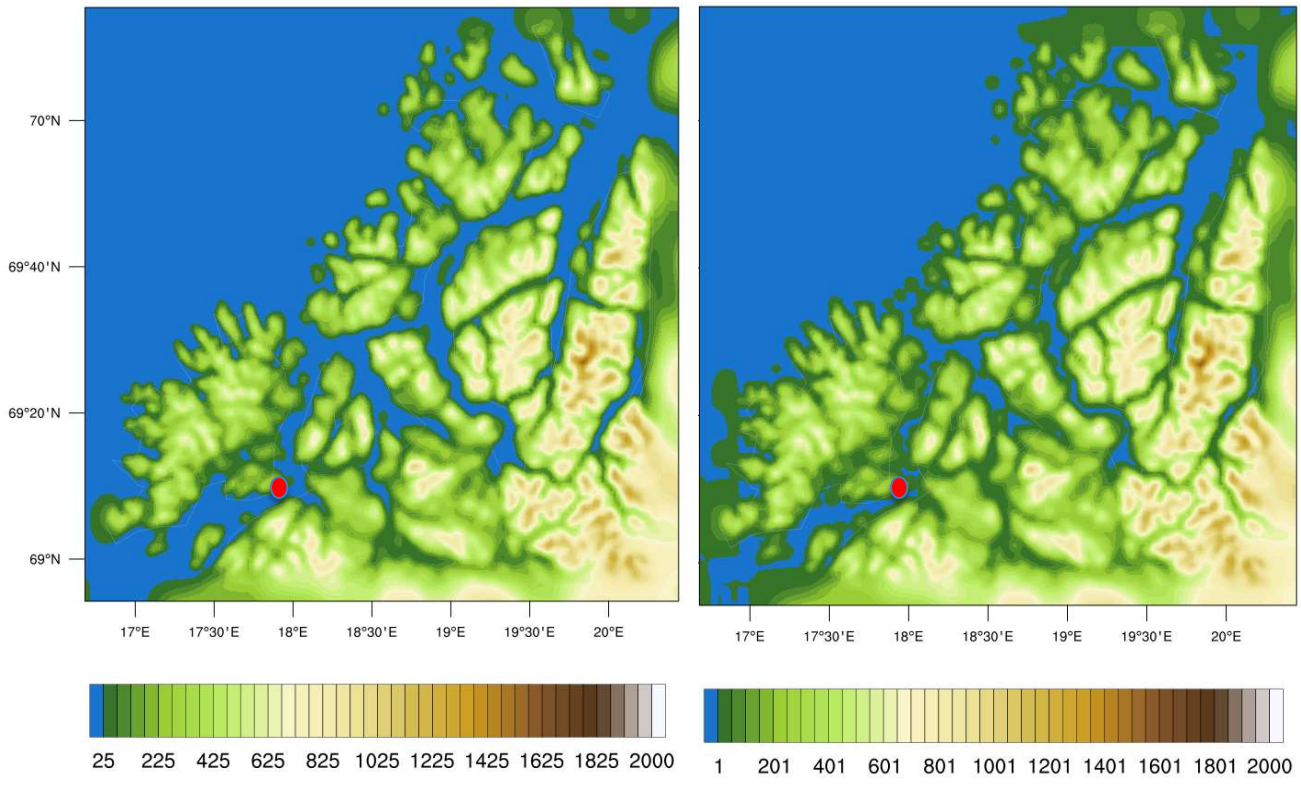

Figure 23: Model terrain height (meter) in domain 3. Solberg is marked with a red dot. The left image sets all terrain under 25m as ocean. In the right image all areas that has a green colour is "seen" as land with elevation in the model. One can see that ocean areas outside Senja has been a part "land". This is due to terrain smoothing in the WRF-model.

Real

In the “Real” program the metgrid files from the WPS is vertically interpolated to the model grid levels and create two files that provides the final initial conditions and boundary layer. These two files are the input data for the real WRF simulation.

Wind turbine schemes

In this thesis two WRF-simulations have been completed over the same area with the same spatial resolution set-up; 25km-5km-1km. The only difference is that in the second simulation, all fourteen wind turbines was placed out in the terrain to simulate the drag and wake effects in the wind farm. The position of each turbine was defined in a separate scheme, called *windturbines.txt*. A wind turbine drag parameterization scheme, called *wind-turbine-1.tbl,* was also added. This scheme contained information about the power curve, hub height, standing trust coefficient, diameter of the rotor and nominal power of the wind turbine [70]. The parameterization scheme was activated in the physics section of the namelist.input.

The kinetic energy extracted from the wind by the turbine is based on the thrust coefficient of the turbine and is a function of wind speed. It is not recommended to run the simulation at a resolution higher than 5 times the rotor diameter, because then the rotor blades could be divided in different grid cells [70]

Post processing

The output files from the WRF-simulation are in NetCDF format, which is a standard format for sharing scientific. The file contains all the simulation variable and is accessible by computers with different ways of storing integers, floating-point-numbers, and characters. Analysis of the data can be done in NCL, Python or MATLAB. In this thesis NCL scripts was used to extract the desirable data and reducing the file size, before further analysis in Python.

3.4 Estimating energy production

The energy production from the wind farm was estimated in two different ways based on two different simulations. Both simulations had the exact same time, domain configuration and resolution. The first simulation was a clean simulation, which means there was no turbines placed out in the terrain. Therefore, the energy production needed to be calculated in python, by applying the power curve on the time series containing the wind speed values. In the second simulation the wind turbine scheme was activated, and estimated energy production was a part of the WRF output file. All wind speed data and energy estimations are done at hub height, 125m above ground level at each location.

As mentioned in section 2.5, the net output from a wind turbine is usually estimated to be 10-15% under the estimated energy production from the power curve [41]. After consulting with people working in the wind energy industry, a total loss factor of 15% was used in this preliminary assessment. This includes loss factors like, wake, ice and maintenance.

3.4.1 Wind turbine

A Vestas wind turbine with a nominal capacity of 6MW was used in this thesis. The turbine has a rotor diameter of 162m and a hub height of 125m. The cut in speed is at 3 m/s and cut off speed at 24 m/s as illustrated by the red lines in figure 24. The turbine produces at rated power in the interval between 12,5m/ and 17,5 m/s and the turbine will gradually decline its production before reaching cut-off speed. A cut-off of strategy like this are called High Wind Ride Trough (HWRT). This stabilizes the energy production at higher wind speed and contribute to a softer cut off strategy. In the following study [73], it was found that a HWRT system increased the power out-put from a wind turbine compared to a turbine without. The main reason for this result, was that the turbine with the HWRT system was operational during a longer period, resulting in higher energy production.

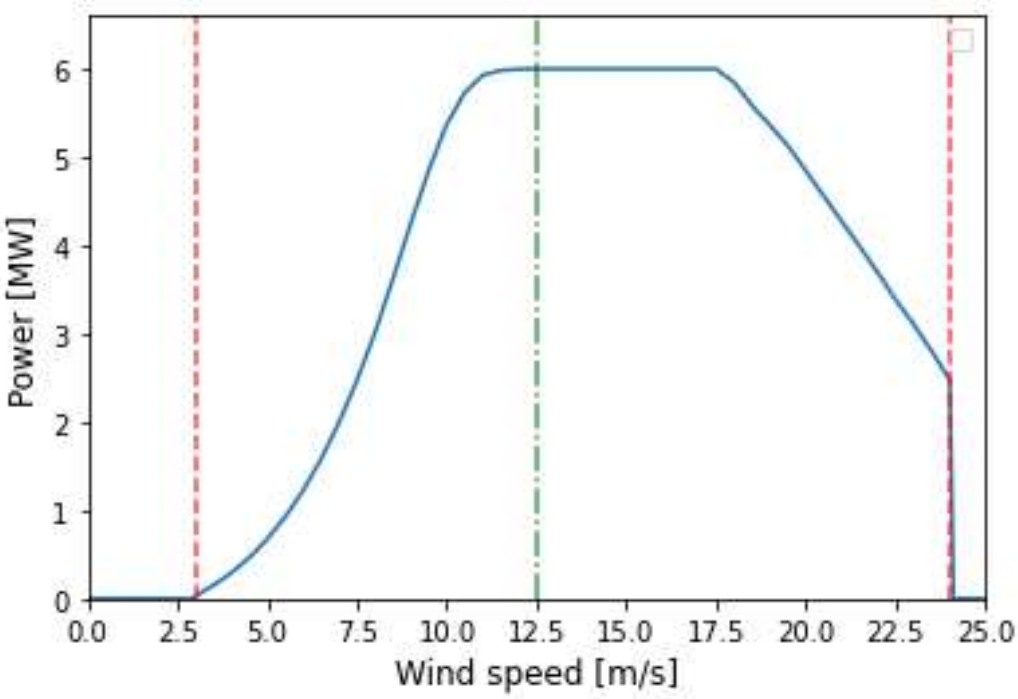

Figure 24: Power curve for a Vestas V162 wind turbine. Cut in speed at 3 m/s, cut off at 24 m/s and rated power at 12,5 m/s and 17,5 m/s. Approximate power curve for the V162, provided by the wind energy industry contact.

3.4.2 Wind energy estimations

First, the energy production was estimated from the clean WRF-simulation. This was done by extracting wind speed data at hub height, 125 meter above ground level, at all turbine locations. To get the correct wind speed at 125magl, a vertical interpolation was done from the horizontally interpolated wind data. Due to the interpolation, all the wind speed series are unique, which makes it possible to discover wind speed variations within the wind farm. This can be used to optimize the placement of the wind turbines. Since no wind turbines was placed out in the model, there was a free stream wind distribution over the wind Solberg in this simulation.

The WRF output file returned wind speed as u and v components, so to get the horizontal wind speed, equation (5) was applied. For the clean simulation, the WRF model returned data values for every 10-minutes through the year. Average wind speed for every hour was calculated since it is more convenient when estimating energy production in (GWh). Finally, the power curve shown in figure 24 was applied on the time series. The power curve holds power production values for every 0.5m/s increase in wind speed. To get an exact power production estimate, the wind speed was interpolated with the power curve.

The estimated power production directly from the power curve was scaled down by 15%. As mentioned earlier, this was done to ger the net energy output from the turbine after losses.

3.4.3 Wind energy estimations from WRF

By activating the wind turbine scheme, the output data from the WRF-simulation returned a variable called “POWER”. This variable stores the energy production values from the wind turbines. If several wind turbines are placed inside the same grid cell, the energy production is added together. By using Ncview, NCAR command language, one can find out how many turbines that are in each grid cell by investigating the “POWER” output data. Figure 25 illustrate 8 grid cells with a different colour than blue, indicating that there was power production in 8 cells. The 14 turbines are therefore distributed inside these cells.

The disadvantage with this method, is that all turbines placed in the same are estimated to produce the exact same amount of power. It is therefore difficult to use this data to optimize wind turbine placement on a fine scale, since all locations in the same cell will return the same amount of power. The advantage is that wake and drag effects is considered in the power output date.

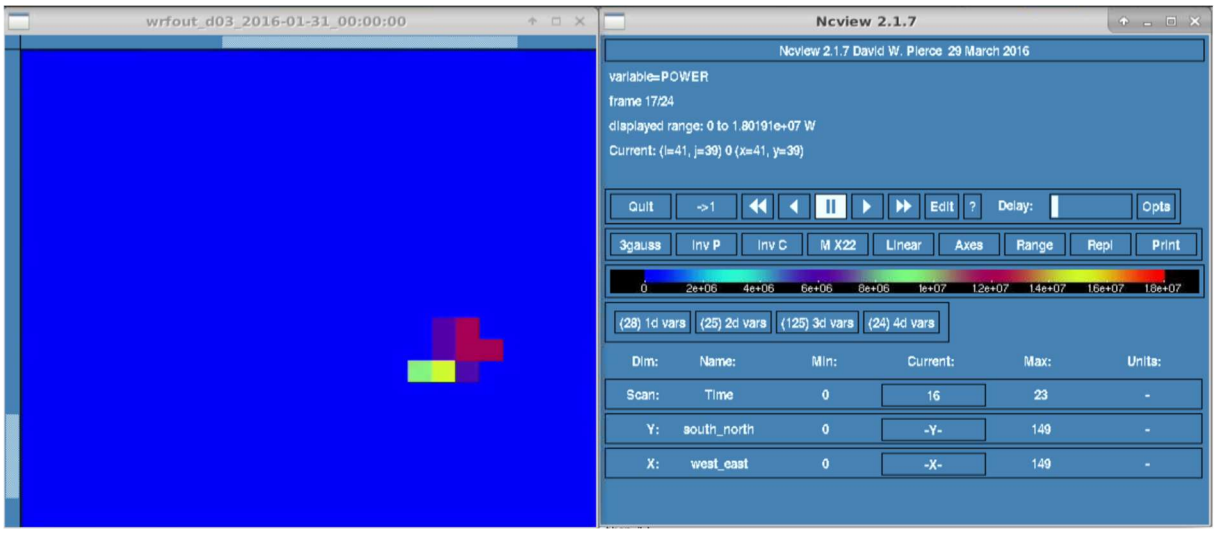

Figure 25: Energy production estimated from the WRF-simulation. Eight cells have a different colour than blue, indicating that all the fourteen wind turbines are placed inside these cells. If several wind turbines are placed inside the same cell, the WRF simulation will return the total power production inside each cell. This limits the possibility to optimize turbine placement within the cell, because the turbine will produce the exact same power at all locations inside the cell.

3.4.4 Wind energy production during simulation year

In this thesis the WRF-simulations are only simulating the weather and wind situation during 2016. As a result, the yearly estimated energy production only reflects the potential energy production back in 2016 at Solberg. Every years have some variation in terms of weather and wind conditions, it's therefore relevant to compare how the wind situation was in 2016 compared to mean wind situation over a longer period.

The NVE report "Vindkraft- produksjon 2016" describes how the wind speed statistics were in 2016 and how wind power plants in Norway performed in terms of energy production compare to a reference period [47]. The average wind speed during the reference period is used to set normal values for mean wind speed and energy production. The mean values are weighted based on installed capacity at the different wind farms. Figure 26 illustrate mean wind speed deviation in percentage in 2016 compared to the reference period. All areas covered with a blue tone had lower mean wind speed in 2016 than what one can expect from a normal year. The South-Eastern part of Norway was the only area with higher wind speed than the reference period. In total, mean wind speed was 94,9% at the wind power plants compared to the reference index. Which means that the mean wind speed in 2016 was 5,1% lower than what one can expect from a average year.

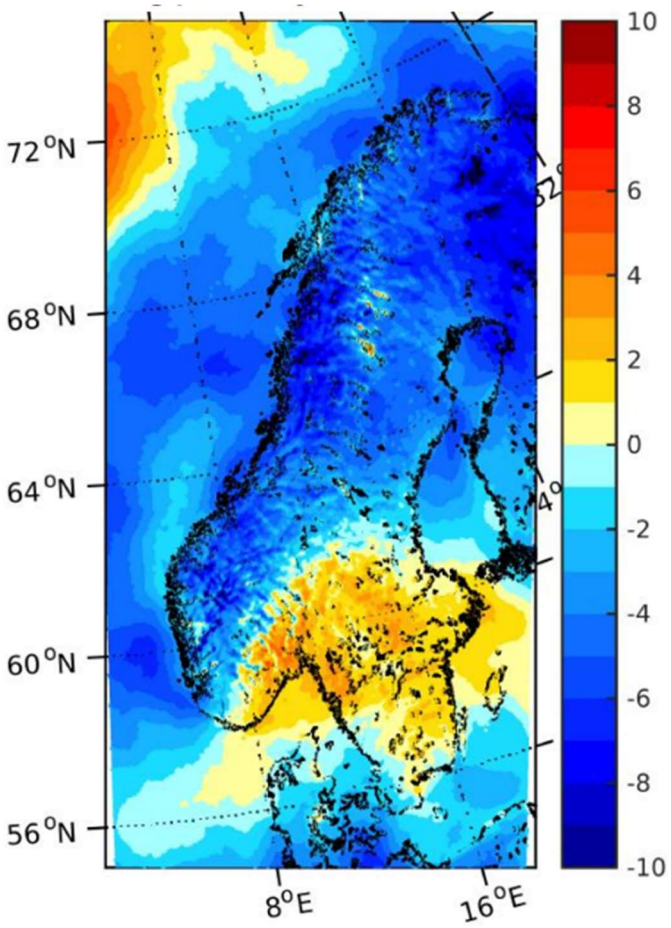

Figure 26: Deviation in mean wind speed given in percentage from 2016 compared with the reference period between 2000-2015 [47].

As a result of lower wind speed than normal in 2016, wind energy production was also lower than normal. For Norwegian wind energy plants, the energy production index was 92% in 2016, which means that the plants produced in average 8% less than what one could expect [47]. Since 2016 was a year with lower mean wind speed and energy production than normally, the estimated energy production from the WRF-simulations will be in the lower range of what we can expect. A wind power plant can operate for 25-30 years dependent on the given concession, so to use an energy production estimate that is in the lower part of the production range will have large impact on the economic part of the project. It would therefore be relevant to make an adjusted energy production estimate, which is scaled up to match the average yearly energy production.

Energy production for wind farms in northern Norway during simulation year

Since Solberg is located at Senja it is relevant to see how wind parks in northern Norway performed during 2016 and use this as a basis for the energy production adjustment. Figure 27 shows the locations of the different wind farms in northern Norway.

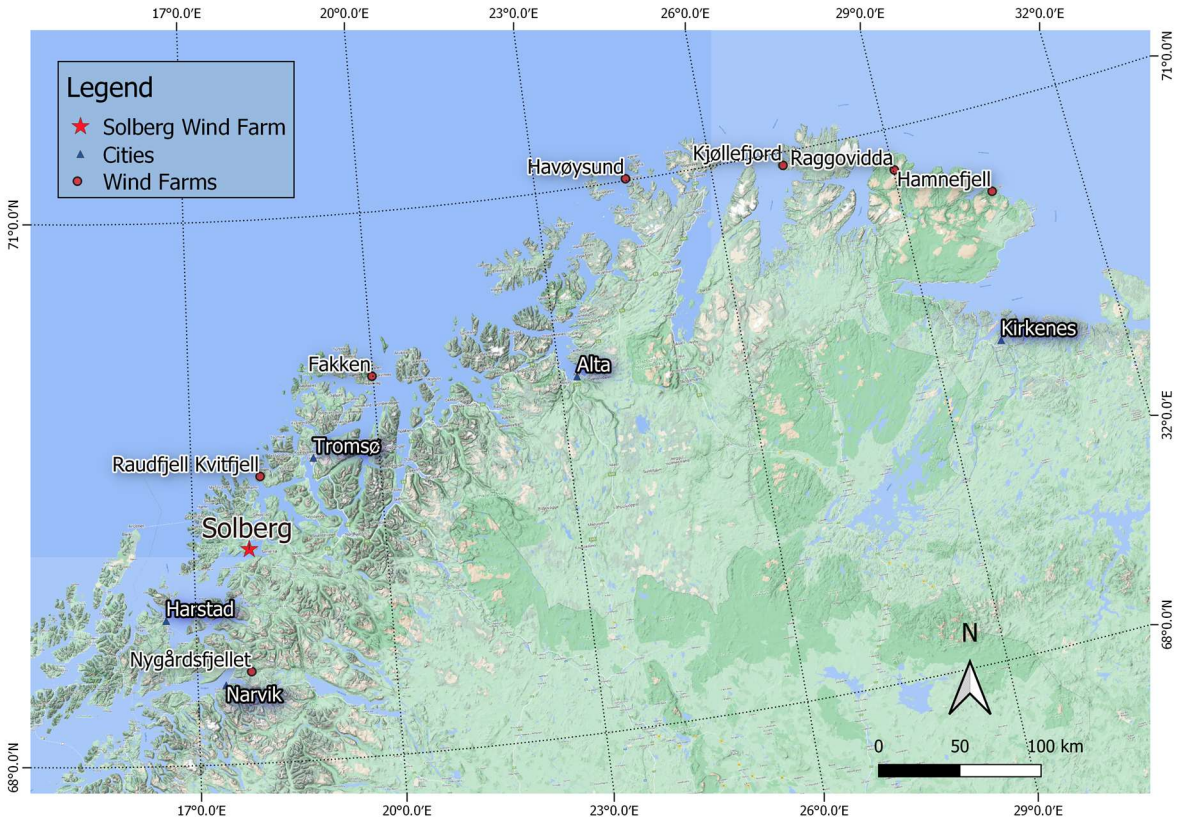

Figure 27: Overview over wind farms in northern Norway.

Table 2 shows the wind and production index for some selected wind parks that was operational in northern Norway in 2016. In general, wind power plants in northern Norway had higher wind and production index than the weighted average throughout Norway in 2016. At Andøya there is only one wind turbine, hence it is not relevant to use this as a basis for comparison to Solberg, when adjusting energy production, because there would not be any wake loss appearing at Andøya.

Nygårdsfjellet and Fakken is located 75km North and 131km South-East for Solberg, respectively. They have a similar production volume to what we can expect at Solberg, with a yearly production of 139GWh and 104GWh during ab average year [47]. Therefore, a combination of the production index data from these three wind farms are most suitable to use when adjusting the energy production from the WRF-simulation. Be aware that Raudfjell and Kvitfjell wind farm started operation in 2020, hence no production data to use for 2016.

Table 2: Selected wind farms in northern Norway. Showing wind index and production index in 2016 compared to reference period (2000-2015) [47]

Wind park	Wind index [%]	Production index [%]	Approx. distance from Solberg [km]
Andøya	96.80	95.50	67
Nygårdsfjellet	95.00	93.70	75
Fakken	95.30	94.10	131
Kjøllefjord	95.20	93.50	407
Havøygavelen	95.50	92.10	327
Raggovidda	93.50	94.10	463

Wind speed and energy production adjustment

Wind and production index data from Fakken and Nygårdsfjellet are used as basis for the energy adjustment on the out-put data from the WRF-simulation. Fakken and Nygårdsfjellet had an energy production of 6,3% and 5,9% below the reference period in 2016, respectively. For Solberg wind farm, a conservative upscaling factor of 5% will be used on the energy production to reflect the energy production during an average year. It is the adjusted energy production that will be used in the economic analysis.

3.5 Economic assessment

The estimated energy production returned directly from the WRF-simulation was used in the economic assessment, because it considers important factors like wake and drag effects. The production data was used to calculate yearly income based on the estimated electricity prices during the lifetime of the project. Key figures related to capital CAPEX and OPEX was obtained from a person working with experience from the wind energy industry. An overview of the NPV calculations for the 5 first years are shown in appendix C. This illustrates the setup used to produce the results.

3.5.1 Capital expenditure

The CAPEX can be divided into sub-segments, as shown in table 3. Civil BoP include costs related to roads and draining, turbine foundation, cable trenches, crane pads, metrological masts, and buildings for electrical switch gear. The electrical BoP include costs related to underground cable networks, switch gear to disconnect turbines from the system, connections to control rooms and connection cables to feed the power from the wind turbines into the grid system. In this thesis an additional cost off 200MNOK is added to connect the wind farm to the external grid. Project and construction management are cost related to the technical execution of the project. It includes among other things, micrositing of turbine placement to maximize energy production and detailed plan for the construction phase. Unforeseen costs are added as a buffer to cover unexpected costs.

Table 3: Overview over CAPEX costs in MNOK. This table reflect the CAPEX cost for the base scenario where 1EUR costs 10NOK.

CAPEX			
Investment budget; 14 turbines @ 6 MW	**#**	**%**	**MNOK**
Vestas Turbines 6 MW	14	56.3 %	630.00
Civil BoP		11.7 %	131.04
Electrical BoP		7.8 %	87.36
Project/construction managment		2.3 %	26.21
Financial cost during construction		1.6 %	17.47
Unforseen		2.3 %	26.21
Investment cost		82.1 %	**918.29**
External grid connection		17.9 %	200.00
Total CAPEX		100.0 %	**1 118.29**

Expecting Increased investment cost for onshore wind

Figure 28 shows the CAPEX trends for onshore wind from between 2015 and 2023, required from IEA's latest renewable energy market update [63]. Numbers for 2022 and 2023 are based on estimates for new contracted projects started under the current high commodity prices. From 2015 to 2020, the CAPEX for onshore wind felt by approximately 20% and solar PV 50%. Compared to 2020 levels CAPEX for onshore wind is estimated to increase by 25% in 2023. The main reason is due to high commodity prices and shortage of metals and minerals. Russia is major supplier of metals and minerals, which are critical for the clean energy transition. As the international community isolate Russia and limits their export of commodities, the commodity market is under strong pressure [57].

As shown in figure 15, CAPEX is traditionally high for renewable power plants. An additional increase of 25% would have a sizeable negative impact on the profitability of wind farm projects. Scenarios with increased CAPEX cost will be shown in the sensitivity analysis.

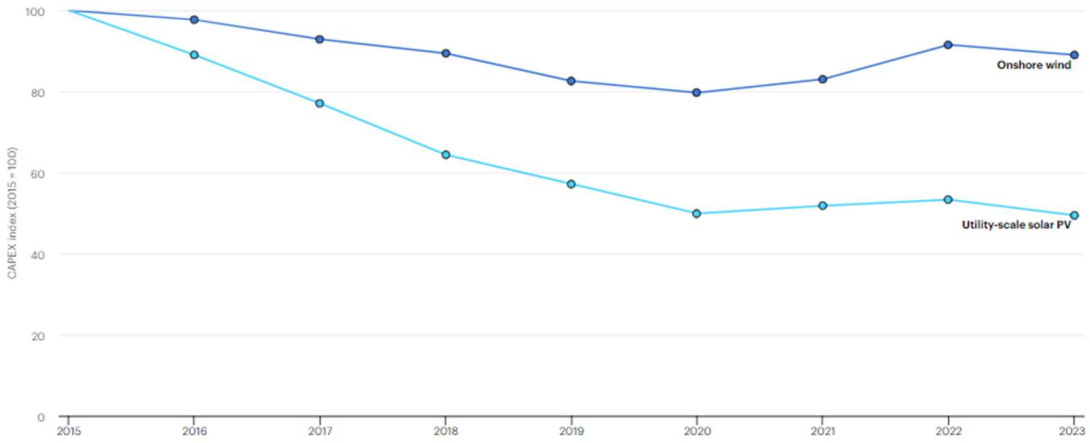

Figure 28: CAPEX development for onshore wind and solar PV. The investment costs felt from 2015 to 2020 with approximately 50% and 20% for solar PV and onshore wind, respectively. In 2023 the CAPEX for onshore wind is expected to increase with 25% compared 2020 [63].

3.5.2 Operational expenses

OPEX is all costs related to the operation and maintenance of the wind farm, see table 4. Costs like land rent and grid rent varies with energy production and gross income. Turbine O&M and technical management costs in table 4 reflect the cost in year one of operation. These costs will be adjusted with an inflation factor of 2% very year in the base case of the project. Insurance and property tax is paid as a percentage of total capex and the value of the property, respectively. The valuation of the land is sat to 52,63 MEUR. In addition, an OPEX buffer cost with a magnitude of 5% of the total OPEX is added to cover unforeseen costs.

Table 4: Overview over all costs related to the operation of the wind farm. The yearly OPEX costs will vary dependent on yearly energy production and the cost related to turbine O&M and technical management will have a yearly inflation adjustment. The numbers shown in table 3 is therefore the cost for the first production year.

OPEX	
Yearly operational costs	
Turbine O&M [MEUR/ turbine]	0.05
Land rent [% of brutto income]	4.00 %
Grid rent [kr/GWh]	30 000
Property tax [% of CAPEX basis for property tax]	0.70 %
Capex basis for property tax [MEUR]	52.63
Insurence [% of capex]	0.07 %
Technical managment [MEUR/ MW]	0.002
Opex buffer [% of opex]	5.00 %

4 Results and discussion

4.1 Wind resources

This section will present the results related to wind speed and wind direction at Solberg. All wind data presented shows the wind conditions at 125m above ground level (magl) with a resolution of 1km. The height of 125magl is chosen to illustrate the wind conditions at the turbine's hub height.

4.1.1 Wind speed

Figure 29 shows the average wind speed at 125m above ground level in 2016 over large parts of Troms County. The height corresponds to the hub height of the turbine and illustrate the wind resources in 2016. The map is based on d03-data from the WRF-simulation, with a resolution of 1km. The dark blue areas indicate low average wind speed and orange to red color illustrate high average wind speeds up to 12m/s. It is evident that mountain tops in general have higher average wind speed than low-laying areas. In addition, coastal areas show signs of having higher average wind speeds compared to inland area. Based on figure 29, the average wind speed at Solberg was in the range between 7-8m/s in 2016.

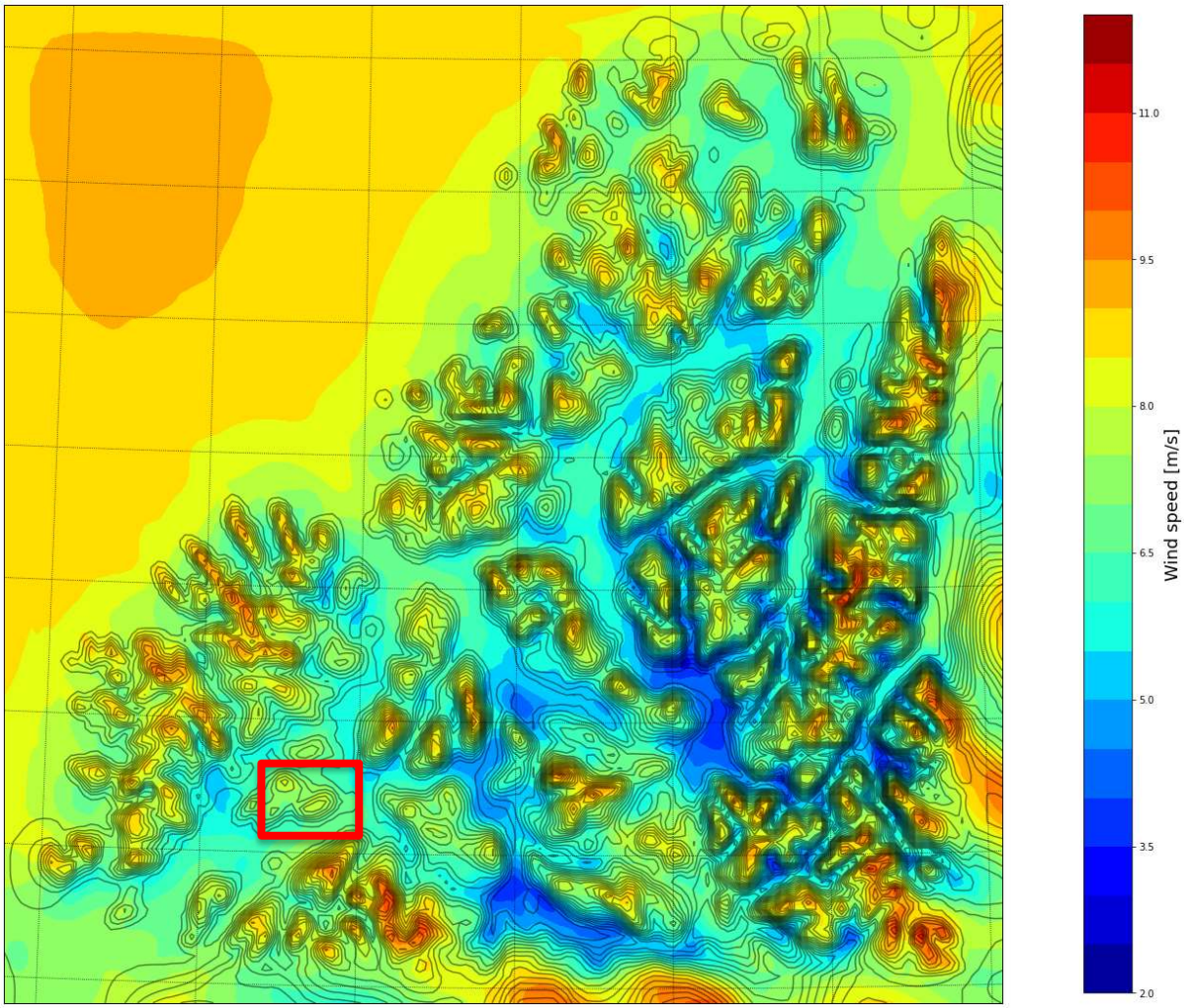

Figure 29: Average wind speed at 125 meter above ground level in 2016. The map shows the innermost domain, d03, with a resolution of 1km from the WRF-simulation. Solberg is located inside the red box.

Wind speeds at Solberg wind farm

The average wind speed for the whole wind farm was estimated to 7.47 m/s in 2016. The blue line in figure 30 shows the average wind speed for the whole wind farm for every 10minute. The red line shows the weekly average wind speed. From the figure one gets an indication of the seasonal wind speed variation with higher wind speed during the winter months.

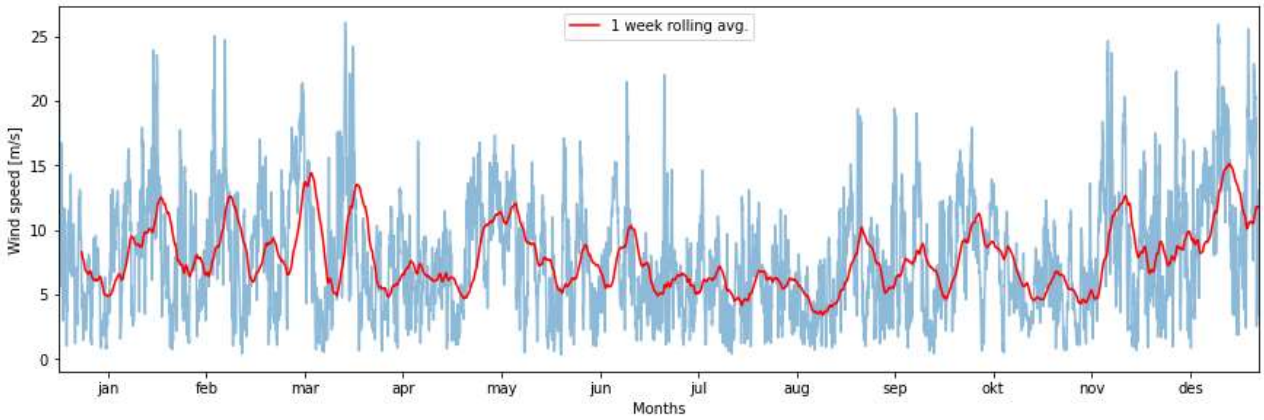

Figure 30: The blue line shows the average wind speed at all the turbines every 10 minutes during the simulation year, 2016. The red line shows weekly average wind speed across all the turbine locations. This visual the seasonal variations, with higher wind speed during the winter and lower wind speed in the summer months. The months tickets on the x-axis are placed in the middle of each month, approximately the 15th every month.

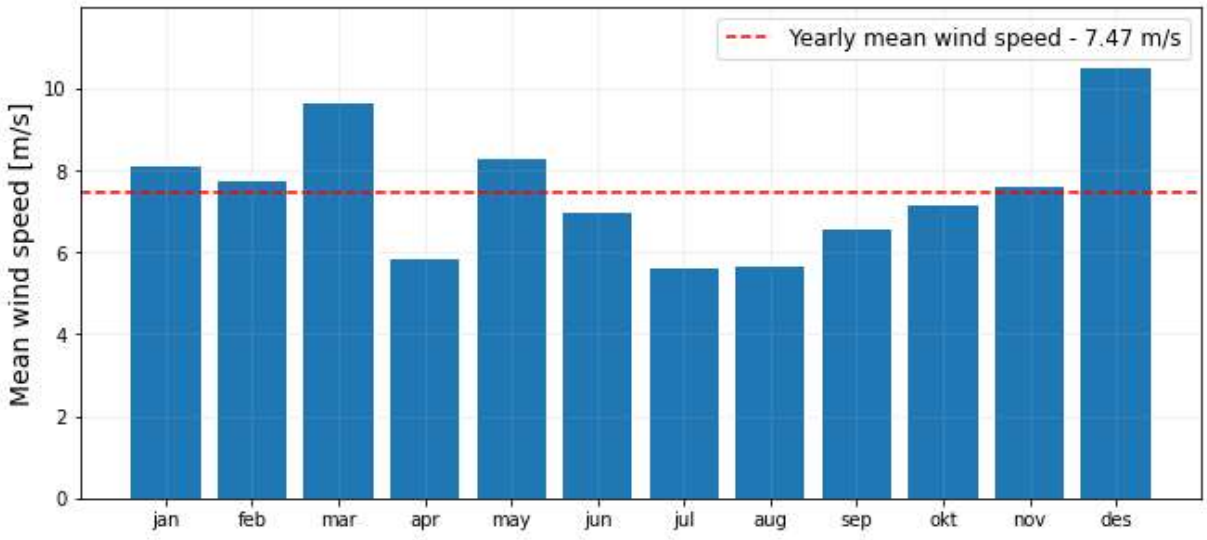

Figure 31: Monthly average wind speed at Solberg wind farm based on a WRF-simulation from 2016. The average wind speed is calculated based on the average wind speed at each turbine location for the respective month. The red line shows the yearly average wind speed for the whole farm.

Figure 31 shows the monthly average wind speed at Solberg wind farm, the red line illustrates the yearly average wind speed for the whole park. The wind farm experienced highest average wind speed in December, with 10,50 m/s. The average wind speed in April, June, July, August, September, and October where all below the mean wind speed for the whole year. This observation indicates higher wind speed during the winter months.

The upper plot in figure 32 shows the wind speed distribution for the whole wind park and illustrate the frequency of how often different wind speeds occurs at Solberg. Most of the wind comes in the speed interval between 4-6 m/s. The bottom plot illustrates the wind speed distribution with respect to the wind direction. The scatter plot consists of 10-minutes data values. There is a clear concentration of data points between 90-130 degrees and at 225 degrees. By examine the terrain around Solberg in figure 17, one can clearly see that these directions are towards the valley formation in the East and the open fjords in SW, respectively. This will be illustrated in more detail under the wind direction section.

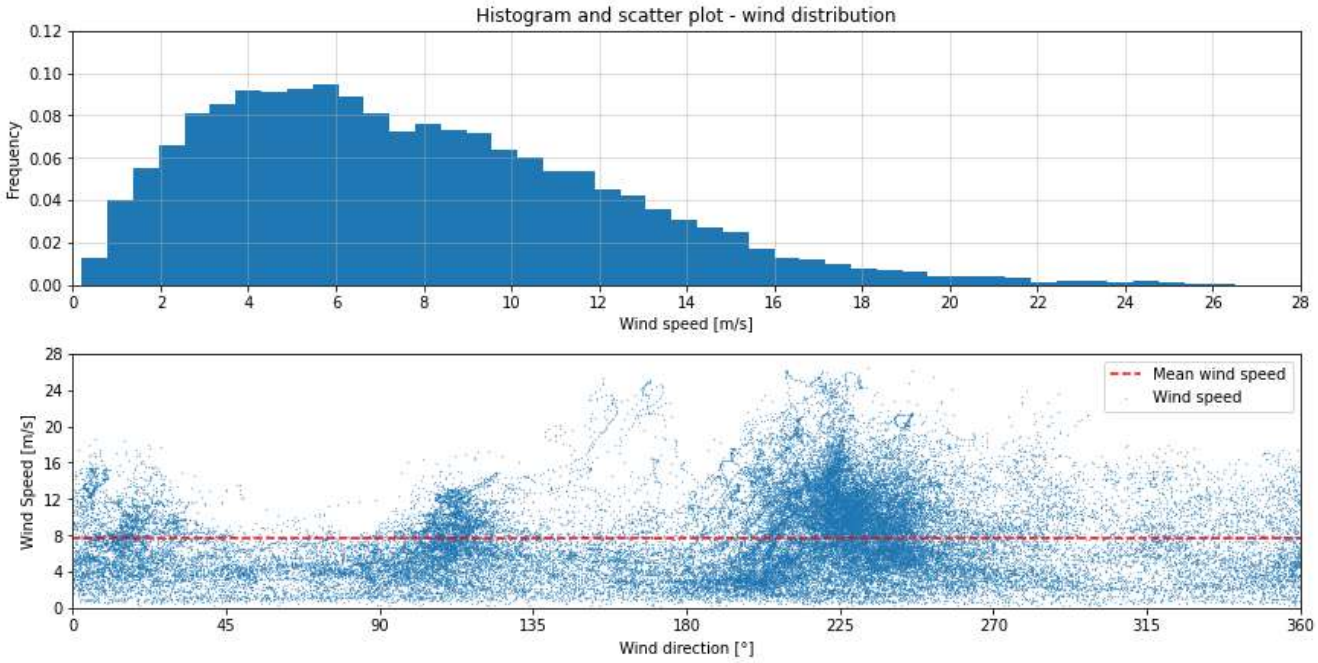

Figure 32: The top figure shows the wind speed distribution for the whole wind park at Solberg. The bottom plot shows the wind speed distribution from different direction in degrees. The main wind direction is from approximately 225 degrees, which is from South-East.

Wind speed at turbine locations

Figure 33 shows the average wind speed in 2016 at the different turbine locations. A clear observation is that the turbines located furthest to the West in each row have the highest average wind speed, which were turbine w1, w5 and w10. The turbines located furthest to the East in each row had the lowest average wind speed, w4, w9 and w14. Gap winds are a phenomenon that can explain this observation, which are formed when the air masses are forced to flow through natural terrain formations. By investigating the terrain formation surrounding Solberg, there is a steep mountain side located in the SW, see figure 17 and 18, that can possibly initiate a gap wind phenomenon.

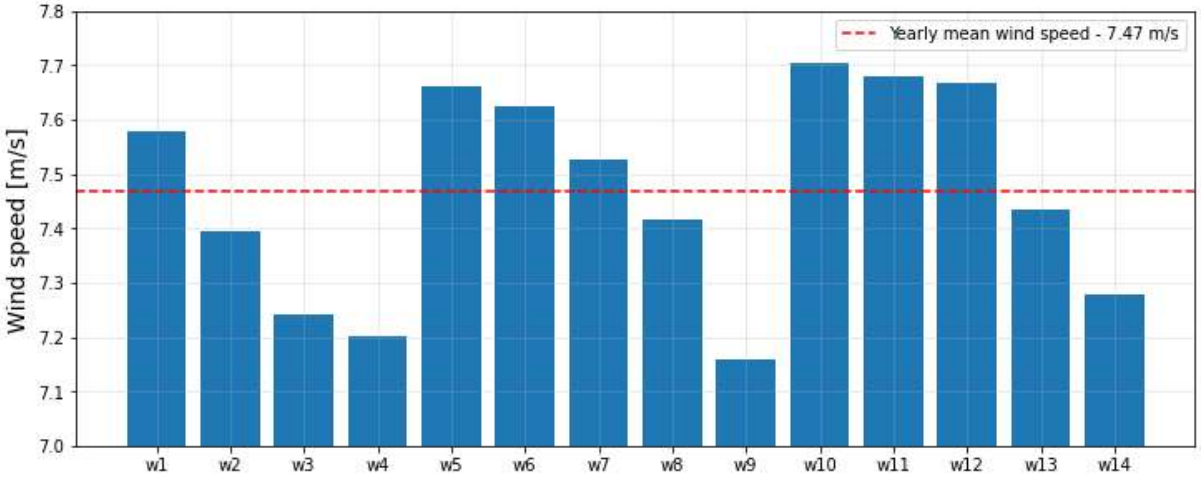

Figure 33: Average wind speed at turbine locations during 2016. Be aware that the y-axis starts at 7.0 m/s to illustrate the wind speed variation between the wind turbines more clearly.

The observations from figure 33 can be used to understand the local wind patterns and optimize the turbine placement at Solberg. Optimalization of turbine placement can result in higher production, hence higher profitability in the project. No further micrositing is performed in this thesis, but some thoughts about improved turbine placement is shared in the end of the result section.

Observations based on the wind speed analysis

The wind farm can be divided in three rows, illustrated by the three red circles in figure 34. As seen in figure 33, the turbines located furthers to the west in each row, had the highest average wind speeds. This was an interesting observation which was used to optimize the turbine placement. At first, turbine w13 was located approximately 800m East for turbine w4, marked by a red triangle. At this location, the average wind speed was 6.992 m/s at hub height, which was by far the lowest between the different locations. It was therefore moved back to the last row, at the location of turbine w13, where the average wind speed was 7,435 m/s. Based on this observation, the second row including turbine w5, w6, w7, w8 and w9, should been moved one notch to the left to test if the turbines achieved higher average wind speeds.

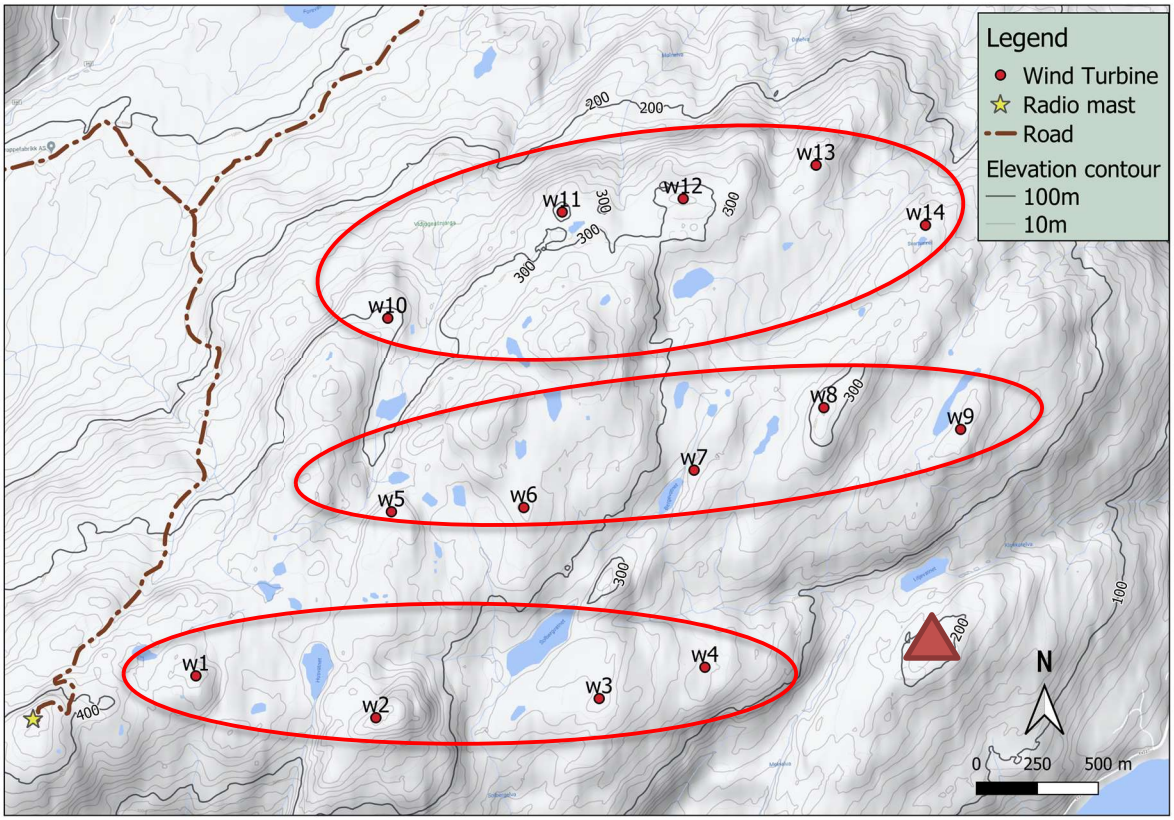

Figure 34: Close up view over turbine placement. The wind farm can be divided in three rows, marked the red circles. The wind speed is highest in the west and decrease as one move eastward.

Another interesting parameter to investigate is the correlation between turbine height placement and the average wind speed. Figure 35 illustrates a visible trend, where higher turbine placement in general results in higher average wind speed. One exception is turbine w2, which is located at the highest point of all the turbines, but has lower average wind speed than w13, which is located approximately 125m lower. Turbine w10, w11 and w12 are all placed at the rear row with respect to the main wind direction, but they have the highest average wind speed. A possible explanation to this observation can be mountain waves, where the wind is pushed up in the front of Solberg in the SW, and as the terrain gradually decrees the wind gain speed towards the ground. It is important to mention that this is wind speed data set are from the clean WRF-simulation, so no wake or drag effect are taken into account. The section covering energy production from the WRF-simulation will show that the wake and drag effect has a considerable effect on these turbines. In general, this shows that a well-placed turbine can compensate for lower height, but height is still an important factor to achieve high average wind speed.

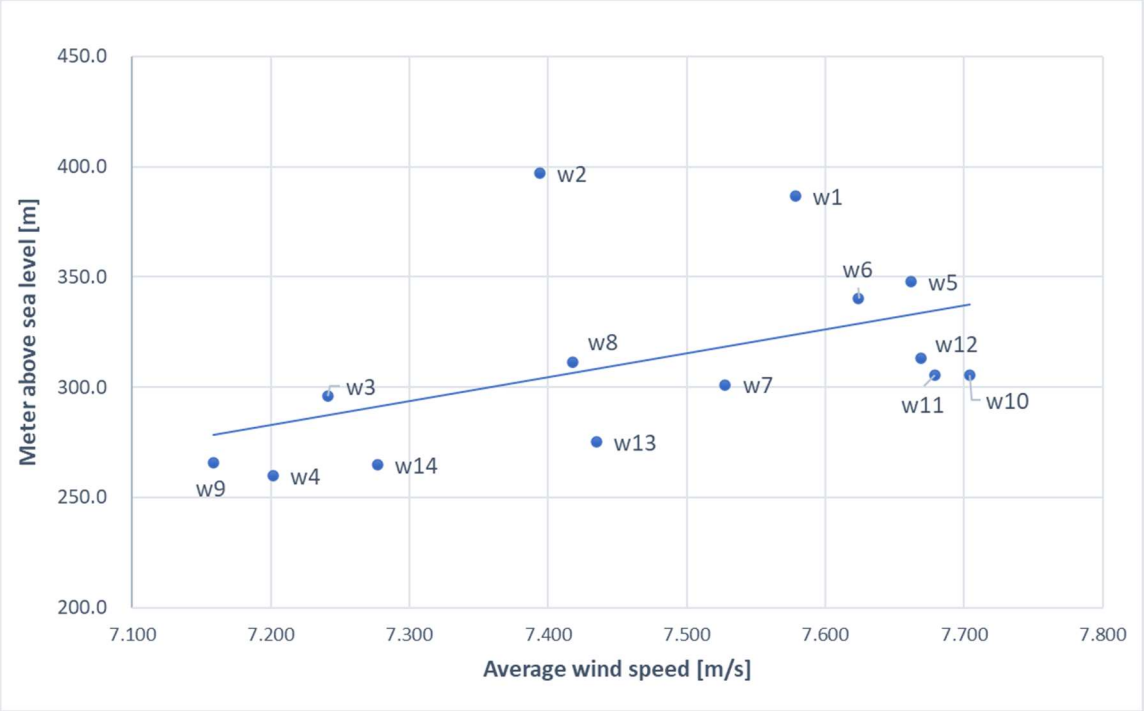

Figure 35: Correlation between turbine placement in meter above the sea and average wind speed. There is a visible trend that the wind speed increases in line with higher turbine placement. The blue line shows the linear regression between the two parameters.

Wind speed adjustment

The wind speed during 2016 was below the reference period from 2000-2015. Table 5 shows the average wind speed at all the turbine locations at hub height after the wind speed is adjusted up 4%. This is done to reflect the average wind speed during an expected wind year.

Table 5: Average wind speed at all turbine locations after the wind speed is adjusted up with 4%. This is to reflect the wind speed during an average year.

Average wind speed at hub height [m/s]		
Turbines	WRF-simulation	Adjusted (+4%)
w1	7.578	7.881
w2	7.394	7.690
w3	7.241	7.531
w4	7.201	7.489
w5	7.661	7.968
w6	7.624	7.929
w7	7.528	7.829
w8	7.418	7.714
w9	7.159	7.445
w10	7.704	8.012
w11	7.679	7.986
w12	7.669	7.975
w13	7.435	7.732
w14	7.277	7.568
Avg	**7.469**	**7.768**

4.1.2 Wind direction

The wind rose in figure 36 shows the wind direction distribution at Solberg wind farm during 2016. The length of each bar indicates how large share the of the total wind that comes from the different directions, and the different colors illustrate wind speed intervals. SW is the most dominant wind direction with almost 24% of the total wind. Approximately 50% of the total wind comes between South and West, in the 180-270 degrees interval. In addition, almost all wind speeds above 12m/s are estimated to come from this direction. This means that only winds from this direction is high enough to induce the turbines to produce at rated power. This should be considered as an important observation when designing the wind farm, to maximizing energy production.

It is visible how the main wind direction at the farm is affected by the terrain and topography surrounding Solberg, see figure 37. Most of the wind comes directly from SW, where the wind comes from an open fjord passage with minimal resistance from obstacles like mountains or forests. The same reason can explain why the highest wind speeds comes from this direction. High mountain formation in the North-West result in minimal wind from this direction.

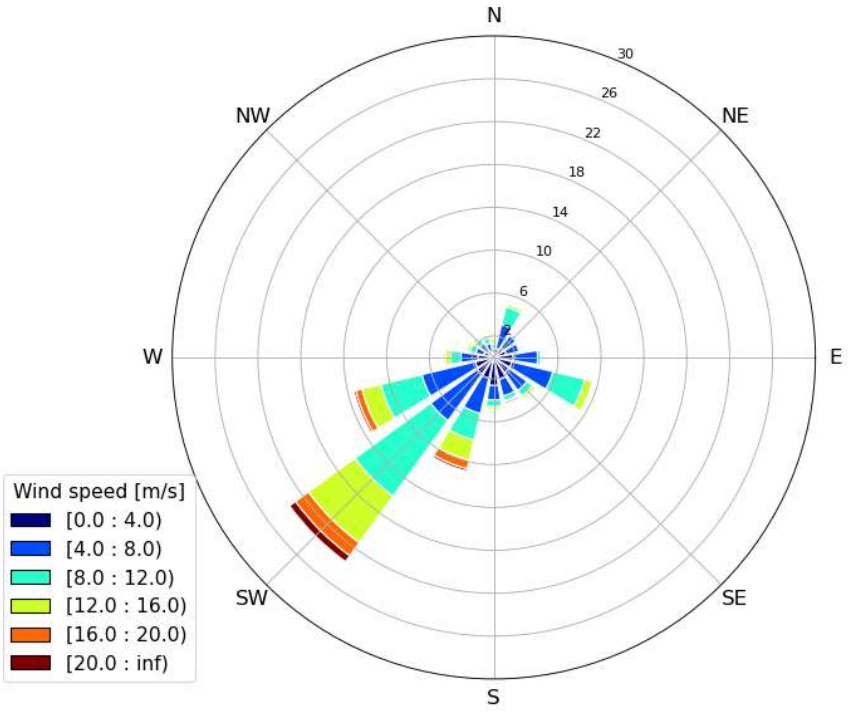

Figure 36: Windrose describing the general wind direction and wind speed distribution at Solberg wind farm. The colours illustrate different wind speed intervals. Most of the wind that comes directly from SE in the interval between 8-12 m/s.

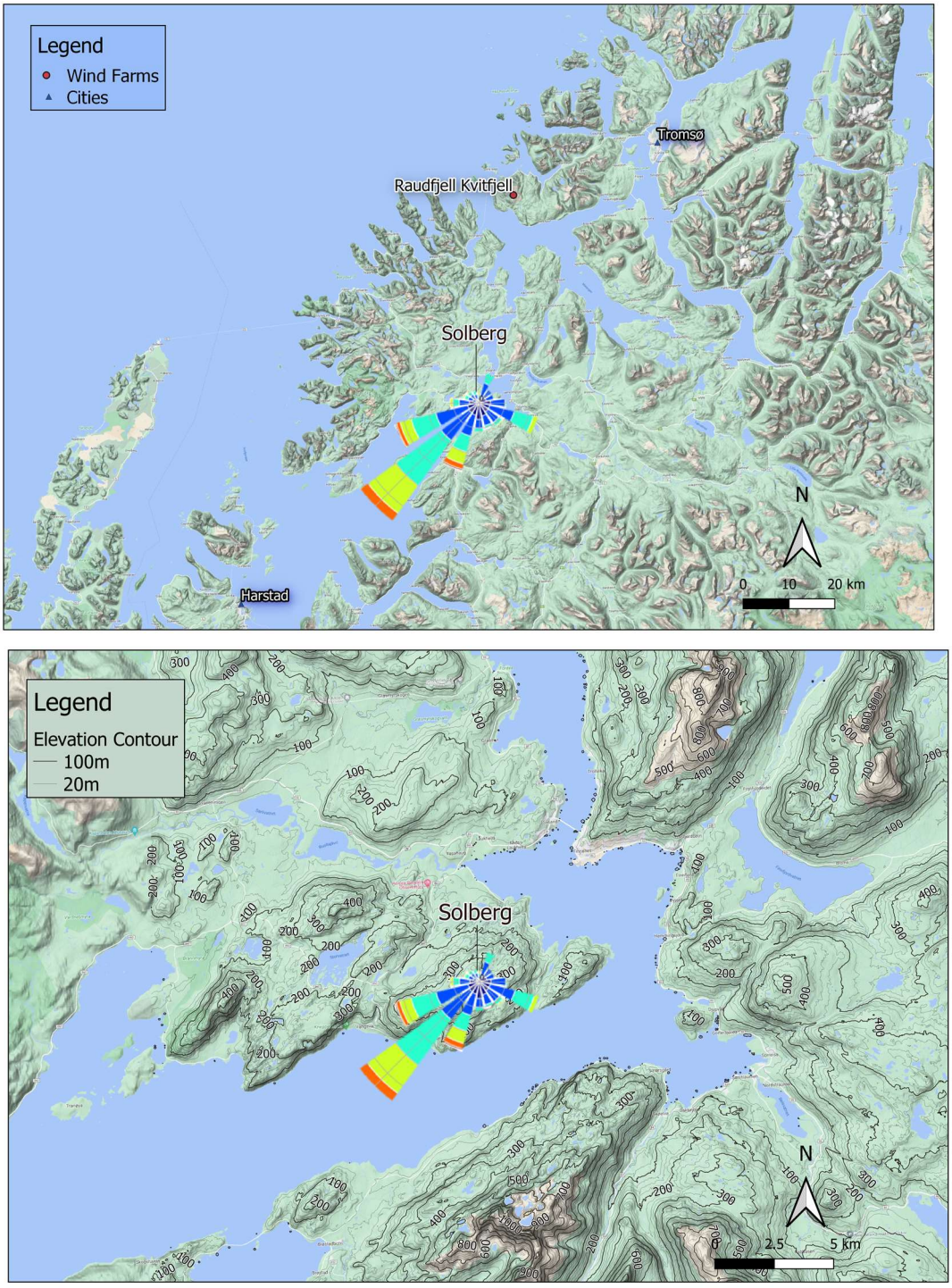

Figure 37: The top image is an overview of the terrain formations around Solberg. The second image is a closer view on the terrain formations with contour lines. The windrose shown in figure 36 is added at the location of the wind farm. SW is the most dominate wind direction and is also the wind direction with the highest wind speeds. In the SW direction there is an open fjord with a length of approximately 70km. There is no high mountains or forest areas for the wind to pass before it reaches Solberg, which can explain the high wind speeds from this direction.

Wind direction and season variations

High wind speed in December

The average wind speed in December at Solberg was 10,5 m/s. This was the month with the highest average wind speed. To investigate which wind direction that was the most dominant during this month, an individual wind rose was plotted for December, see figure 38. Approximately 65% of the wind came between South and West, and 50% of the wind from SW was above 12m/s.

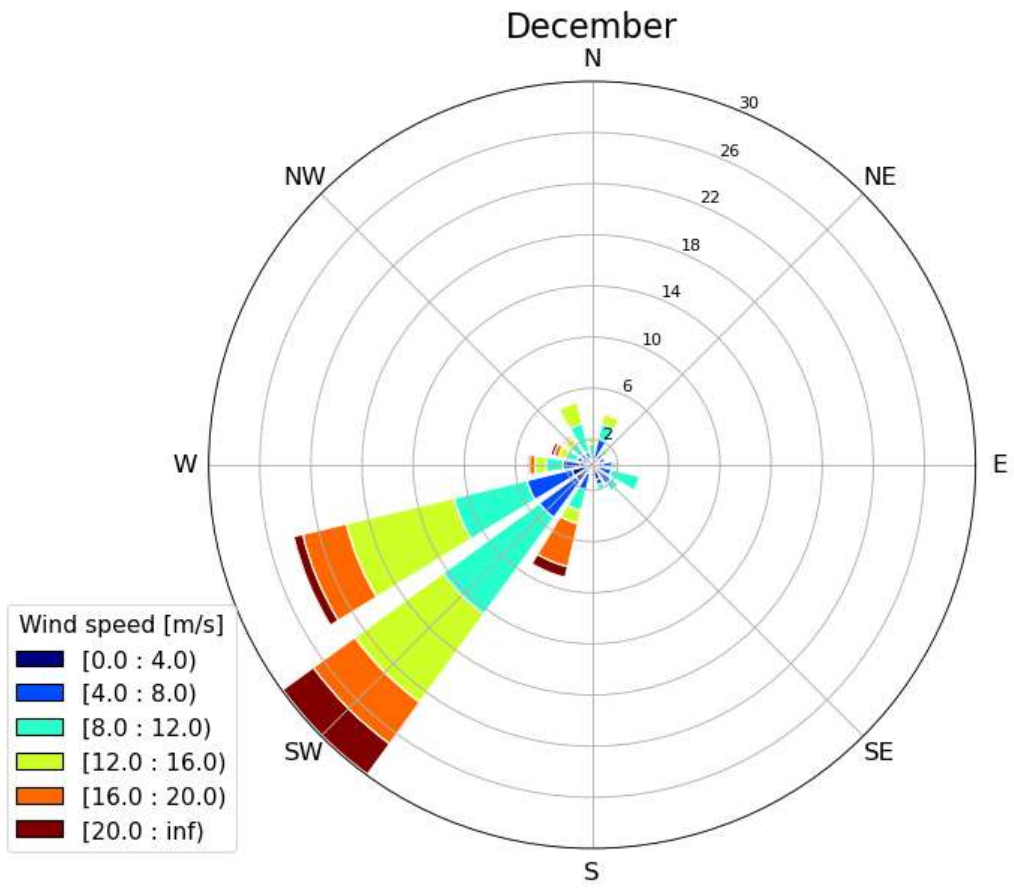

Figure 38: Wind rose for December at Solberg wind farm.

Low wind speed in July

In July, the average wind speed at Solberg was 5,61 m/s, almost 50% lower than in December. Figure 39 shows the wind direction distribution for this month. The main wind direction was WSW, which is a shift towards the West compared to the main wind direction for the whole year. In addition, more wind came from a Nort-Eastly direction. There was almost no wind above 12 m/s, which indicating that the turbines will have few hours at rated power in July.

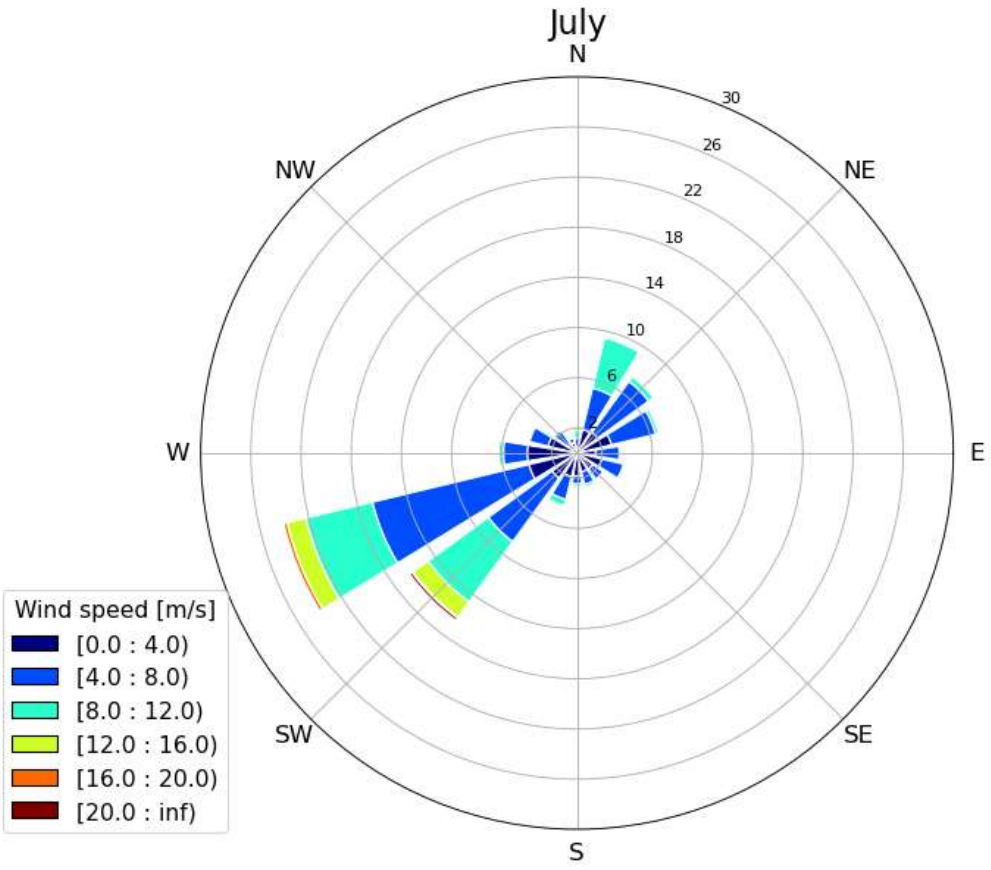

Figure 39: Wind rose for July at Solberg wind farm

4.1.3 Limitations and uncertainties

The WRF-model is a great tool for assessing the wind resources for a distinct are in the preliminary phase of a wind farm project. The model returns a large set of different parameters that will give an overview of the available wind resources. However, the model simplifies both the terrain and physical conditions in the atmosphere, which results in some uncertainties related to the results.

Firstly, the WRF-model simplifies the terrain by smoothing mountain tops and valley bottoms, as illustrated in figure 23. Therefore, the height of the turbine placement in the WRF-simulation are lower than it would be in the real terrain. Higher elevation placement of the turbines correlated with higher average wind speed, see figure 35. Therefore, the average wind speed achieved in operational use can be assumed to be some higher than found in this thesis. In addition, earlier studies evaluating the WRF model with respect to complex terrain in northern Norway, has found that the WRF-model tends to underestimate the wind resources and the wind speeds under high winds [2][3]. Underestimating the general wind resources will have impact on the energy production and result in lower production. The projects economic sensitivity related to variation in energy production is presented in the economic part and will illustration the effects of both under- and overestimating wind speeds.

Another effect of terrain smoothing in the WRF-model, is that the RIX value presented in figure 19, will generally be lower. By smoothing the complex and steep terrain, the frequency of turbulence will decline. Less turbulence is positive for a wind farm and will rise the energy production. There were only one nearby weather masts close to Solberg with data from 2016. This mast was located at Kistefjell, at an elevation of approximately 920m. Do to the known smoothing effect of terrain elevation in the WRF-model, it was assumed that a comparison between real measurements and WRF data at Kistefjell would not be representative for the situation a Solberg. In order to validate the wind speed estimations from the WRF-simulation at Solberg, it would have been desirable to compare the data with real measurements from a weather mast at the exact site.

In total, the smoothing effect has both positive and negative contributions to the estimation of wind resources. The magnitude between these effects is not known and highlights the complexity and uncertainties related to wind modelling in complex terrain.

4.2 Energy production

In this section the energy production data for the whole farm and the individual turbines will be presented. This will give an overview of total monthly production and variations between the turbines in the wind farm. Energy production estimates from the two WRF-simulations will be compared to illustrate the impact of wake loss effect. The estimated yearly energy production will be adjusted with +5%, based on the production index from 2016 for wind farms close to Solberg, as discussed in section 3.4.

The estimation of the energy production assumes that the wind farm operates 365 days a year, which equals to 8760 hours. Be aware that 2016 was a leap year, resulting in an extra day with production. For the economic analysis, a net energy production is estimated by assuming a total loss of 15%. The wake loss is accounted for in the simulation, so the remaining losses related to icing and operational down time due to maintenance is adjusted based on estimates and numbers from a person with experience from the wind energy industry.

Figure 40 gives an overview of the energy production in during the simulation year. The blue line indicates the hourly energy production in MWh, and the red line shows the weekly rolling average. The figure shows that the production in general was lower during the summer months in 2016.

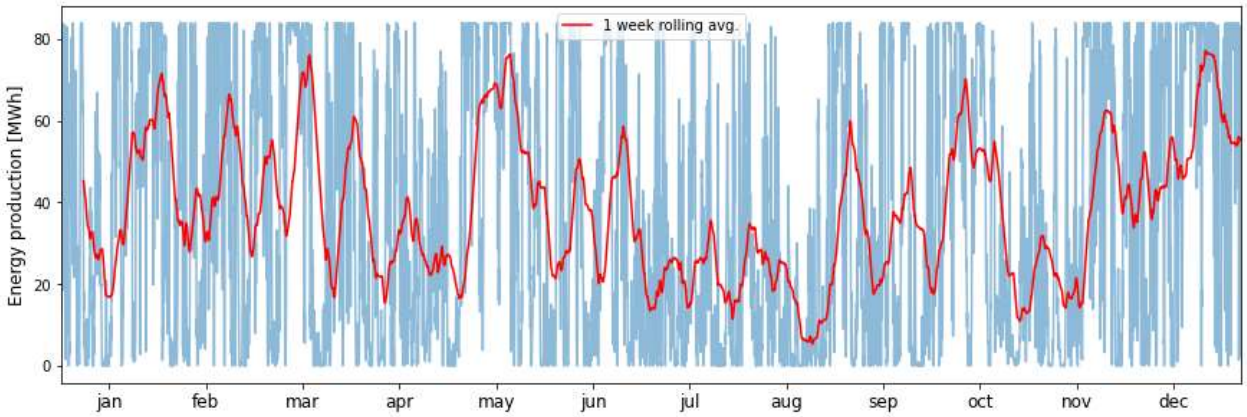

Figure 40: Overview of energy Production for Solberg wind farm. Dates on the x-axis are placed in the center of each month. The blue line shows the hourly production, and the red line shows 1 week rolling average in [MWh].

4.2.1 Wake effect on energy production

Wind Farm production

Table 6 shows the energy production comparison between the two WRF-simulations. In total, the energy production felt with approximately 8,6%, or 27,5GWh, when the wake effect was considered. There was a large variation in production decline among the different months. November had the largest production decline with 16,4%, but October had a rise in production by 0,4%. March had the second highest energy production and just a slightly decline by 0,7%. To analyze these observations in more detail, wind roses were plotted for some months, see figure 41.

Table 6: Monthly estimated energy production for Solberg wind farm. The table compare the production estimates between the two WRF-simulations for every month, and present the difference in GWh and precentage change.

Monthly gross energy production [GWh]				
Month	**Clean WRF**	**Turbines in WRF**	**Differance [GWh]**	**%-change**
Jan	31.99	27.88	- 4.11	-12.85 %
Feb	26.87	25.96	- 0.91	-3.39 %
Mar	35.97	35.72	- 0.25	-0.70 %
Apr	17.33	15.11	- 2.22	-12.81 %
May	35.35	31.68	- 3.67	-10.38 %
Jun	23.66	21.04	- 2.62	-11.07 %
Jul	16.40	14.66	- 1.74	-10.61 %
Aug	16.58	15.48	- 1.10	-6.63 %
Sep	21.44	20.43	- 1.01	-4.71 %
Oct	26.46	26.56	0.10	0.38 %
Nov	26.66	22.28	- 4.38	-16.43 %
Dec	41.32	35.73	- 5.59	-13.53 %
Sum	**320.03**	**292.53**	**- 27.50**	**-8.59 %**

Figure 41 compares monthly energy production between the two WRF-simulations. The blue bars show the gross energy production from the clean simulation and the grey bars show the simulation including wake effects. The dark blue line shows the change in percentage in energy production between the two simulations. Be aware that the y-axis for the percentage is inverted.

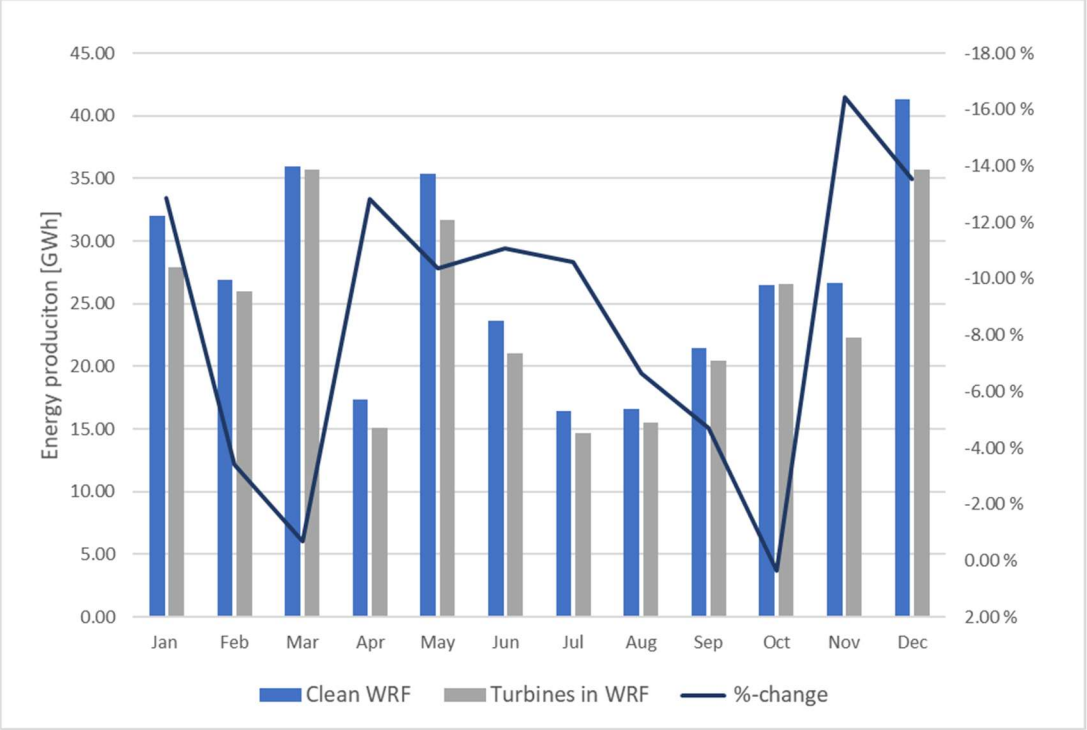

Figure 41: Monthly energy production comparison between the two WRF-simulations. The blue bars are the estimated gross energy production from the "clean" simulation and the grey bars shows the estimated energy production when wake and drag effect is considered. The dark blue line shows the percentage difference between the two simulations for every month in 2016. Be aware that the dark blue line is inverted to illustrate increased decline in energy production with an ascending line.

December vs March – large difference in estimated wake loss

December and May were the months with highest energy production. When adjusting for wake loss from the clean simulation, December had a decline in energy production with 13,5% and March only 0,7%.

Figure 42 shows wind roses for December and March. The most distinct difference is that the magnitude of the wind direction bar from SW is almost 8 percentage points larger in December than in March. In addition, there came almost three times as much wind from WSW in December then in March. Another noteworthy observation is that March had considerably more wind from an Eastly direction than in December.

Based on these observations, the wind farm is more sensitive for wake effects when the wind comes from a WSW direction. The current wind farm design has lower wake losses when the wind comes directly from SW. Based on observations from the windrose in March, winds from the east causes minimal wake losses in the farm. The relative wake effect should in general decline when the wind speed increase, because when the wind speed reach rated power, the turbine is not able to extract more energy out of the wind. Even though December has a higher frequency of high wind speeds, the wake effect is very prominent, which means that the wind direction must be the leading factor for the distinction in wake losses.

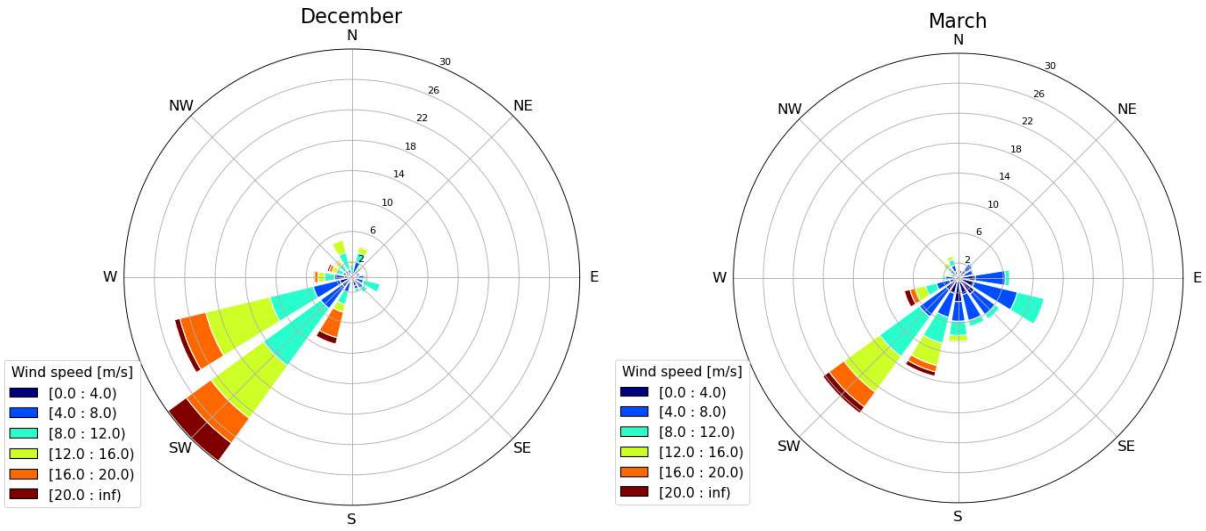

Figure 42: Wind roses for December and March at Solberg wind farm. This was the two months with highest energy production.

Turbine production

Table 7 sums up the energy production at each turbine from the two WRF-simulations. By comparing the two data sets, the impact of the wake effect for each turbine are visualized. In colon "Turbines in WRF", see table 7, several of the turbines has similar energy production. This is because these turbines are placed in the same grid cell and the value presented is the average energy production for each turbine in the cell. Due to this, the wake loss effect presented in table 7 cannot be seen as exact, but more as a rough estimate.

Table 7: Gross energy production at each wind turbine before adjusting for wind speed and losses. The table compares the estimated energy production for both the "clean" WRF-simulation and the WRF-simulation where wind turbines are placed in the terrain. The absolute and percentage difference

Gross energy production for each turbine [GWh]				
Turbines	**Clean WRF**	**Turbines in WRF**	**Differance [GWh]**	**%-change**
w1	23.13	22.22	- 0.90	-3.91 %
w2	22.37	22.22	- 0.15	-0.68 %
w3	21.87	20.73	- 1.14	-5.20 %
w4	21.75	20.20	- 1.55	-7.13 %
w5	23.71	20.73	- 2.98	-12.58 %
w6	23.53	20.73	- 2.80	-11.90 %
w7	23.09	21.01	- 2.07	-8.98 %
w8	22.67	21.01	- 1.66	-7.30 %
w9	21.73	19.68	- 2.05	-9.44 %
w10	23.98	22.36	- 1.61	-6.73 %
w11	23.71	21.95	- 1.77	-7.44 %
w12	23.58	20.00	- 3.58	-15.19 %
w13	22.70	20.00	- 2.71	-11.92 %
w14	22.21	19.68	- 2.53	-11.38 %
Sum	**320.03**	**292.53**	**- 27.50**	**-8.59 %**

Figure 43 is a graphic illustration of table 7, illustrating how the energy production for each turbine changed when wake was considered. The blue bars are the clean simulation, and the grey bars are the simulation considering wake. The dark blue line shows the percentage decline in power production after wake effect is considered. Be aware that the y-axis is inverted for the percentage, meaning the line rises with larger decline in energy production.

The row consisting of turbine w1, w2, w3 and w4 had the lowest energy production loss after the wake was considered. These turbines are placed at the front row of the farm with respect to the main wind direction, which is likely why they have the smallest decline. Turbine w12 on the rear row had a decline of 15,19%, due to its close position to W11, especially when the wind comes from a WSW direction. These observations are relevant to use during farm design optimalization which will be discussed later.

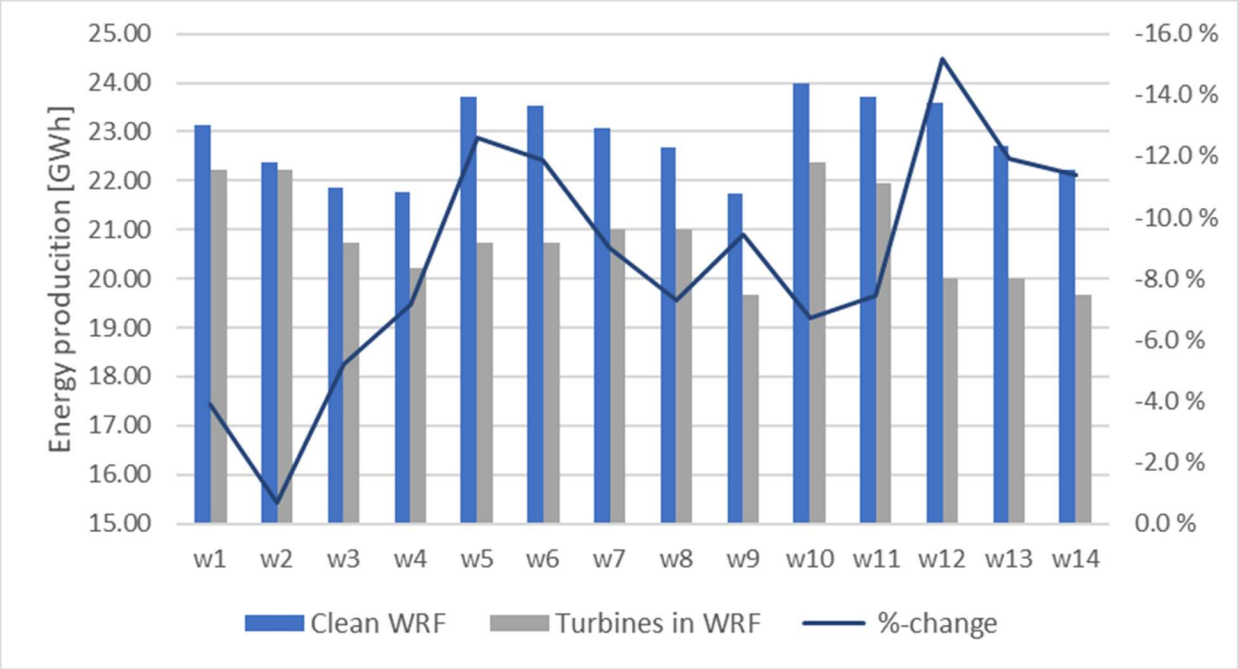

Figure 43: Gross power production at each turbine in both WRF-simulations. Be aware that the Y-axis for the energy production starts at 15 GWh and not zero. This is to visualise the production variations between the turbines better. The dark blue line illustrates the negative percentage change from the "Clean WRF" and the "Turbine in WRF" simulation. The Y-axis for the percentage change is shifted to better illustrate increasing change in between the two simulations.

4.2.2 Icing

During an average weather year its expected 301-500 hours with icing above 10g/h at 80m above sea level for the two southern most rows in the wind farm, see icing map from NV, figure 4 [67]. For the rear row, 201-300 hours with icing can be expected.

As mentioned in section 2.5.2, thicker surfaces have shown a lower capability to accumulate ice than thinner surfaces [20]. This can suggest that larger turbines with thicker blades are beneficial compared to smaller turbines under conditions where ice can accumulate. At Solberg wind farm the wind turbines have a rotor diameter off 162m, which should be considered as a large turbine blade, hence beneficial regarding icy conditions. No exact assessment of possible loss due to icing is performed in this thesis, but ice loss is included in the total 15% loss factor which is applied on the gross energy production.

4.2.3 Net energy production

In this section the yearly net energy production for Solberg wind farm is presented. This is based on the WRF-simulation including wind turbines; hence the wake effect is already considered in the energy output. The energy production was first adjusted with (+5%) based on the production index for nearby wind farms in 2016. This is to reflect the average expected energy output from the farm.

A degradation factor of 10-15% on the gross energy production is often used to reflect the total losses from an operating wind farm [41]. After discussions with a person in the wind energy industry, a total loss of 15% from gross energy production was recommended. In this thesis, the wake loss, 8,6%, is already included in the out-put data from simulations. To adjust for losses related to icing, a factor of 5% is used based on the simulation done at Kvitfjell Raudfjell wind farm [22]. This is a rough estimate, but used due to Kvitfjell and Raudfjell proximity to Solberg, only 45km, and its location similarity, regarding height and topography.

Wind farm production

Figure 44 shows the net energy production in the different months, the total production was 288.53 GWh. The net energy production was highest in December, with 35,22 MWh. The red line indicates the average wind speed for each month.

Figure 44: Total Monthly energy production at Solberg wind farm after losses. The value on top of each bar indicates the monthly energy production. The red line shows the average wind speed in the farm during the months.

Turbine production

Figure 45 shows the yearly net energy production for each turbine. Turbine w10 had the highest production with 22.05 MWh, and w14 and w9 had the lowest production with 19.41MWh.

Figure 45: Yearly net energy production per turbine. Turbine w10 had the highest net production

Some of the turbines had the same production volume because they were placed in the same grid cell in the model. When several turbines are placed in the same cell, the total energy production from the cell is divided on the number of turbines inside the cell, as shown in figure 25. The disadvantage is that it is not possible to visualize exact production variations within the cell, which makes it harder to optimize turbine placement. For example, turbine w5 and w6 are placed in the same cell. The total net energy production in this cell is 40,88GWh, hence the average production per turbine is 20,44 GWh. A possible solution to avoid the averaging between several turbines in the same cell is to run the model with a finer resolution and place 1 turbine inside each cell.

4.2.4 Energy potential

Figure 46 shows the gross energy potential at Solberg wind farm. The red line indicates the energy potential based on the average wind speed distribution for the whole park. Most of the incoming wind has wind speed between 3-7 m/s, but this interval represents just a small fraction of the total energy production potential. The largest energy potential is in the 9-12 m/s wind speed interval.

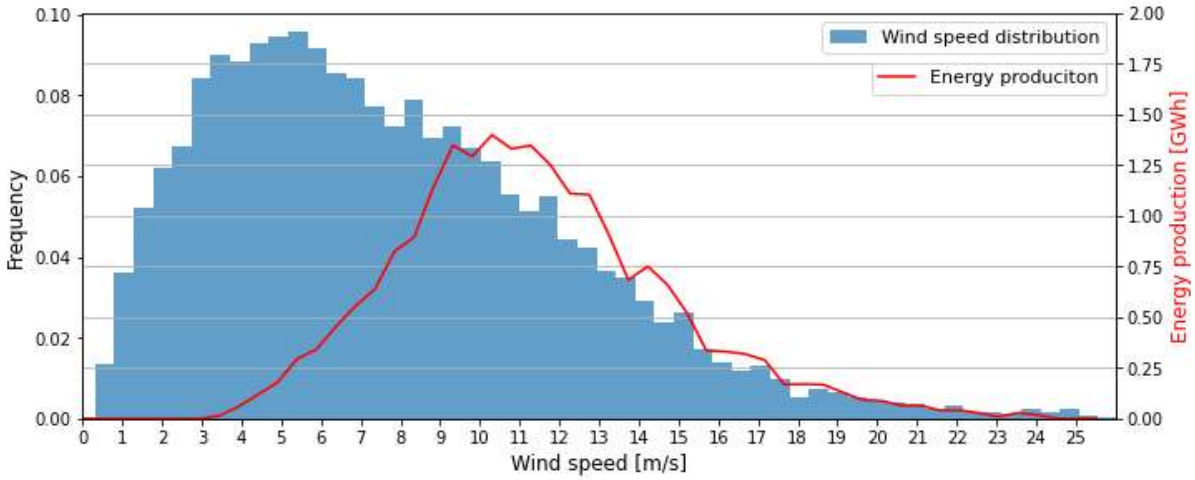

Figure 46: Yearly gross energy potential at Solberg wind farm. The blue bars show the average wind speed distribution for the whole farm after wind speed adjustment. The red line indicates the energy potential for the farm at different wind speeds.

4.2.5 Capacity factor

The capacity factor describes the ratio between the produced energy and the total possible energy that the wind farm could have produced based on its installed capacity. Solberg wind farm has an installed capacity of 84MW and is estimated to produce 288.53 GWh during an average year, which result in capacity factor of 39,10% for the whole wind farm.

Table 8 shows the installed capacity, yearly expected energy production, hub height and estimated capacity factor for wind farms located in the vicinity of Solberg. The expected production volumes are from NVE [54]

Table 8: Overview of installed capacity, expected production, hub height and capacity factor for Solberg and some selected wind farms located in the vicinity of Solberg. The capacity and expected production data are from NVE [54].

Wind park	Installed capacity [MW]	Expected production [GWh]	Hub height [m]	Capacity factor
Solberg	84.00	288.53	125.00	39.10 %
Raudfjell	84.00	227.35	85.00	30.90 %
Kvitfjell	197.40	541.00	85.00	31.29 %
Fakken	54.00	139.00	80.00	29.38 %
Ånstadblåheia	50.40	154.00	87.00	34.88 %
Nygårdsfjellet	32.20	104.00	80.00	36.87 %

Table 8 shows that Solberg wind farm is estimated to have the highest capacity factor among the listed wind farms. With a hub height of 125m, Solberg stands out among the other wind farms with an additional height off approximately 40m. Based on observations from this thesis and wind maps at different heights over Norway [55], the wind speeds are in general higher at 125m compared to 80m above the ground. The energy output is strongly correlated with the wind speed and vary with respect to the third power of the wind speed, which can explain the higher capacity factor at Solberg.

In 2021 the average capacity factor for Norwegian onshore wind power plants was 32,9%. It is important to mention that the production index was only 93,6% in 2021, meaning that the energy production was 6,5% lower than during the reference period, 2003-201 [56]. In 2018, the global weighted average capacity factor was 34% for onshore wind farms [40].

4.2.6 Relevant observations for further micrositing

This thesis does not include a detailed micrositing of each turbine, because after re-placement of a turbine, the WRF-simulation need to be run again, which is time consuming on a fine resolution. However, from the wind speed, wind direction and energy production data presented above, several observations were found which can be used to optimize turbine placement and the design of the wind farm. Based on the observations, some suggestions for improvements are presented below.

Firstly, the wind speed was highest at the turbines located furthest to the west, possibly due to the combination of the open fjord passage and a possible funnel effect. All turbines in the middle row, w5, w6, w7, w8 and w9, could therefore been moved one notch to the west in further micrositing to test if this assumption is correct.

Secondly, height placement was also found as one important factor that had a correlation with higher wind speed. Turbine w2 deviated from this observation, by having lower average wind speed than turbine w13, even though w13 was placed 125m lower in the terrain. Based on this observation, height placement should be prioritized, but need to be emphasized in proportion to the wind farm design. For example, placing a wind turbine lower in the terrain to improve the overall wind farm design, would be beneficial if it reduces the wake loss for the turbines behind.

Finally, the current wind farm design appears to have higher wake losses when the wind comes from WSW than from SW. This was observed in the production volume for May and December. These months had approximately the same energy production in the “clean” WRF-simulation, but when the wake was considered, December had a decline of 13,5% and May only 0,7%. In figure 20, one can observe that if the wind comes from a WSW direction, the wind farm appears to have five rows of turbines, in contrast to only three rows if the wind comes directly from the South. This can explain why the wake losses were higher in December than in March. Since WSW is the second most prominent wind direction at Solberg, the wind farm design should be optimized to reduce the wake loss from this direction to obtain higher energy production.

4.2.7 Limitations and uncertainties

The wind speed is the most important factor when it comes to potential energy output from a wind turbine. It is therefore important to be aware of possible consequential errors that can occur if the wind speeds used in the energy assessment are under- or overestimated.

The wind speed has a cubic relationship with the energy output form a wind turbine. Hence, if the wind energy resources are underestimate in the WRF simulation, as earlier studies have shown [2], it will result in lower energy production. Lower energy production will again affect the economic aspect of the project, which will be illustrated in the economic assessment.

An overestimation or underestimation of the wind speed within the wind turbines rated power range, will not affect the total energy production, since the power production is constant in this range. When the wind speed is close to the cut-off speed, the power production will be sensitive for overestimations, because a wind speed with a magnitude slightly above the cut-off speed will result in no energy production. The model is also sensitive for errors in the lower wind speed intervals between the cut-in and rated power level. Small deviation in wind speed will result in larger deviation in energy production due to the cubic relationship between the wind speed and the energy production.

In the WRF-simulation where the wind turbine scheme was activated, the resolution of the model limits the possibility to investigate the energy production for each turbine individually. The simulation returned total energy production within each grid cell, making it hard to use the data for further micrositing of wind farm. However, the simulation was useful to estimate the wake effect that occurred in the wind farm.

From the clean WRF-simulation, the wind speeds extracted at hub height was not affected by any wake loss or wind shadow from close by turbines. This resulted in a significantly higher energy production, compared to the wake simulation. However, the data from this simulation made it easier to map local variations within the wind farm. However, one should be careful to use this wind speeds to optimize turbine placement, since wake affects, and wind shadows are not included.

4.3 Economic assessment

In this section the results from the economic analysis of Solberg wind farm are presented. The goal of the analyze is to calculate the Net Present Value (NPV) and Levelized Cost of Electricity (LCOE) for the wind farm. These results will reflect the profitability of the project and will form the basis of an investment decision. A sensitivity analysis is conducted, to investigate the vulnerability of the investment in relation to major changes in electricity price and variation in energy production.

Assumptions

The yearly net energy production for Solberg wind farm was estimated to 288.53 GWh and will be used in the basis scenario for the economic assessment. A yearly degradation rate of 0,25% will be applied from year two (Espen E., VP Business Development Magnora, personal comment, 27.05.2022). It is assumed that all the yearly production volume is sold in the spot market.

The projecting and license application phase for a wind farm was discussed with a person working in the wind energy industry. For a preliminary project like Solberg, production start in 2030 was suggested as a rough estimate. Based on the price trajectories shown in figure 12 and 13, it would be beneficial for wind farm to start production closer to 2030, due to higher electricity prices. It is therefore assumed that Solberg wind farm is operational from 2030. In addition, it is assumed a cost of EUR/NOK of 10kr in the base case scenario.

Significance

For wind turbines sat in production before 31.12.2021 there were two economic government subsidies available in Norway. Firstly, a linear depreciation of the capex over the first five years was allowed. Secondly, a green electrical certificate gave renewable energy producers an additional 5øre/kWh for each kWh. These subsidies will not be relevant for Solberg wind farm since the farm is sat in production after 31.12.2021.

4.3.1 Capital expenditure

The initial expense varies between different wind energy project, dependent on the terrain and infrastructure in the area. For this project, a total cost of 1,33 million euro per installed MW was used. This number was obtained from a person with experience from the wind energy industry, with experience from the wind energy industry. A cost of 200 MNOK related to external grid connection is a part of the initial costs. In the base case scenario, it is assumed that 1 EUR cost 10 NOK. The total cost of turbine installation and external grid connection was then estimated to 1 118 290 000 NOK, see table 9.

Table 9: Overview over CAPEX costs in MNOK. This table reflect the CAPEX cost for the base scenario where 1EUR costs 10NOK. The wind turbines stand for 56.3% of the installation costs and is the most expensive part of the CAPEX.

CAPEX			
Investment budget; 14 turbines @ 6 MW	**#**	**%**	**MNOK**
Vestas Turbines 6 MW	14	56.3 %	630.00
Civil BoP		11.7 %	131.04
Electrical BoP		7.8 %	87.36
Project/construction managment		2.3 %	26.21
Financial cost during construction		1.6 %	17.47
Unforseen		2.3 %	26.21
Investment cost		82.1 %	**918.29**
External grid connection		17.9 %	200.00
Total CAPEX		100.0 %	**1 118.29**

As shown in figure 28, the CAPEX for onshore wind projects is estimated to increase by 25%, from 2020 to 2022. The numbers presented in table 10 should reflect the price situation of May 2022, but the costs could increase even further due to the tight commodity market with high mineral and metal prices. The projects sensitivity regarding increased CAPEX cost will be covered in the sensitivity analysis.

4.3.2 Operational expenses

Table 10 shows the estimated OPEX in year one of the wind farm. As mentioned in 3.5, these costs will vary with time dependent on energy production, gross income, the need of maintenance and inflation. Grid rent and operational and maintenance costs related to the turbines are the largest expenses. In total, the OPEX was estimated to 25.36 MNOK in year 1 of the project.

Table 10: Estimated OPEX cost in year 1 for Solberg wind farm.

OPEX-year 1			
Yearly operational costs			**MNOK**
Turbine O&M [50 000 EUR/ turbine]	50 000		7.00
Land rent [% of brutto income]	4 %		2.64
Grid rent [kr/GWh]	30 000		8.54
Property tax [% CAPEX basis for property tax]	0.70 %		3.68
Capex basis for property tax [MEUR]	52.63		
Insurence [% of capex]	0.07 %		0.61
Technical managment [MEUR/ MW]	0.002		1.68
OPEX			24.16
Opex buffer [% of opex]	5.00 %		1.21
Total OPEX			**25.36**

4.3.3 Electricity prices

The electricity prices have a large impact on the profitability of a wind farm. In section, “Power market outlook”, there was presented different pris trajectories in the short and long term. They included both basis, high and low scenarios for the electricity price in NO4.

In figure 47 three different price trajectories are conducted based on the data from NVE [4] and Ishavskraft [6]. The different trajectories represent a basis, high and low scenario. Data from Ishavskraft was used for the prices towards 2032. Since there was no low scenario from Ishavskraft, the basis prices are also used in the low scenario for the first 2 years. From 2032 and towards 2040 the NVE prices was used. Since the price estimates from NVE stopped at 2040, the 2040 estimate was extended to cover the lifetime of the wind farm.

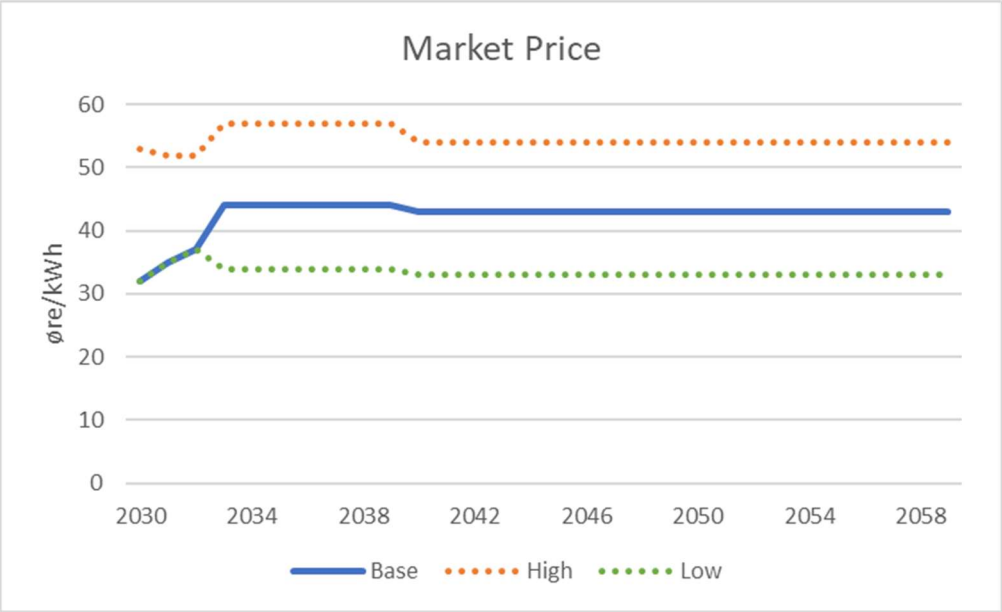

Figure 47: Three different market price scenarios in NO4 based on data from Ishavskraft and NVE. Since the project is assumed to start production in 2030, only prices in 2031 and 2032 are from Ishavskraft. There are no price trajectories from NVE after 2040, it is therefore assumed the same prices to the end of the project as in 2040.

The average electricity price for the basis, high and low scenario are 42,40 øre/kWh, 52,20 øre/kWh and 31,6 øre/kWh, respectively. As mentioned in the section "Market outlook", it is associated large uncertainties to these price trajectories due to expected demand growth in both NO4 and SE1 towards 2030 and 2050. The basis price trajectory presented in figure 46 was discussed with a person working in the wind energy industry and was seen as a conservative estimate.

4.3.4 Power Purchasing Agreement and price hedging

Power Purchasing Agreements (PPA) was disused with a person working in the wind energy industry (Espen E., VP Business Development Magnora, personal comment, 27.05.2022) and has recently traded between 25-30 øre/kWh in NO4. By implement a PPA, parts of the production volume are hedged at a fixed price and entails larger security for the project. PPA has traditionally been a requirement from lenders, in order to have a debt share towards 50%. Lately these requirements have shown signs to be milder (Espen E., VP Business Development Magnora, personal comment, 27.05.2022). Since the cost of debt is lower than

cost of equity, it would be valuable for a wind farm project to achieve a good PPA to have a higher debt share. This would only be valid, as long as the spot price doesn't increase in a large extent and make the PPA less valuable.

For this preliminary project, no PPA or price hedging is applied. A PPA would be entered much closer to the production start of the farm. Therefore, all production volumes are assumed to be sold in the spot market.

4.3.5 Weighted Average Cost of Capital

This section shows the parameters used to find the nominal WACC, which is used in the NPV and LCOE calculations.

Table 11 shows the parameter used to calculate the *cost of equity* by using the Capital Asset Pricing Model (CAPM). The Norwegian 10-year government bond is the most used *risk-free rent* in the Norwegian market. For this project, a normalized long-term risk-free rent at 3% is used [59]. The beta value of 0.875 was obtained from NVE [60], and indicates that the project is less volatile, hence less risky, than the general market. The market risk premium of 5% was acquired from PWC [59] and reflect the median risk premium in the Norwegian market from 2021. This resulted in a cost of equity at 7,38%.

Table 11: Capital Asset Pricing Model (CAPM). The cost of equity was estimated to 7.38% for Solberg

Capital Asset Pricing Model (CAPM)	
Risk free rent	3.00 %
Beta	0.875
Market risk premium	5.00 %
Cost of Equity	**7.38 %**

Table 12 shows the input values and the calculated average cost of capital (WACC). An equal weight between debt and equity is assumed. The cost of equity was found to be 7,38% in table 12, and the cost of debt is based on the weighted average cost of long-term debt for power companies, required by IEA [62]. In the following thesis [49], it was fond that the cost of debt related to onshore wind farms in Sweden were between 1%-2% in 2019. This is significantly lower than 3,4%, which is used in this thesis. The low cost of debt in Sweden was related to a widespread use of PPA, which resulted in stable revenues and cheaper lending [49].

For this thesis, an average cost of capital of 5% was used as a rough estimate. This is in line with future estimates on average WACC for onshore wind farms [61].

Table 12: Weighted average cost of capital was calculated to 5% for this project.

Weighted average cost of capital (WACC)	
Equity	50.0 %
Debt	50.0 %
Cost of Equity	7.38 %
Cost of Debt	3.40 %
Tax	22.0 %
WACC	5.01 %

4.3.6 Net Present Value

This section presents the result related to the NPV calculations. There are three main scenarios based on the three different electricity price trajectories presented in figure 47. Table 13 present the average electricity prices for the different price trajectories, but in the calculations the yearly values are used.

Based on the basis scenario it is found that Solberg wind farm is profitable. The NPV was 55,5MNOK and the project had an IRR of 5,5%. As shown in equation 23, the IRR need to be equal or higher than the discount rate, to be profitable. The high scenario showed a NPV of 491.8MNOK and an IRR of 9,0%, illustrating the value of a higher electricity prices. In the low scenario, with an average electricity price of 31,6 øre/kWh, the project was not a sustainable investment. However, had the project had equal a discount rate as onshore wind project in Germany and Denmark in 2019, at 2-3% [49], the project would be feasible even in the low-price scenario. It worth mentioning that the low WACC values in 2019 was strongly connected with the historical low 10-y government bond yield in both Denmark and Germany and is not representable for the situation today.

Table 13: Net Present Value and Internal Rate of Return for the three scenarios with different electricity price. It is used the same WACC, inflation and production volumes for all scenarios. Electricity price is the only factor that is changed.

Scenarios with different electricity prices			
	Basis	High	Low
WACC	5.0 %	5.0 %	5.0 %
inflation	2.0 %	2.0 %	2.0 %
Average Electricity price [øre/kWh]	42.40	54.53	33.40
NPV [MNOK]	**55.42**	**491.75**	**-201.30**
IRR	**5.46 %**	**8.99 %**	**3.13 %**

4.3.7 Levelized Cost of Electricity

The LCOE value represent the average net present cost of producing electricity during the lifetime of the wind farm. For the basis scenario with a yearly estimated energy production of 288.53 GWh, it was found that the wind farm had a LCOE of 39.65 øre/kWh. Figure 48 illustrate the sensitivity of the LCOE with respect to variation in WACC.

There are many different causes that can increase the WACC. Increased financial risk would result in higher cost of equity, since the shareholders would require a higher rate of return, hence higher WACC. Also, unfavorable loan terms, will result in higher cost of debt and increasing the WACC. The high sensitivity of LCOE with respect to WACC, shown in figure 48, is in line with earlier study's [53] as mentioned in section 2.7.2.

NVE have estimated the LCOE for onshore wind project in Norway to be at 22,15 øre/kWh in 2030 [14-endre]. This is significantly lower than in this thesis with a difference of 17,5 øre/kWh. Possible reasons for this difference are discussed later in this chapter.

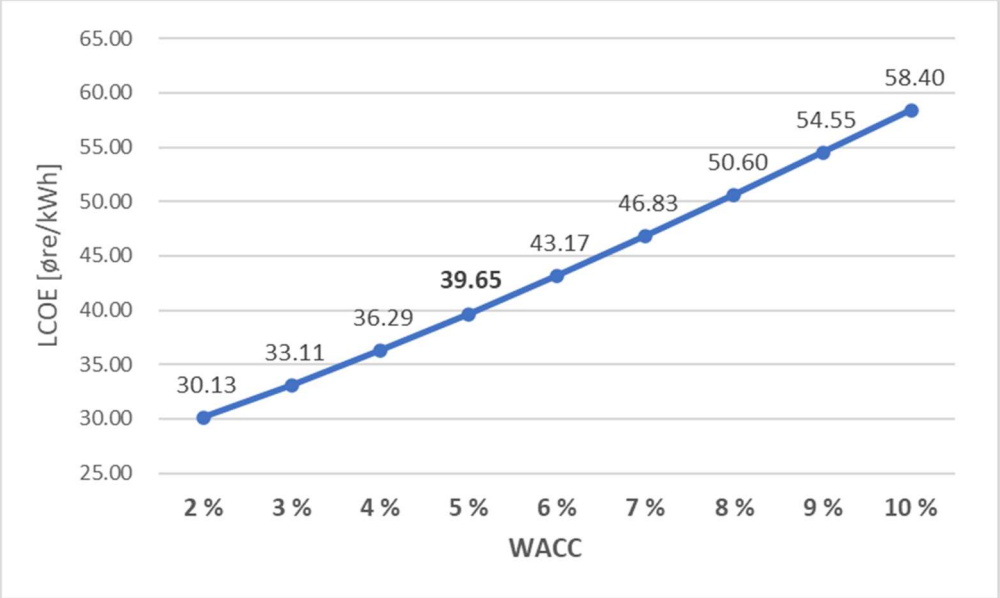

Figure 48: The sensitivity of LCOE with respect to WACC for Solberg wind farm. The base case has a WACC of 5%, hence a LOCE at 39,65 øre/kWh

4.3.8 Sensitivity analysis

For an investor it is important to be aware of the possible downside risks for a project. The goal of this section is to map some of these risk factors to see how the project performs when main parameters changes.

Figure 49 illustrate how the LCOE changes with respect to fluctuations in yearly energy production. The blue "Basis" bar represents the estimated yearly energy production of 288.53 GWh. With higher production volumes, the cost of energy production decline. At 15% higher production volumes, the LCOE is at 34,42 øre/kWh. This LCOE is still higher than the low scenario for electricity prices, indicating that 15% higher production volumes will not be able to equalize for the loss if the low-price scenario becomes a reality.

At a production decline at -5%, the LCOE increases to 41,74 øre/kWh. The project will still be economically viable whit respect to the basis scenario, since the LCOE is lower than the average market price during the lifetime.

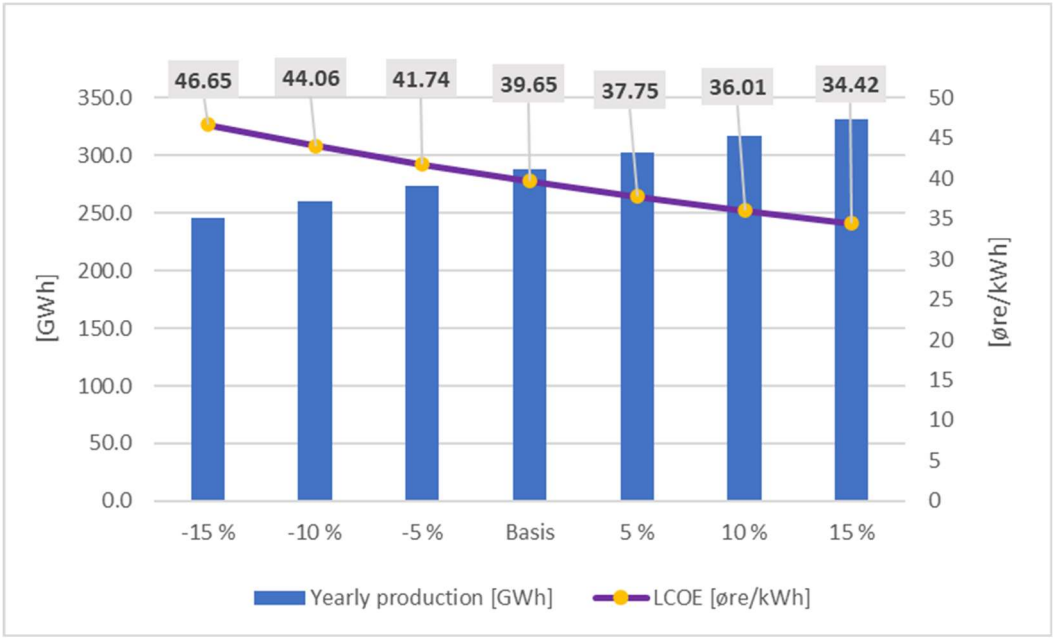

Figure 49: Sensitivity in LCOE with respect to changes in yearly energy production. All the other parameters are similar as in the basis scenario. The plot shows the changes in LCOE when the yearly energy production varies from -15% to +15% from the basis estimated energy production of 288.53 [GWh].

Figure 50 illustrate the sensitivity of LCOE and NPV when CAPEX varies between -15% and +15% from the basis scenario, all the other factors are hold constant. The blue bars represent the NPV of the project, and the purple line indicate the LCOE. With a reduction of 25% of the initial costs, the LCOE decline to 31,19 øre/kWh. Towards 2023 CAPEX for wind power plants were estimated to increase with 25% compared to 2020 [63]. An equal increase for Solberg wind farm would have a large impact on both the NPV and increasing the LCOE to 48,11 øre/kWh.

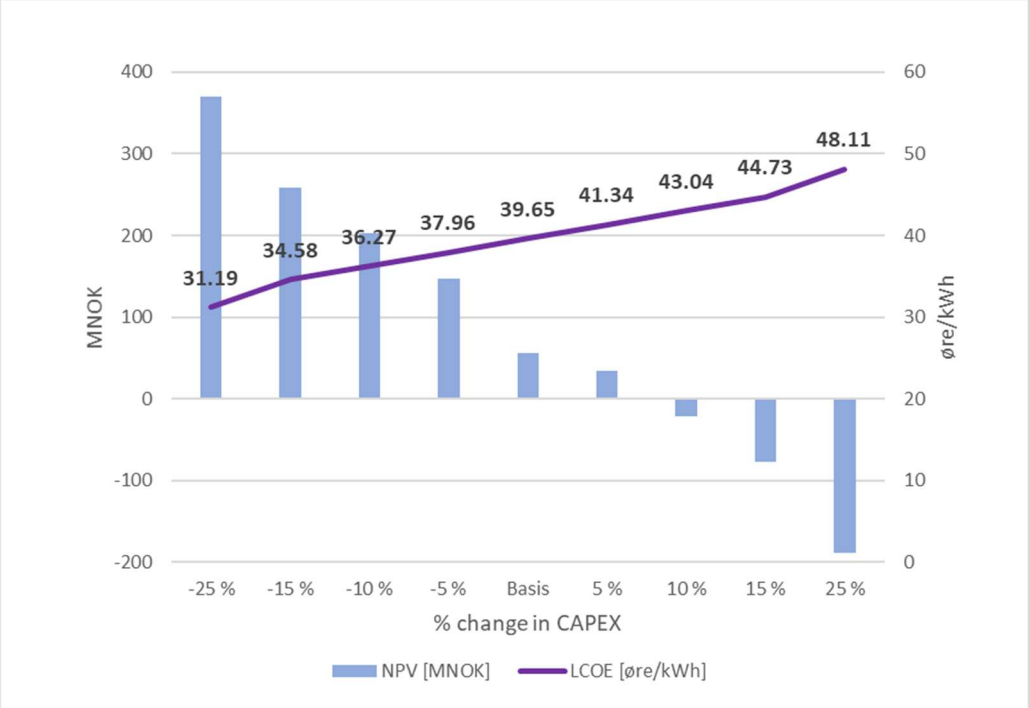

Figure 50: LCOE sensitivity with respect to %-changes in CAPEX. The blue bars indicate the NPV, and the purple line illustrate the LCOE at the different %-changes.

Figure 51 give an overview of the sensitivity of LCOE with respect to the main parameters if they change between -15% and +15% from the basis scenario. It is evident that fluctuation in energy production, dark blue line, have the largest influence on the LCOE. This highlights the importance of correct wind resource assessments and energy production estimates in the projecting phase. It is therefore important to have knowledge about the limitations and uncertainties that incorporate by using WRF, and that overestimation and underestimation of wind speed would have large impact on the final LCOE of the wind farm.

Changes in CAPEX has also a significant impact on the LCOE, indicated by the blue line. Lower costs in the initial phase of the project indicates a significantly decrease in the LCOE, hence making the project more profitable. The WACC has also an impact on the LCOE, indicated by the green line in figure 50. Increased WACC result in increased LCOE. An increase of 15%, result in a WACC off 5,75%, which cannot be considered as a high scenario. See figure 48 for a more complementary illustration of the WACC's impact on the LCOE at higher values. In the sensitivity study of EUR/NOK, it is assumed that all CAPEX is paid in EUR and that all electricity volumes are sold in EUR. As visible in figure 51, this has a minimal effect on the LCOE, because the effects equalize each other. However, if the CAPEX is paid in EUR and the electricity sold in NOK, an increase in EUR/NOK would have increase the LCOE and have a negative impact on the profitability.

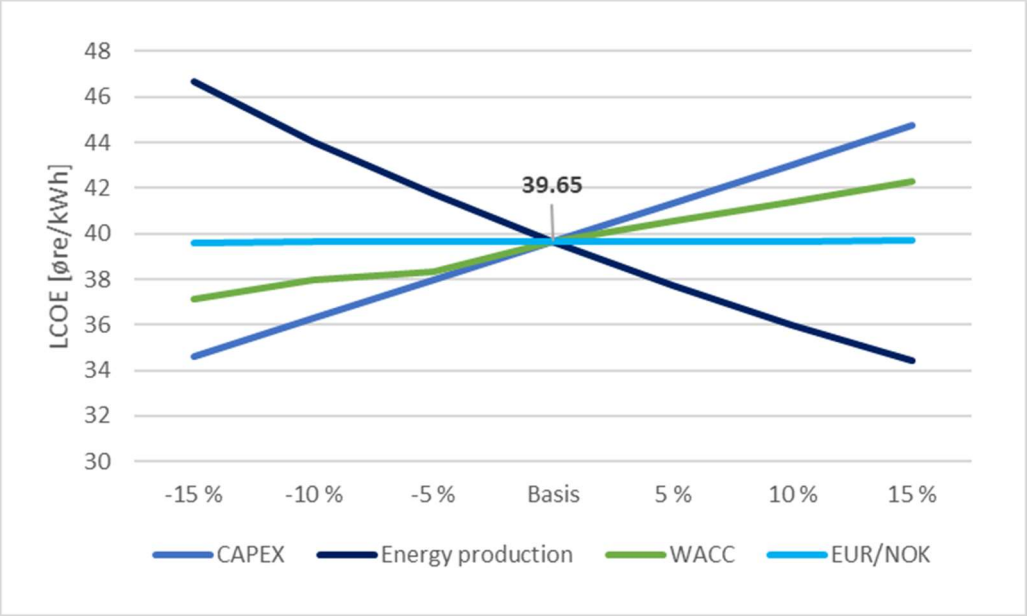

Figure 51: LCOE sensitivity with respect to changes in main parameters. For the EUR/NOK case, it is assumed that all CAPEX cost is in EUR and the electricity is sold in EUR.

Comparing Solberg wind farm with estimates from NVE

NVE has estimated the future LCOE on onshore wind in Norway, based on information from, Ministry of Finance, Statistics Norway and *EnergiRapporten* [65][71]. In this section a comparison between the main foundlings in this thesis and the general numbers from NVE's are performed. Table 14 shows the available parameters [71] that NVE used to estimate the LCOE for onshore wind in Norway in 2030.

The main difference between Solberg wind farm and NVE's estimates are the LCOE. There are several possible causes for this large difference. Firstly, NVE's estimate are based on an average farm size of 474MW, which is significantly larger than Solberg. With higher installed capacity, the cost per MW installed will normally reduce due to scale. A degradation rate of 0,10% is used by NVE, which result in less loss from the energy production during the lifetime. Finally, the CPAEX is not presented by NVE, but their numbers were updated 31.01.2022, meaning the latest increased cost of commodities are not included in theirs estimates. The duration of high commodity prices is uncertain, but they will affect the CAPEX for all renewable projects the next 2 years [63][57].

Table 14: Comparison between Solberg wind farm and estimates from NVE regarding future LCOE of onshore wind in 2030.

	Solberg	NVE
LCOE (2030)	39.65	22.15
Size [MW]	84	474
Lifetime	30	25
OPEX [øre/kWh]	9.2	10
Degradiation	0.25 %	0.10 %

4.3.9 Limitations and uncertainties

Small errors in the wind resource assessment would propagate trough the energy production and finally affect the economic assessment. To cover these uncertainties and how they affect different outcomes of the project, a sensitivity analysis was performed.

Besides the uncertainty related to energy production, the future electricity prices represent a large uncertainty in the economic assessment. Three different price trajectories have been used based on market outlook analysis from NVE, Statnett and Ishavskraft. Nobody can predict the future price, but by mapping the future demand and supply situation for Norway NO4 and SE1 can return a rough estimate. The main findings are that the demand will increase more than the supply, which in general should result in increasing prices. The limited transmission line capacity between North and South are today causing large price differences, both in Norway and Sweden. There are stated plans to expand this capacity towards 2030, but the timeline is rough. However, increased transmission capacity will result in higher prices.

For the economic assessment, the calculations of the CAPM and WACC was based on consensus parameters in the Norwegian market. For this individually case, some investors could have required higher market risk premium, due to the uncertainty regarding the electricity prices. This would result in a higher WACC, hence increasing the LCOE, as shown in figure 48.

Finally, it is linked a large uncertainty regarding the future CAPEX for onshore wind power plants. As shown in figure 28, the CAPEX has increased since 2020 due to a thigh commodity market and high prices on minerals and metals. However, the trend before this was descending. It was found that increased CAPEX cost resulted in significantly higher LCOE, which make the future commodity price trends an important parameter to watch for wind farms developers.

4.4 Summary of main limitations and uncertainties

The results from this thesis have shown that small under- or over estimations in wind speed estimations from the WRF-simulation, will propagate trough the wind energy assessment and to the economical assessment. As shown, the LCOE of the wind farm sowed largest sensitivity to variations in yearly energy production.

Since the energy output from a turbine has a cubic relationship with the available wind speed, small variations in the wind speed estimations will propagate to larger variations in estimated energy production. These effects would be largest in the wind speed range between 3-10m/s due to the properties of the power curve. This highlights the importance of knowing the WRF-models' limitations when it comes to wind modelling in complex terrain, hence real observations from a weather mast on-site are desirable to validate the results.

The wake loss effect was estimated to 8,6% for Solberg. Due to the model's resolution, the energy production was averaged within each grid cell, hence it must bee seen as a rough estimate. Energy loss due to icing was assumed to be 5% based on a study at Raudfjell and Kvitfjell. However, no detailed ice loss assessment was performed at Solberg, which increase the uncertainties in the energy estimations. For a preliminary project like Solberg, a total loss factor of 15% was applied, which should be considered as a rough estimate.

For the economical assessment, the main input value was the estimated energy production. As mentioned above, several steps with subsequent uncertainties were performed to obtain the estimated energy production of 288.53GWh. In addition, there are large uncertainties related to the future electricity prices. The economic analysis showed that the LCOE had highest sensitivity to variation in yearly energy production. This illustrates, the importance of having an accurate and trustworthy wind resource assessment, when using the WRF-model in the preliminary phase of a wind farm project.

From the three different price trajectories, the NPV showed high sensitivity for the different scenarios. However, from the market outlook its evident that the demand will increase, which will form the basis for higher electricity prices if additional energy production is not developed.

5 Conclusion

This thesis has proven that Solberg wind farm is an economic sustainable investment, with operational energy production from 2030. This result was found by a compilation of the results in the three main segments of the thesis: Wind resources assessment, estimations of the energy production and the economic assessment.

The wind farm consists of 14 Vestas V162 wind turbines and has a total installed capacity of 84MW. The average wind speed for the whole wind farm was 7,47 m/s at hub height of 125m, and the main wind direction was SW. The yearly net energy production in an average weather year was estimated to 288,53 GWh and resulted in a capacity factor of 39,10%. The capacity factor was above all the other wind farms in Solberg's vicinity. An additional hub height of approximately 40m above the other wind farms was suggested as one possible reason. In the basis scenario, the LCOE was estimated to 39.65 øre/kWh, NPV to 55,4MNOK and the IRR to 5,46%. In total, this made the Solberg wind farm an economic sustainable investment.

The wind resource assessment was performed by running two WRF simulations with a resolution of 1km. The first simulation was a "clean" simulation. In the second simulation, a wind turbine scheme was activated along with the power curve of the turbine. By comparing these two simulations, the wake loss effect on the yearly energy production on the wind farm was found to be 8,6%. Additional loss for icing and maintenance was included, resulting in a total loss factor of 15%. December and March had similar production volumes, but the wake loss was much larger in December. The difference in wind direction was suggested to be one of the reasons, where December had more high wind speeds from WSW. Based on this observation, the wind farm design was suggested to be optimized with respect to winds from WSW in order to decrease wake loss and increase energy production.

The economic assessment showed that the wind farm was an economic sustainable investment with respect to the basis scenario. This assumed an average electricity price for the lifetime of the project of 42,4 øre/kWh. The profitability of the project showed largest sensitivity to variations in yearly energy production and electricity prices. Future electricity prices are not possible to predict, hence a carefully wind resource assessment is important. WRF is a good tool in a preliminary phase but should be completed with data from weather mast to increase the accuracy of the energy production estimations.

5.1 Further research

Validating WRF energy estimations with a real wind farm

To evaluate the accuracy of the WRF-simulation with the wind turbines, a simulation over a wind farm site should be performed. The turbines should be placed out in the model at the exact same coordinates as in the wind farm. Instead of running one simulation for one year at the same site, one should prioritize to cover several wind farms in northern Norway. This will give a broader validation of the model with respect to different locations. This will show how the energy production estimations from the WRF-simulation correlate with real data from the wind farms. The results from such a study would be valuable when mapping new possible areas for wind energy production, such as Solberg.

Combining WindSim and WRF

To optimize turbine placement and minimize wake loss at Solberg, a new assessment with WindSim, a Wind Park Design Tool, in combination with WRF could be performed. Optimalization of turbine placement and micrositing is important to increase the energy production. As shown in the sensitivity analysis, the LCOE of the project is sensitive for variations in energy production. This highlights the importance of a good wind resource assessment.

Automate wind energy assessments

Making a more streamlined system for mapping and comparing several areas over a shorter period. When the WRF simulation is done, a designed script should analyse and plot the most important parameters automatically, for both the whole farm and the turbine locations; windspeed distribution, windrose, monthly wind speed variation, yearly average wind speed, energy production etc. Based on the energy production, a rough estimate of the LCOE could have been made for each site automatically. This would make it easier and faster in a preliminary phase to pick out the locations with lowest available resources.

Green hydrogen production

For periods with high energy production and low energy consumption, there would be interesting to map the possibilities for producing green hydrogen at Solberg. This could be mapped by analysing seasonal energy consumption at Senja and compare it to the seasonal estimated energy production from Solberg. The high density of fishing vessels at Senja makes this an interesting case, due to the proximity to the end users.

6 Appendix

Appendix A: Wind turbine locations at Solberg Wind farm

Wind turbine placement Solberg			
Turbine	Latitude	Longitude	Real height [m]
w1	17.81946	69.17818	386.8
w2	17.83785	69.17634	397.0
w3	17.86099	69.17667	295.8
w4	17.87206	69.17763	259.9
w5	17.84050	69.18388	347.7
w6	17.85417	69.18380	340.4
w7	17.87189	69.18488	301.1
w8	17.88557	69.18694	311.2
w9	17.89957	69.18591	265.6
w10	17.84097	69.19098	305.4
w11	17.85949	69.19458	305.6
w12	17.87205	69.19486	313.3
w13	17.88646	69.19665	275.2
w14	17.89694	69.19347	264.8

Appendix B: Namelist for WRF simulation

Namelist.wps

```
&share
 wrf_core = 'ARW',
 max_dom =3,
 start_date = '2016-01-01_00:00:00','2016-01-01_00:00:00','2016-01-01_00:00:00'
 end_date   = '2017-01-01_00:00:00','2017-01-01_00:00:00','2017-01-01_00:00:00'
 interval_seconds = 21600,
 io_form_geogrid = 2,
 opt_output_from_geogrid_path = './',
 debug_level = 0,
/

&geogrid
 parent_id         = 1,1,2,
 parent_grid_ratio = 1,5,5,
 i_parent_start    = 1,37,40,
 j_parent_start    = 1,54,27,
 e_we          = 96,136,151,
 e_sn          = 96,96,151,
 geog_data_res = 'default', 'default', 'default',
 dx = 25000,
 dy = 25000,
 map_proj =  'polar',
 ref_lat   = 66.5,
 ref_lon   = 19,
 truelat1  = 66.5,
 truelat2  = 90,
 stand_lon = 19,
 geog_data_path ='/cluster/projects/nn9426k/geog',
 opt_geogrid_tbl_path = './',
/

&ungrib
 out_format = 'WPS',
 prefix = 'FILE',
/

&metgrid
 fg_name = 'FILE',
 io_form_metgrid = 2,
 opt_output_from_metgrid_path = './',
 opt_metgrid_tbl_path = './',
/

!&mod_levs
! press_pa = 201300 , 200100 , 100000 ,
!             95000 ,  90000 ,
!             85000 ,  80000 ,
!             75000 ,  70000 ,
!             65000 ,  60000 ,
!             55000 ,  50000 ,
!             45000 ,  40000 ,
!             35000 ,  30000 ,
!             25000 ,  20000 ,
!             15000 ,  10000 ,
!              5000 ,   1000
/
```

Namelist.input for activating wind turbine scheme

```
a&time_control
run_days                  = 32,
run_hours                 = 00,
run_minutes               = 00,
run_seconds               = 00,
start_year                = 2016,     2016,     2016,
start_month               = 12,       12,         12,
start_day                 = 01,       01,         01,
start_hour                = 00,       00,         00,
start_minute              = 00,       00,         00,
start_second              = 00,       00,         00,
end_year                  = 2017,     2017,     2017,
end_month                 = 01,       01,         01,
end_day                   = 01,       01,         01,
end_hour                  = 00,       00,         00,
end_minute                = 00,       00,         00,
end_second                = 00,       00,         00,
interval_seconds          = 21600,
input_from_file           = .true.,   .true.,  .true.,
history_interval          = 60,       60,      60,
frames_per_outfile        = 24,       24,      24,
restart                   = .false.,
restart_interval          = 5760,
io_form_history           = 2,
io_form_restart           = 2,
io_form_input             = 2,
io_form_boundary          = 2,
!ofields_filename        ="myoutfields.txt","myoutfields.txt",
debug_level               = 0,
/

&domains
time_step                 = 90,
time_step_fract_num       = 0,
time_step_fract_den       = 1,
max_dom                   = 3,
e_we                      = 96,       136,   151,
e_sn                      = 96,       96,    151,
e_vert                    = 38,       38,    38,
p_top_requested           = 5000,
num_metgrid_levels        = 38,
num_metgrid_soil_levels   = 4,
dx                        = 25000,    5000,   1000,
dy                        = 25000,    5000,   1000,
grid_id                   = 1,        2,        3,
parent_id                 = 1,        1,        2,
i_parent_start            = 1,       37,       40,
j_parent_start            = 1,       54,       27,
parent_grid_ratio         = 1,        5,        5,
parent_time_step_ratio    = 1,        5,        5,
feedback                  = 0,
smooth_option             = 0,
!eta_levels                = 1.0000, 0.9980, 0.9955, 0.9925, 0.9890, 0.9850,
 0.9805, 0.9755, 0.9700, 0.9640, 0.9575, 0.9505, 0.9430, 0.9350, 0.9265, 0.9170,
 0.9060, 0.8930, 0.8775, 0.8590, 0.8363, 0.8104, 0.7803, 0.7456, 0.7059, 0.6615,
 0.6126, 0.5594, 0.5041, 0.4479, 0.3919, 0.3384, 0.2897, 0.2474, 0.2107, 0.1792,
 0.1523, 0.1293, 0.1093, 0.0917, 0.0763, 0.0629, 0.0513, 0.0413, 0.0328, 0.0255,
 0.0194, 0.0144, 0.0104, 0.0071, 0.0000,

smooth_cg_topo                    = .true.,
/
```

```
&physics
mp_physics                = 8,        8,       4,
ra_lw_physics             = 4,        4,       4,
ra_sw_physics             = 4,        4,       4,
radt                      = 15,       3,       1,
sf_sfclay_physics         = 2,        2,       2,
sf_surface_physics        = 2,        2,       2,
bl_pbl_physics            = 5,        5,       5,
bldt                      = 0,        0,       0,
cu_physics                = 6,        0,       0,
cudt                      = 5,        5,       5,
isfflx                    = 1,
ifsnow                    = 1,
icloud                    = 1,
surface_input_source      = 1,
num_soil_layers           = 4,
sf_urban_physics          = 0,        0,       0,
windfarm_opt             = 1, 1, 1,
windfarm_ij              = 0,
windfarm_tke_factor       = 0.25,
bl_mynn_tkeadvect         = .true., true., true.,
/


/

&fdda
/

&dynamics
w_damping                 = 0,
diff_opt                  = 1,          1,       1,
km_opt                    = 4,           4,
epssm                        = 0.1,       0.1,
diff_6th_opt              = 0,           0,
diff_6th_factor           = 0.12,      0.12,
base_temp                 = 290.,
damp_opt                  = 0,
zdamp                     = 5000.,     5000.,
dampcoef                  = 0.2,       0.2,
khdif                     = 0,         0,
kvdif                     = 0,         0,
non_hydrostatic           = .true.,    .true.,
moist_adv_opt             = 1,         1,
scalar_adv_opt            = 1,         1,
/

&bdy_control
spec_bdy_width            = 5,
spec_zone                 = 1,
relax_zone                = 4,
specified                 = .true.,  .false.,    .false.,
nested                    = .false.,   .true.,    .true.,
/

&grib2
/

&namelist_quilt
nio_tasks_per_group       = 0,
nio_groups                = 1,
/
```

Wind turbine table for WRF simulation - Example

Top row: Number 43 indicate number of wind speed values

Second row: 125= hub height in m, 132= rotor diameter, 0.130= standing trust coefficient (used standard value from scheme), 6= installed capacity MW

The three colons: Left colon indicates wind speeds, mid colon is drag coefficient and right colon is power output in watt.

```
43
125. 132. 0.130 6.0
3.0   0.805    32.0
3.5   0.805   150.0
4.0   0.805   292.0
4.5   0.805   467.0
5.0   0.805   676.0
5.5   0.805   927.0
6.0   0.805  1229.0
6.5   0.805  1584.0
7.0   0.805  2000.0
7.5   0.805  2476.0
8.0   0.805  3017.0
8.5   0.805  3624.0
9.0   0.805  4264.0
9.5   0.795  4859.0
10.0  0.790  5380.0
10.5  0.750  5734.0
11.0  0.740  5932.0
11.5  0.720  5983.0
12.0  0.700  5998.0
12.5  0.500  6000.0
13.0  0.400  6000.0
13.5  0.350  6000.0
14.0  0.300  6000.0
14.5  0.270  6000.0
15.0  0.250  6000.0
15.5  0.220  6000.0
16.0  0.200  6000.0
16.5  0.180  6000.0
17.0  0.160  6000.0
17.5  0.150  6000.0
18.0  0.140  5846.0
18.5  0.130  5581.0
19.0  0.120  5360.0
19.5  0.110  5128.0
20.0  0.100  4844.0
20.5  0.090  4555.0
21.0  0.080  4268.0
21.5  0.750  3985.0
22.0  0.070  3690.0
22.5  0.065  3383.0
23.0  0.060  3102.0
23.5  0.058  2801.0
24.0  0.055  2479.0
```

Appendix C – NPV calculations for Solberg

NPV calculations for the five first years in the basis scenario.

NOK						
År	0	1	2	3	4	5
Production [GWh]		288.53	287.81	287.09	286.37	285.66
Electricity price						
Base		32.0	35.0	37.0	44.0	44.0
High		53.0	52.0	52.0	57.0	57.0
Low		32.0	35.0	37.0	34.0	34.0
Inncome		92 329 600	100 733 036	106 222 987	126 003 429	125 688 421
Turbine O&M		- 7 000 000	- 7 140 000	- 7 282 800	- 7 428 456	- 7 577 025
Land rent		- 3 693 184	- 4 029 321	- 4 248 919	- 5 040 137	- 5 027 537
Grid rent		- 8 655 900	- 8 655 900	- 8 655 900	- 8 655 900	- 8 655 900
Property tax		- 3 684 030	- 3 757 711	- 3 832 865	- 3 909 522	- 3 987 713
Insurance		- 642 803	- 655 659	- 668 772	- 682 148	- 695 791
Technical managment		- 1 680 000	- 1 713 600	- 1 747 872	- 1 782 829	- 1 818 486
OPEX		- 25 355 917	- 25 952 191	- 26 437 129	- 27 498 992	- 27 762 451
Opex buffer		- 1 267 796	- 1 297 610	- 1 321 856	- 1 374 950	- 1 388 123
Total OPEX		- 26 623 713	- 27 249 801	- 27 758 985	- 28 873 942	- 29 150 574
EBITDA		65 705 887	73 483 236	78 464 002	97 129 487	96 537 847
Depreciation turbin (saldogruppe d)		- 161 817 600	- 129 454 080	- 103 563 264	- 82 850 611	- 66 280 489
Depreciation nett (saldogruppe e)		- 10 000 000	- 9 500 000	- 9 025 000	- 8 573 750	- 8 145 063
EBIT		- 106 111 713	- 65 470 844	- 34 124 262	5 705 126	22 112 296
Tax		-	-	-	-	-
Net income		- 106 111 713	- 65 470 844	- 34 124 262	5 705 126	22 112 296
Depreciation turbin		161 817 600	129 454 080	103 563 264	82 850 611	66 280 489
Depreciation grid		10 000 000	9 500 000	9 025 000	8 573 750	8 145 063
Investeringskostnader (capex)	- 1 118 290 000					
Beregnigsgrunnlag	- 1 118 290 000	65 705 887	73 483 236	78 464 002	97 129 487	96 537 847

Figure 52: Five first years of NPV calculations in the basis scenario

Deficit carried forward due to large depreciations. Year nine was estimated to be the first year of tax payment due to deficit carried forward.

Taxable Income After Depreciation and Loss Carryforwards									
year	1	2	3	4	5	6	7	8	9
Taxable income after deprecition, before loss caryyforwards						35 178 963	45 568 888	53 813 213	60 336 976
Loss carryforwards	- 106 111 713	- 65 470 844	- 34 124 262	5 705 126	22 112 296				
Sum loss carryforwards	- 106 111 713	- 171 582 557	- 205 706 819	- 200 001 693	- 177 889 398	- 142 710 434	- 97 141 546	- 43 328 333	17 008 642
Taxable income after deprecition and loss carryforwards									
Tax to pay (22%)									3 741 901.31

Figure 53: No tax paid before year 9 due to deficit carried forward.

7 Bibliography

[1] Stortingsmelding 13 (2020–2021) klimaplan for 2021–2030 [online] [accessed 10.10.2021]

Available at: https://www.regjeringen.no/no/dokumenter/meld.-st.-13-20202021/id2827405/

[2] A.A. Fossem, «Wind resource assessment using weather research and forecasting model", 2019

[3] M. Bilal, K. Solbakken and Y. Birkelund, *"Wind speed and direction predictions by WRF and WindSim coupling over Nygårdsfjellet",* 2016

[4] Henriette Birkelund, Fredrik Arnesen, Jarand Hole, Dag Spilde, Silje Jelsness, Frida H. Aulie og Ingrid E. Haukeli, «*Langsiktig kraftmarkedsanalyse 2021 – 2040*», The Norwegian Water Resources and Energy Directorate, 2021 [online] [accessed 10.02.2022]

Available at: https://publikasjoner.nve.no/rapport/2021/rapport2021_29.pdf

[5] Nettutviklingsplan for Norge 2021 *"Nettutviklingsplan 2021"*, Statnett, 2021

[online] [Accessed 23.04.2022]

[6] Energy price trajectory towards 2032 received from *Markedssjef* at Ishavskraft, [accessed 03.04.2022]

[7] Newsletter from Statnett regarding opening of Nordlink [online] [accessed 20.04.2022]

Available at: https://www.statnett.no/vare-prosjekter/mellomlandsforbindelser/nordlink/nyhetsarkiv/stromforbindelsen-mellom-norge-og-tyskland-er-ferdig-bygget/

[8] Newsletter from Statnett regarding opening of North-Sea-link [online] [accessed 20.04.2022]

Available at: https://www.statnett.no/vare-prosjekter/mellomlandsforbindelser/north-sea-link/

[9] Information about the Smart Senja project

Available at: https://smartsenja.no/om-oss/

[10] Al-Yahyai S., Charabi Y., Gastli A., "*Review of the use of Numerical Weather Prediction (NWP) models for wind energy assessment",* 2010.

[11] Carvalho D., Rocha A., Gómez-Gesteira M. and Santos C. "*A sensitivity study of the wrf model in wind simulation for an area of high wind energy. Environmental Modelling & Software",* 2012

[12] Documentation about Sigma [online] [accessed 2022.05.18]

Available at: https://documentation.sigma2.no/

[13] Solbakken K., Birkelund Y.," *Evaluation of the Weather Research and Forcasting (WRF) model with respect to wind in complex terrain, 2018",* Phys.: Conf. Ser. 1102 012011.

[14] Ahrnes C. D., Henson R., "*Meteorology today: An introduction to Weather, Climate, and the Environment",* 2008, edition 12.

[15] Wallace J., Hobbs P. V., *Atmospheric Science, second Edition: An introductory Survey,* February 2006.

[16] Ulazia, A., Nafarrate, A., Ibarra-Berastegi, G., S´aenz, J. & Carreno-Madinabeitia, S. "*The consequences of air density variations over Northeastern Scotland for offshore wind energy potential. Energies",* 2019

[17] Gary L. J., "*Wind Energy Systems",* November 2001

[18] De Lellis M., Reginatto R., "*The Betz limit applied to Airborn Wind Energy",* 2018

[19] González-Longatt F., Wall P., Terzija V., "*Wake effect in wind farm performance: Steady-state and dynamic behaviour",* 2012

[20] Homola, M. C., '*Atmospheric icing on wind turbines: Modeling and consequences for energy production',* 2011

[21] Gao L., Hong J., "*Wind turbine performance in natural icing environments: A filed characterization"*, 2021.

[22] Kjersem H.A., *"Estimation of Production Losses due to Icing on Wind Turbines at Kvitfjell Wind Farm"*, 2019

[23] Jia Yi J., Rizwan G., Muhammed Virk S., "*Wind Turbine Wake Effects on Wind Resource Assessments – a Case Study*", 2020 [online] [accessed 10.03.2022]

[24] Bjørnebye H., Hagem C. and Lind A., *"Optimal location of renewable power",* 2017

[online] [accessed 23.05.2022]

Available at:
https://www.ssb.no/en/forskning/discussionpapers/_attachment/313894?_ts=15cd4ccda30

[25] Byrne R., Astolfi D., Castellani F., Hewitt N., *«A Study of Wind Turbine Performance Decline with Age trough Operation Data Analysis"*, April 2020

[online -pdf] [accessed 24.05.2022]

[26] Kalmikov, A., "*Wind Energy Engineering"*, 2017 [accessed 10.04.2022]

[27] Gunnerød J., Bøhnsdalen E., Vagner D., Hytten L.M., Christiansen L., "*Kortsikig markedsanalyse 2021-2026*", Statnett, December 2021 [accessed 20.05.2022]

https://www.statnett.no/contentassets/914a67b2c52343d29bf5d34709d25e25/kortsiktig-markedsanalyse-2021-2026.pdf

[28] Gunnerød J., Bøhnsdalen E., Vagner D., Hytten L.M., Christiansen L., «*Long-term market analysis 2020-2050*», Statnett, Spring 2021

https://www.statnett.no/globalassets/for-aktorer-i-kraftsystemet/planer-og-analyser/lma/lma-update-2021.pdf

[29] *"Nordic grid development perspective 2021"*, report from Energinet, Fingrid, Statnett and Svenska Kraftnet, 2021

[online] [accessed 10.05.2022]

Available at: https://www.statnett.no/globalassets/for-aktorer-i-kraftsystemet/planer-og-analyser/nordic-grid-development-perspective-2021.pdf

[30] European Commission – Press release *"REPowerEU: Joint European action for more affordable, secure and sustainable energy",* March 2022

[31] Døskeland I. H., Nybø A., Kringstad A., Gustafsson M. and Winsnes M.M., "*Prisforskjeller og kapasitet nord-sør*», april 2022 [online] [accessed 10.10.2022]

Available at:

https://www.statnett.no/contentassets/1d183d99f1d943e1bc67c5ef98887052/presentasjon-webinar-prisforskjeller-og-kapasitet-nord-sor.pdf

[32] Forster H., Gores S., Nissen C., Siemons A., Renders N., Dael S., Sporer M. and Tomescu M., "*Trends and projections in Europe 2021*", 2021 (European Environment Agency)

[33] The Norwegian Petroleum Directorate, "*Kraft fra land*", report, 2020

Available at: https://www.npd.no/globalassets/1-npd/publikasjoner/rapporter/2020/kraft-fra-land-til-norsk-sokkel/kraft-fra-land-til-norsk-sokkel-rapport-2020.pdf

[34] Presentation by Troms Kraft, held 24.05.06

[35] Impact assessment for Wisting, by Equinor "*Wisting PUD del 2: Konsekvensutreding*", februar 2022 [online] [Accessed 15.05.2022]

https://cdn.sanity.io/files/h61q9gi9/global/d099700b5ec5825bfec9e5ecadc7c72fe7e592c9.pdf?pud-del-ii-konsekvensutredning-wisting-equinor.pdf

[36] Ministry of the Environment and Energy, "*The Swedish climate policy framework", 2020* [online] [Accessed 20.05.2020]

Available at:
https://www.government.se/495f60/contentassets/883ae8e123bc4e42aa8d59296ebe0478/the-swedish-climate-policy-framework.pdf

[37] Report about the electrification in the Nordic region, "*Study on opportunities and barriers to electrification in the Nordic region*", Prepared by DNV on behalf of Nordenergi, 2020 [online] [Accessed 20.05.2022]

Available at: https://www.energiforetagen.se/globalassets/dokument/nordenergi/electrification-in-the-nordics---nordenergi_19_05_2021.pdf

[38] Information about the electrification of LKAB, *"Frågor och svar, vår nya strategi»*, LKAB, 2020, [online] [Accessed 20.05.2022]

[39] Haukeli I. E., Stavseng A., Splide D., Hole J., Skaansar E., Skotland C. H., Holm I., Heine M. H., Verlo K. R. and Røv V., *«Elektrifiseringstiltak i Norge, hva er konsekvensene for Norge?*», 2020

[40] International Energy Agency (IEA), Average annual capacity factors by technology [online] [accessed 18.04.2022]

Available at: https://www.iea.org/data-and-statistics/charts/average-annual-capacity-factors-by-technology-2018

[41] Olivera W.S, Fernandes A. J., *"Investment Analysis for Wind Energy Projects"*, 2013 [Online] [Accessed 15.05.2022]

[42] D'Angelo M., *"Onshore Wind Energy Market Analysis - of Sweden, Poland, and Romani",* 2020 [online] [accessed 09.05.2022]

[43] Terrain complexity in Norway, *"Terrengkompleksitet, RIX-verider, målestokk 1:600 000"*, by Kjeller Vindteknikk for NVE

[online] [accessed 02.05.2022]

Available at: https://www.nve.no/media/2461/terrengkompleksitet_kartbok2a_rev1.pdf

[44] Info about ERA-Interim data [online] [accessed 21.03.2022] https://www.ecmwf.int/en/forecasts/datasets/reanalysis-datasets/era-interim

[45] WRF V3.9 user guide [Accessed 15.01.2022]

Available at: https://www2.mmm.ucar.edu/wrf/users/docs/user_guide_V3/user_guide_V3.9/ARWUsersGuideV3.9.pdf

[46] Geographical Static Data Downloads page [online]

https://www2.mmm.ucar.edu/wrf/users/download/get_sources_wps_geog.html)

[47] David E.W., «*Vindkraft - produksjon i 2016»,* NVE, 2017

[48] Dag S., «*Strømforbruk mot 2040 - Analyse av strømforbruk i Fastlands-Norge, Norden og utvalgte EU-land*», 2019

[49] Roth A., Brückmann R., Jimeno M., "*Renewable energy financing conditions in Europe: survey and impact analysis",* March 2021

[50] Angelopoulos D., Bruckmann R., Jirous F., Konstantinaviciute I., Noothout P., Psarras J., Tesniere L. and Breitschopf B., *"Risks and cost of capital for onshore wind energy investments in EU countries"* 2016, [online] [Accessed 2022-05-15]

[51] Information about the MSCI World Index [online] [accessed 2022.05.15]

Available at: https://www.msci.com/World

[52] Dukan M., Kitzing L., Brückmann R., Jimeno M., Wigand F., Kielichowska I., Klessmann C., and Breitschopf B., "*Effect of auctions on financing conditions for renewable energy",* 2019 [online] [accessed 28.04.2022]

[53] International Renewable Energy Agency (IRENA), *"Future of wind: Deployment, investment, technology, grid integration and socio-economic aspects"*, 2019 [online] [accessed 28.04.2022]

Available at: https://www.irena.org/-/media/files/irena/agency/publication/2019/oct/irena_future_of_wind_2019.pdf

[54] Map over wind farms in Norway with information about installed capacity and excepted production. Delivered by NVE.

[Accessed 25.05.2022]

Available at: https://www.nve.no/energi/energisystem/vindkraft/kart/

[55] Map book showing wind speeds over Norway at 50m, 80m and 120m. Made by Kjeller vindteknikk for NVE.

Available at: https://www.nve.no/energi/energisystem/vindkraft/vindressurser/

[accessed 25.05.2022]

[56] Simonsen A. H., Brennan K., «*Vind- og produksjonsindekser for vindkraft i Norge, 2021*», NVE report, February 2022

[online] [accessed 23.05.2022]

Available at: https://2021.nve.no/media/13401/mev-ws-2022-001-vind-og-produksjonsindekser-for-vindkraft-i-norge-2021.pdf

[57] Newsletter from IEA regarding the high commodity prices, *"Critical minerals threaten a decades-long trend of cost decline for clean energy technologies",* [online] [accessed 26.05.2022]

https://www.iea.org/commentaries/critical-minerals-threaten-a-decades-long-trend-of-cost-declines-for-clean-energy-technologies?utm_content=buffer6288d&utm_medium=social&utm_source=twitter.com&utm_campaign=buffer&s=07

[58] Discussion with Espen Erdal, VP Business Development in Magnora. Experience from developing wind farms. [27.05.2022]

[59] Report about the risk premium in the Norwegian market by PWC *"Risikopremien i det norske markedet"*, 2021

[online] [accessed 10.05.2022]

Available at: https://www.pwc.no/no/publikasjoner/pwc-risikopremie-2021.pdf

[60] The WACC-model, NVE [online] [accessed 12.10.2022]

Available at: https://2021.nve.no/norwegian-energy-regulatory-authority/economic-regulation/the-wacc-model/

[61] Feldman D., Bolinger M., *"Curretn and Future Cost of Renewable Energy Project Finance Across Technologies",* 2020 [online] [accessed 02.05.2022]

Available at: https://www.nrel.gov/docs/fy20osti/76881.pdf

[62] International Energy Agency (IEA), *"World Energy Investment 2020*", 2020 [online] [accessed 20.05.2022]

Available at: https://iea.blob.core.windows.net/assets/ef8ffa01-9958-49f5-9b3b-7842e30f6177/WEI2020.pdf

[63] International Energy Agency (IEA), *"Renewable Energy Market Update, outlook for 2022 and 2023"*, 2022 [online] [accessed 27.05.2022]

Available at: https://iea.blob.core.windows.net/assets/d6a7300d-7919-4136-b73a-3541c33f8bd7/RenewableEnergyMarketUpdate2022.pdf

[64] Depreciation rules in Norway [online] [accessed 27.05.2022]

Available at: https://www.skatteetaten.no/rettskilder/type/handboker/skatte-abc/gjeldende/driftsmiddel--avskrivning-painntektsforing-av-saldo/D-2.008/D-2.027/

[65] EnergiRapporten – report about the energy market and industry

Available at: https://www.tekniskenyheter.no/energirapporten.573794.no.html

[66] Milligan M., Frew B., Clark K. and Bloom A., *"Marginal Cost Pricing in a World without Perfect Competition: Implications for Electricity Markets with High Shares of Low Marginal Cost Resources"*, by National Renewable Energy Laboratory (NRL), 2017

[67] Overview of expected icing at 80m in Norway, made by Kjeller Vindteknikk for NVE [online] [accessed 14.05.2022]

Available at: https://www.nve.no/energi/energisystem/vindkraft/vindressurser/

[68] Presentation held by Ishavskraft (03.03.2022) for students at UiT

[69] Map of the Nordic grid system

Available at: https://www.svk.se/en/national-grid/map-of-the-national-grid/

[70] Fitch A. C., et al, *"Local and Mesoscale Impacts of Wind Farms as Parameterized in a Mesoscale NWP Model. Monthly Weather Review"*, 2012

[71] Costs related to power production. Estimated LCOE by NVE. [online] [accessed 10.04.2022]

Available at: https://www.nve.no/energi/analyser-og-statistikk/kostnader-for-kraftproduksjon/

[72] Rydsaa J., *"WRF tutorial on FRAM ",* tutorial available for students taking "*Wind modelling in complex terrain"*, autumn 2021 at UiT

[73] Castellani F., Natili F., Astolfi D. and Cianetti F., *"Mechanical behaviour of wind turbines operating above design conditions"*, 2019 [online] [accessed 27.05.2022]

Available at: https://www.sciencedirect.com/science/article/pii/S2452321620302705

[74] Power curve [online] [accessed 28.05.2022]

Available at: https://wind-power-program.com/turbine_characteristics.htm